THERMAL AND DIAGENETIC EVOLUTION OF CARBONIFEROUS SANDSTONES, CENTRAL APPALACHIAN BASIN

by

Jason S. Reed

Dissertation submitted to the Graduate Faculty of

Virginia Polytechnic Institute and State University

in partial fulfillment of the requirements for the degree of

DOCTOR OF PHILOSOPHY

in

GEOLOGICAL SCIENCES

Kenneth A. Eriksson, Chair
Robert J. Bodnar
Susan C. Eriksson
Michal Kowalewski
J. Fred Read
J. Donald Rimstidt

April 15, 2003

Blacksburg, Virginia

Keywords: diagenesis, paleothermometry, sandstone, Appalachian basin

THERMAL AND DIAGENETIC EVOLUTION OF CARBONIFEROUS SANDSTONES, CENTRAL APPALACHIAN BASIN

Jason S. Reed

ABSTRACT

The thermal and diagenetic evolution of Carboniferous sandstones in the central Appalachian basin has been resolved using various techniques. Paleothermometers including vitrinite reflectance and fluid inclusions indicate that burial of Lower and Upper Pennsylvanian strata of the Appalachian Plateau in West Virginia exceeded 4.4 km during the late Permian and occurred at a rate of ~100 m/m.y. Exhumation rates of ~10-30 m/m.y. from maximum burial to present depth were constrained using published apatite fission track and radiogenic helium ages.

Quartz, lithic and feldspar-rich sandstones from different stratigraphic intervals and locations were sampled from core (95 %) and outcrop (5%) to qualitatively and quantitatively evaluate sandstone diagenesis. A compositional multivariate data set compiled from point counts served as the basis for quantitative analysis of controls on sandstone diagenesis such as framework grain composition, paleoclimate and depositional environment. *A priori groups* (independent variables) corresponding to the controls were compared using digenetic products (dependent variables). Major conclusions of the analysis are, first, minerals that formed early appear to have been influenced by stratigraphic position. The distribution of siderite and iron-oxide/oxyhydroxide may reflect the second order paleoclimatic signature recognized throughout the Carboniferous, where siderite formed during everwet periods and iron-oxide/oxyhydroxide during semi-arid conditions, reflecting differences in redox. Second, framework grain composition controlled the distribution of diagenetic alterations and quartz cementation in the burial environment. Lithic arenites are deficient in authigenic quartz, yet have undergone various degrees of illitization. The quartz deficiency is attributed to compaction-related loss of primary porosity relatively early, which inhibited flow of silica-bearing fluids. Finally, no correlation can be demonstrated between depositional environment and diagenesis.

Anomalously high fluid inclusion homogenization temperatures (> 215 °C) from Upper Pennsylvanian sandstones adjacent to the Alleghany Thrust Front indicate that tectonic setting played an important role in quartz authigenesis. The discrepancy between the fluid inclusion and vitrinite reflectance data imply that warm silica-bearing fluids, likely sourced from low-grade metamorphic reactions, were injected into Pennsylvanian sandstone aquifers during thrust loading associated with the Alleghanian orogeny.

ACKNOWLEDGEMENTS

This project and its presentation has greatly benefited from guidance and support provided by my dissertation advisor, Kenneth Eriksson. He is thanked for contributing to my development as a critical thinker, scientist and communicator. In addition, the results presented here would not be possible without the input of an exceptional dissertation committee. Bob Bodnar, Mike Kowalewski and Don Rimstidt have served as co-authors and greatly improved one or more manuscripts extracted from this dissertation. Chapter 2 on diagenesis has been enhanced significantly by discussions with Fred Read and Susan Eriksson. Jim Spotila is also thanked for his contributions to the burial and exhumation chapter and the resulting manuscript.

Contributions by West Virginia Geological and Economic Survey (WVGES) including core samples, wire-line logs and supplementary vitrinite reflectance data are acknowledged and appreciated. The United States Geological Survey, Mettiki Coal, Ackenheil Engineering, Consol Energy, the Army Corp of Engineers and Consol Energy are thanked for generously donating core samples and accompanying wire-line logs. Ron Martino is acknowledged for providing additional samples and also for valuable conversation and inspiration that directed me toward continuing studies in clastic sedimentology after earning a B.S. Much of the data presented here would not have been possible without the technical support of Bob Tracy, Jay Thomas, Jim Craig, Viktor Liogys and Claudia Mora. Moreover, completing five years of research and study cannot occur without numerous logistical problems and the Department of Geological Science staff (Connie, Mary, Linda, Carolyn, Charles, Mark^2) is thanked for their incessant help whenever asked.

Financial supporters of this research are acknowledged and include Mobil Oil, Geological Society of America student grants (6791-00 and 7250-02) and Virginia Tech. Funding from Virginia Tech occurred in the form of the Byron Nelson Cooper Memorial Fellowship, Heath Robinson – Roy J. Holden Geoscience Scholarship, and Graduate Student Assembly Student Development Grant.

My tenure in the Department of Geological Sciences at Virginia Tech has been extremely enjoyable. Strong bonds with many members of the department have contributed to my positive experience. Specifically, I will never forget the meaningful friendships I have built over the past five years and the help that so many have selflessly provided when needed: Dr. Kendall, Cappy, Greg, Trace, Katy, Young Andrew, Megan, Kevin, Brian, Mark, Jesse, Jay, John V., John W., Joel, Jim, Jeane, Pope, et al. My ability to persevere through difficult times and reach personal and academic goals would not have been possible without the continuous support of my mother, father, sister and best friend and to them I owe all I have and will potentially accomplish.

INTRODUCTION

Resolving the thermal and diagenetic history of sedimentary basins is important for many reasons. First, constraining the geodynamic evolution of an ancient foreland basin provides insight into the mechanics contributing to subsidence and inversion. Second, diagenetic interpretations linked to thermal constraints facilitates a more comprehensive understanding of reservoir quality and development, which can be applied to hydrocarbon and water extraction as well as fluid sequestration. Third, many thermal studies of sedimentary basins have targeted questions involving hydrocarbon generation and maturation and the approaches presented here can refine our current understanding of this phenomena. This study employs an integrated approach to answer questions concerning the thermal and diagenetic history of a foreland basin. Specifically, diagenetic mineral reactions like those presented in Chapters 2 and 3 can be more accurately constrained by using a thermal framework like that presented in Chapter 1.

The results from Chapter 1 provide a scheme that can be applied to many types of geologic problems including basin analysis, geomorphology and diagenesis. The integration paleothermometric and thermochronologic techniques addresses questions concerning the burial and exhumation of sedimentary rock and provides a template for thermally calibrating other ancient sedimentary basins.

Chapter 2 explores the diagenetic evolution of foreland basin sandstones. Specifically, it focuses on a detailed petrographic data set to qualitative and quantitative investigate Carboniferous sandstone diagenesis. Some mineral species were also examined using various geochemical methods. Evaluation of controls on sandstone diagenesis was accomplished using multivariate statistical methods that are not commonly used in sedimentary petrologic studies.

The integrated approach highlighted in Chapter 2 emphasizes the usefulness of multivariate statistics.

Chapter 3 addresses the controversial issue involving quartz authigenesis. Quartz is volumetrically one of the most important cements present in sandstones. Therefore, numerous studies have attempted to identify the most significant sources of silica and general transport mechanisms. One of the least cited mechanisms is proposed in Chapter 3. The paleothermometric results presented allowed us to postulate that warm silica-rich fluids were derived from low-grade metamorphic reactions below the Alleghany structural front. The potential mechanics of fluid flow in a foreland basin support our conclusions, i.e. contemporaneous fluid expulsions from the hinterland driven by active thrusting during the Alleghanian orogeny. Alternative sources of silica including clay mineral transformations and pressure dissolution between quartz framework grains cannot be excluded, although we suspect that they were only minor contributors to the total volume of quartz cement present in the studied sandstones.

TABLE OF CONTENTS

LIST OF FIGURES

LIST OF TABLES

CHAPTER 1: BURIAL AND EXHUMATION HISTORY OF PENNSYLVANIAN STRATA, APPALACHAIN FORELAND BASIN: INTEGRATING PALEOTHERMOMOTRY AND THERMOCHRONOLOGY

ABSTRACT

An inferred burial and exhumation history of Pennsylvanian strata in the central Appalachian foreland basin has been constrained based on the integration of paleothermometers, geochronometers and estimated paleogeothermal gradients. Vitrinite reflectance data and fluid inclusion homogenization temperatures indicate that burial of Lower and Upper Pennsylvanian strata of the Appalachian Plateau in West Virginia exceeded ~4.4 km during the late Permian and occurred at a rate of ~100 m/m.y. Exhumation rates of ~10 m/m.y. from the late Permian to the early Cretaceous were constrained using maximum burial conditions and published apatite fission track ages. Apatite fission track and radiogenic helium ages indicate exhumation rates of ~30 m/m.y. from the early to late Cretaceous. Radiogenic helium dates and present day sampling depths indicate that of exhumation rates from the late Cretaceous to present were ~25 m/m.y. Exhumation rates determined for Upper and Lower Pennsylvanian strata within the Appalachian Plateau are remarkably similar. Early slow exhumation was possibly driven primarily by isostatic rebound associated with Triassic rifting. The later, more rapid exhumation can be attributed to thermal expansion followed by lithospheric flexure related to sediment loading along the passive margin.

Keywords: foreland basin, burial, exhumation, Appalachian Plateau, vitrinite reflectance, fluid inclusions, radiogenic helium dating, apatite fission track dating

INTRODUCTION

Combining various geothermometers can be a valuable means to address many important geologic problems including thermal calibration of sedimentary basins, resolution of inversion histories of foreland basins, and understanding the post-orogenic evolution of ancient mountain systems like the Appalachians. Reconstructions of thermal and burial histories of ancient sedimentary basins traditionally have been based on vitrinite reflectance (e.g., Chyi et al., 1987; Hower and Rimmer, 1991; Zhang and Davis, 1993), fluid inclusion microthermometry (e.g., Goldstein and Reynolds, 1994; Burruss, 1989; Walderhaug, 1994; Wojcik et al., 1994), or a combination of both methods (e.g., Barker and Goldstein 1990; Tobin and Claxton, 2000). More recently, exhumation histories of sedimentary basins have been constrained using thermochronology. Apatite fission track (AFT) dating is the most widely used thermochronologic technique to evaluate the exhumation of sedimentary rocks (e.g., Naeser et al., 1989; Roden, 1990; Blackmer et al., 1994; Boettcher and Milliken, 1994) and can be integrated with vitrinite reflectance for more comprehensive reconstructions of exhumation history (e.g., Feinstein et al., 1989; Arne and Zentilli, 1994; Kamp et al., 1996; O'Sullivan, 1999). Integrating paleothermometers and thermochronometers is desirable because: 1) paleothermometers help justify the use of thermochronometers by predicting whether or not closure temperatures (T_c) were exceeded (Arne and Zentilli, 1994), and 2) tracking the complete thermal evolution of sedimentary basins can be useful for studies involving hydrocarbon generation, basin analysis, diagenesis and geomorphology.

Recent studies of helium diffusion in apatite have validated the use of the (U-Th)/He system for low-temperature thermochronology (e.g., Wolf et al., 1996). Traditionally, radiogenic helium dating of apatite grains has been used in diverse geologic settings to resolve problems

involving isostacy and tectonics (e.g., Spotila et al., 1998; Reiners et al., 2001; Kirby et al., 2002). This method has been applied less frequently to basin analysis, although it can be an effective tool for constraining the latest exhumation history of sedimentary basins (Crowhurst et al., 2002; House et al., 2002).

The purpose of this study is to use an integrated approach to evaluate the thermal inversion history of Pennsylvanian rocks in the Appalachian foreland basin (Fig. 1.1). Specific goals are to 1) investigate the post-orogenic evolution of an ancient foreland basin, 2) demonstrate the applicability of combined techniques to evaluate the burial and exhumation history of the basin, and 3) establish a thermal framework from deposition to deep burial that can be applied to sandstone diagenesis. Sandstones and associated strata in the Appalachian basin are ideally suited to apply these techniques. Fluid inclusions found in quartz cements and vitrinite in surrounding coal and shale provide the means to study the burial history, whereas AFT and (U-Th/He) data from detrital apatite grains recovered from the sandstones constrain exhumation. A secondary contribution of this study supplements our current understanding of the post-Alleghanian evolution the central Appalachians (e.g., Beaumont et al., 1987; Slingerland and Furlong, 1989).

GEOLOGIC SETTING

The Appalachian foreland basin formed in response to three orogenic events; the final episode of subsidence was caused by the Alleghanian orogeny (Quinlan and Beaumont, 1984). This orogeny produced highlands that served as an important source of sediment during the late Paleozoic. Basin subsidence dynamics varied during each of the orogenies and the basin was relatively wide and shallow during the Alleghanian event (Tankard, 1986). Major causes of

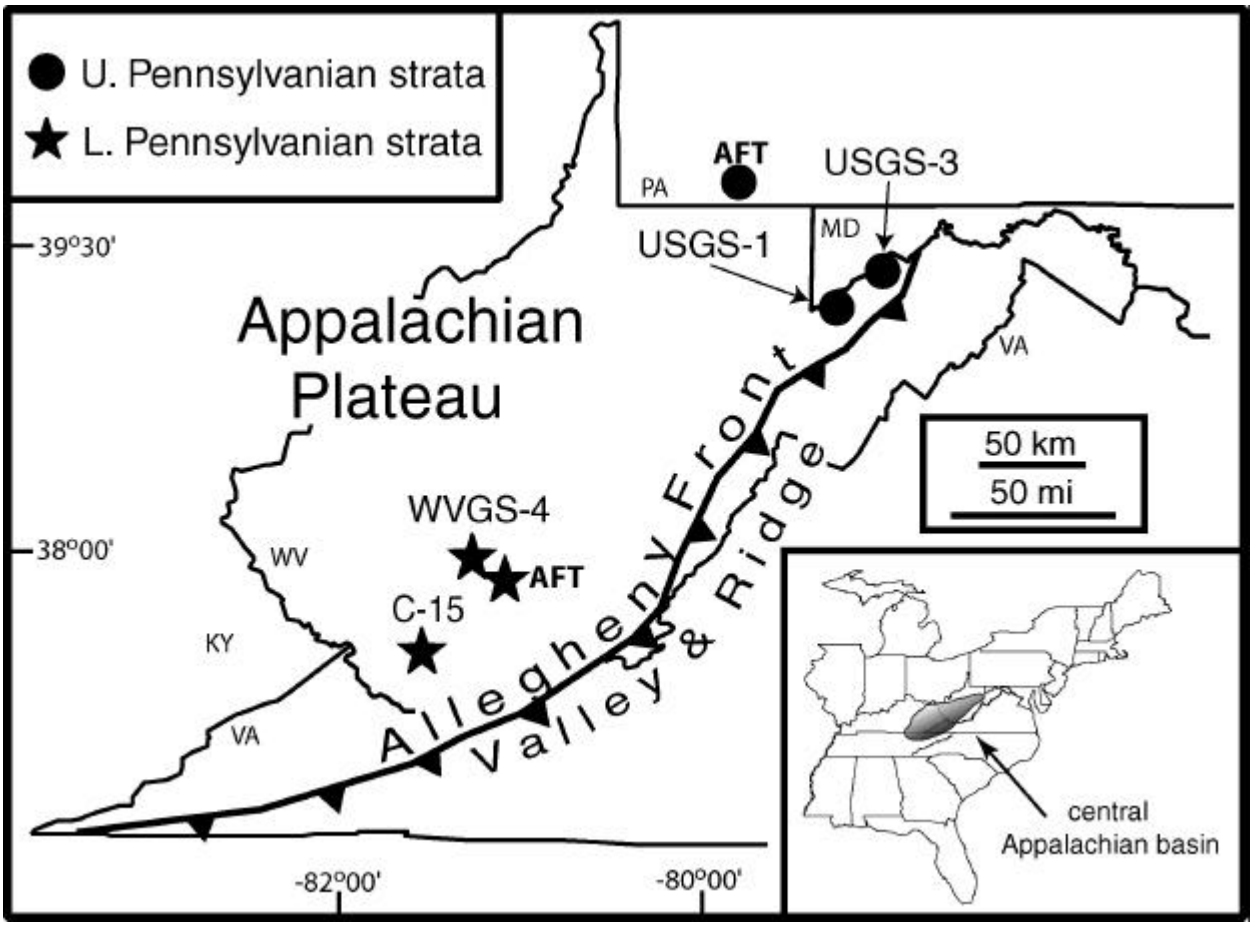

Figure 1.1 Map showing the location of borehole cores and published apatite fission track ages used for this study in relation to the Allegheny Thrust Front.

subsidence during the late Paleozoic were related to tectonic flexure of the lithosphere and sediment loading associated with the rejuvenation of the Appalachian foreland basin. Basin geometry was primarily controlled by the long-term rheological response of the lithosphere to tectonic loading and a general thickening of the crust (Dickinson, 1974; Allen et al., 1986, 1991; Klein, 1991; Sinclair, 1997; Castle, 2001), although short-term responses to tectonic loading have also been recognized (Tankard, 1986). Upper Carboniferous basin fill is primarily composed of siliciclastic sedimentary rocks including sandstone, mudstone, coal, and rare conglomerate and limestone.

Various stratigraphic markers subdivide the late Phanerozoic stratigraphic record. Coals and unconformities have been especially useful for regional correlations of Carboniferous strata in the central Appalachian basin. Upper and lower Pennsylvanian sections used in this study are identified and dated by such markers. The New River Formation in southern West Virginia consists predominantly of nonmarine strata that filled the basin following the development of the early Pennsylvanian unconformity (Korus, 2002). The Upper Pennsylvanian Glenshaw Formation (lower Conemaugh Group) in northeastern West Virginia and western Maryland also consists predominantly of continental siliciclastic units (Belt and Lyons, 1989). Both of the study intervals contain quartz and lithic arenites as well as carbonaceous rocks, all of which are ideal for paleothermometric and thermochronologic studies (Fig. 1.2).

METHODS

Data were collected from core-sampled sandstones and organic-rich strata from four different locations and two stratigraphic intervals within the central Appalachian basin (Figs. 1.1 and 1.2). Selection of sample locations was based on an important structural feature in the

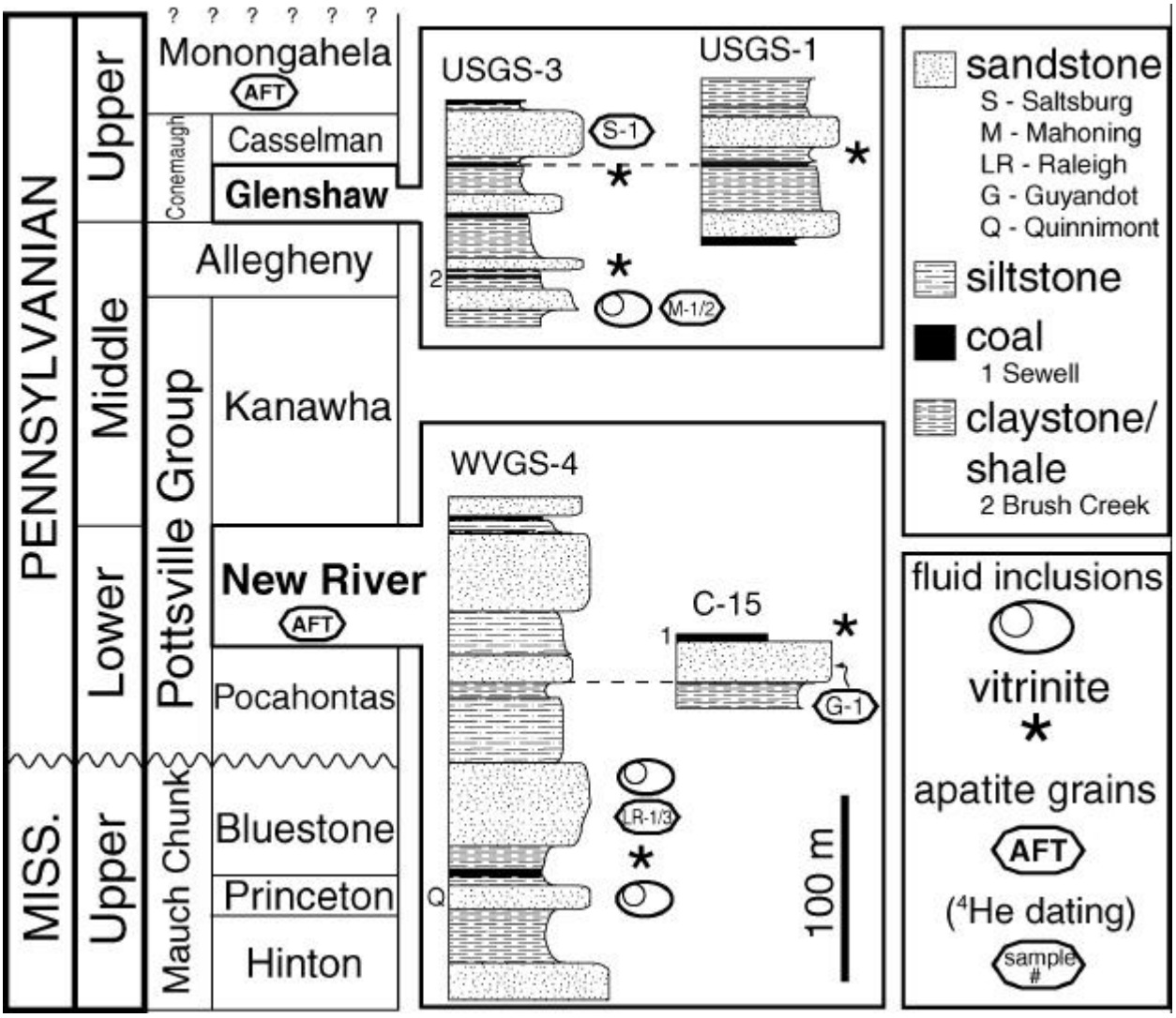

Figure 1.2 Stratigraphy of Upper Mississippian and Pennsylvanian strata. Study intervals are represented on lithostratigraphic columns based on borehole cores. Selected sandstones and organic-rich intervals are labeled.

region. Samples were collected 1) adjacent to the Allegheny structural front, which divides sub-horizontal strata of the Appalachian Plateau from folded Paleozoic sedimentary rocks of the Valley and Ridge. Two additional locations were selected well within the Appalachian Plateau (Fig. 1.1) to evaluate potential differences in the burial and exhumation histories between these sites. Core samples were targeted to ensure that weathering had not significantly altered quartz overgrowths and apatite grains. Quartz-rich intervals were sampled to maximize the probability of finding primary fluid inclusions within quartz overgrowths, while lithic-rich sandstones were selected for potentially high apatite yield (Fig. 1.2). Lower Pennsylvanian samples were recovered from 300 and 640 meters above sea level (300 and 40 meters below the surface, respectively) in the Appalachian Plateau of south-central West Virginia. Upper Pennsylvanian samples are from 460 and 370 meters above sea level (180 and 270 meters below the surface, respectively) in northeastern West Virginia (Fig. 1.1).

Paleothermometric data were collected using standard techniques. Vitrinite was extracted from shale and coal, mounted in epoxy and polished. Reflectance measurements were made using a McCrone MPA1 photometer. Mean maximum reflectance values were recorded and calibrated using glass standards. Vitrinite reflectance temperature estimates were determined using the thermal model SIMPLE-R_o (Suzuki et al., 1993). A heating rate of ~2 °C/m.y. was used for thermal reconstructions and was estimated based on sedimentation rates and an average geothermal gradient for the region (Hulver, 1997). Homogenization temperatures (T_hs) of primary fluid inclusions found within quartz overgrowths were measured with a Linkam THMSG 600 heating and cooling stage following techniques outlined by Goldstein and Reynolds (1994). We assume that T_h is approximately equal to the trapping temperature for reasons outlined in Reed et al. (in review).

Apatite grains used for (U-Th)/He dating were hand selected from crushed sandstone (~14 grains per sample). Radiogenic helium was outgassed at 920 °C and measured by ^{3}He spike using a quadrupole mass spectrometer at Virginia Tech. Line calibration was verified using Durango fluorapatite. Uranium and thorium concentrations of dissolved apatite grains were measured using ICP-MS. Procedures for age determination followed Wolf et al. (1996), Farley (2000), and Spotila et al. (in review). Published AFT ages are limited for the central Appalachian basin, although a few ages are available for samples from comparable locations and stratigraphic intervals selected for this study (Figs. 1.1 and 1.2; Blackmer et al., 1994; Roden et al., 1992).

RESULTS

Fluid inclusion homogenization and vitrinite reflectance temperatures are comparable (see Table 1.1). Therefore, we conclude that these methods serve as reasonable proxies for deep burial conditions. Homogenization temperatures for lower Pennsylvanian samples range from 143 to 163 °C (mean = 150 °C) and reflectance values range from 139 to 147 °C (mean = 143 °C). Vitrinite reflectance values cited here are consistent with values from other sources collected from comparable stratigraphic intervals in the central Appalachian basin (Hower, 1978; Pennsylvania State University Coal Database; West Virginia Geological and Economic Survey, unpublished data). In addition, conodont alteration indices (CAI) for Upper Mississippian strata in southern West Virginia range from 2 to 2.5 (Epstein et al. 1977) and are consistent with our vitrinite reflectance results. High T_h (>215 °C) are recorded in upper Pennsylvanian samples. These values are interpreted to record a high temperature fluid flow event(s) related to the injection of metamorphic fluids during active Alleghanian thrusting (Reed et al., in review) and

	Method	Paleotemp.[1]	Age (Ma)[2]	sample interval	source
Burial			***Upper Pennsylvanian, Allegheny Front***		
	R_o	132 °C	263 ± 3	unamed shale	this study
	R_o	143 °C	263 ± 3	unamed shale	this study
	R_o	171 °C	263 ± 3	Brush Creek Sh.	this study
			Lower Pennsylvanian, Appalachian Plateau		
	R_o	147 °C	274 ± 4	Sewell coal	this study
	R_o	144 °C	274 ± 4	unamed shale	this study
	R_o	141 °C	274 ± 4	unamed shale	this study
	R_o	139 °C	274 ± 4	unamed shale	this study
	F.I.	148 °C	274 ± 4	Upper Raleigh Ss.	this study
	F.I.	145 °C	274 ± 4	Upper Raleigh Ss.	this study
	F.I.	163 °C	274 ± 4	Upper Raleigh Ss.	this study
	F.I.	143.5 °C	274 ± 4	Quinnimont Ss.	this study
Exhumation			***Upper Pennsylvanian, Allegheny Front***		
	^4He	~60 °C	105 ± 11	Saltsburg Ss. (S-1)	this study
	^4He	~60 °C	170 ± 17	Mahoning Ss. (M-1)	this study
	^4He	~60 °C	69.6 ± 7	Mahoning Ss. (M-2)	this study
	AFT	100 ± 20 °C	142 ± 12	Monongahela Fm.	Blackmer *et al.* 1994
			Lower Pennsylvanian, Appalachian Plateau		
	^4He	~60 °C	72.7 ± 7	Guyandot Ss. (G-1)	this study
	^4He	~60 °C	98.6 ± 10	Lower Raleigh Ss. (LR-1)	this study
	^4He	~ 60 °C	93.9 ± 9	Lower Raleigh Ss. (LR-3)	this study
	AFT	100 ± 20 °C	138[(3)]	New River Fm.	Roden *et al.* 1992

Table 1.1 Summary of paleothermometric and thermochronologic results: vitrinite reflectance (R_o), fluid inclusions (F.I.), apatite fission track (AFT), and radiogenic helium (^{4}He).
[1] values reported for vitrinite reflectance and fluid inclusions are paleotemperatures, whereas those reported for and AFT and (U-Th)/He dating are based on annealing and closure temperatures for apatite.
[2] age reported for vitrinite reflectance and fluid inclusions marks time of maximum burial (see text). Age was constrained by rates calculated using estimated subsidence, paleothermometers and burial estimates of Blackmer et al. (1994).
[3] no standard deviation reported.

are not used in basin reconstruction. However, vitrinite reflectance values reported for the Glenshaw Formation appear to be good burial proxies, because resulting temperatures suggest that the rocks were not greatly affected by the high temperature fluid event cited above.

Published AFT ages from detrital apatites in the New River Formation and Monongahela Group are 138 Ma (standard deviation not cited) and 142 ± 12 Ma, respectively. (U-Th)/He ages are from cores USGS-3, WVGS-4 and C-15 (Table 1). Two New River Formation sandstones yield ages of 72.7 ± 7 Ma (Guyandot), 98.6 ± 10 Ma (Raleigh) and 93.9 ± 9 Ma (Raleigh, duplicate age), whereas ages from Glenshaw Formation sandstones are 105 ± 11 Ma (Saltsburg), 170 ± 17 Ma (Mahoning) and 69.6 ± 7 Ma (Mahoning, duplicate age). The older age from the Mahoning was excluded from the calculations because it is counterintuitive that the age is much older than the Saltsburg (105 ± 11 Ma) and may represent the presence of U-rich inclusions in the analyzed apatite grains, which are common but difficult to identify in detrital samples.

Well-constrained geothermal gradients are necessary to accurately estimate burial depths using paleothermometric and thermochronologic data. The average present day geothermal gradient for the study area is ~20 °C/km (Blackwell et al., 1989; Hulver, 1997). Assuming the geothermal gradient in the Appalachian foreland basin was 50% higher at the time of sedimentation than today (Vitorello and Pollack, 1980; Chyi et al., 1987), then a paleogeothermal gradient of ~30 °C/km can be assumed for the late Paleozoic. This estimate is consistent with thermal model results (31 to ~33 °C/km) based on vitrinite reflectance and heat flow parameters compiled by Zhang and Davis (1993) for the Appalachian Plateau near the Allegheny structural front. In addition, Hulver (1997) calculated the paleogeothermal gradient for the Permian to be ~36 °C/km for the study area using various thermal indicators including vitrinite reflectance, conodont color alteration indices and AFT. Thus a present day value of 20

°C/km and paleogeothermal gradient of 35 °C/km were used to calculate burial depths. The inferred paleogeothermal gradient is consistent with values cited for Cenozoic foreland basins (e.g., Bachu et al., 1995; Law et al., 1998; O'Sullivan, 1999; Appendix H). Geothermal gradients corresponding to the estimated time of maximum burial, AFT and (U-Th)/He ages (i.e., instantaneous values) have been interpolated using an exponential decay function (assuming conductive heat loss) fit to the past and present geothermal gradients cited above (Fig. 1.3; Appendix E). Resulting maximum burial depths for the central Appalachian basin of ~4.4 km are comparable to load thicknesses associated with the Alleghanian orogeny predicted by geodynamic models of Beaumont et al. (1987).

Burial rates were constrained using two complementary methods. Subsidence rates were calculated based on average stratigraphic thicknesses in the study area and chronostratigraphic markers for upper Mississippian, lower Pennsylvanian and upper Pennsylvanian strata (Fig. 1.4). Age estimations of the New River (ca. 316 Ma) and Glenshaw (ca. 306 Ma) formations are based on megafloral zones (Blake, 1997), chrono- and lithostratigraphic correlations in the central Appalachian basin (Gillespie and Pfefferkorn, 1979), and the timing of the Wanganui paleomagnetic reversal (Opdyke et al., 2000). All stratigraphic thicknesses reported here are decompacted based on ratios established for nonmarine deposits of sandstone, shale/siltstone and coal (Nadon and Issler, 1997; Nadon, 1998; Appendix F). Miller and Eriksson (2000) estimated that the 750 meter-thick upper Mississippian Mauch Chunk Formation was deposited in approximately 7 Myr whereas the ~350 meter thick New River Formation spanned approximately 3 Myr (Chesnut, 1994; Korus and Eriksson, submitted). Upper Pennsylvanian rates have been constrained using sedimentary cycles. Up to twelve paleosol-bounded cycles have been identified within a 160 m

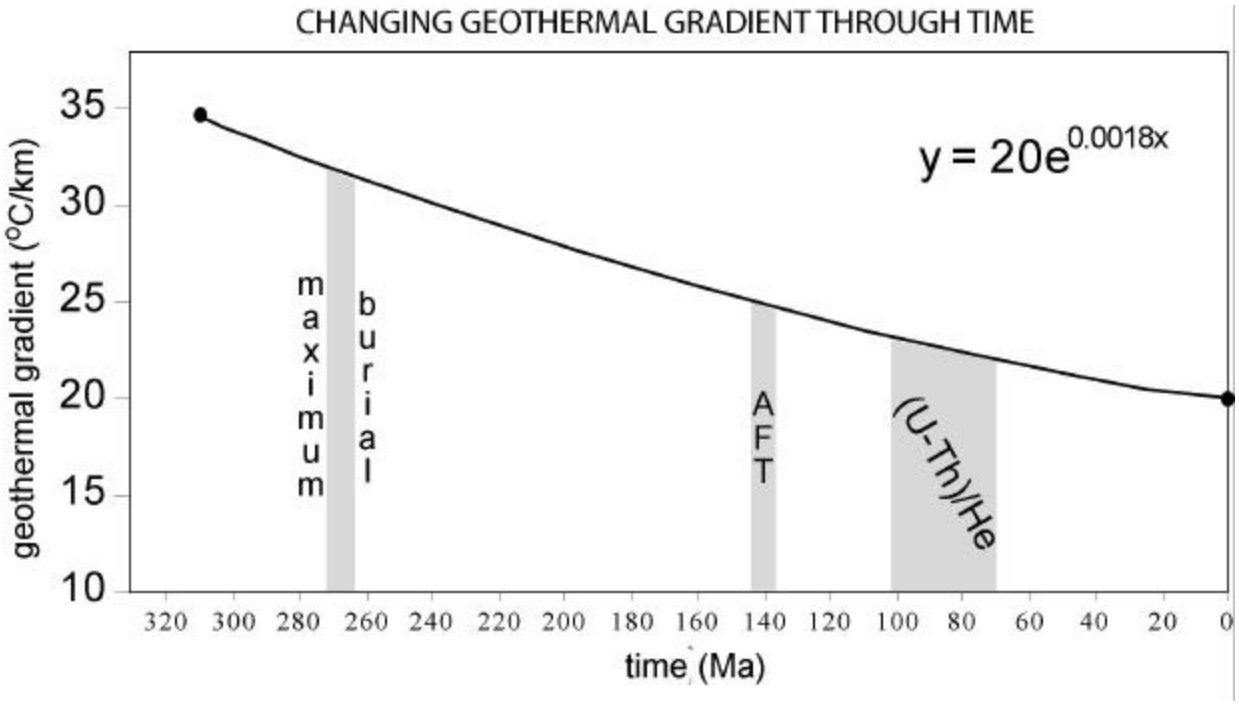

Figure 1.3 Exponential heat loss curve for the central Appalachian basin. Paleogeothermal gradients are interpolated for times corresponding to paleothermometric and thermochrologic results.

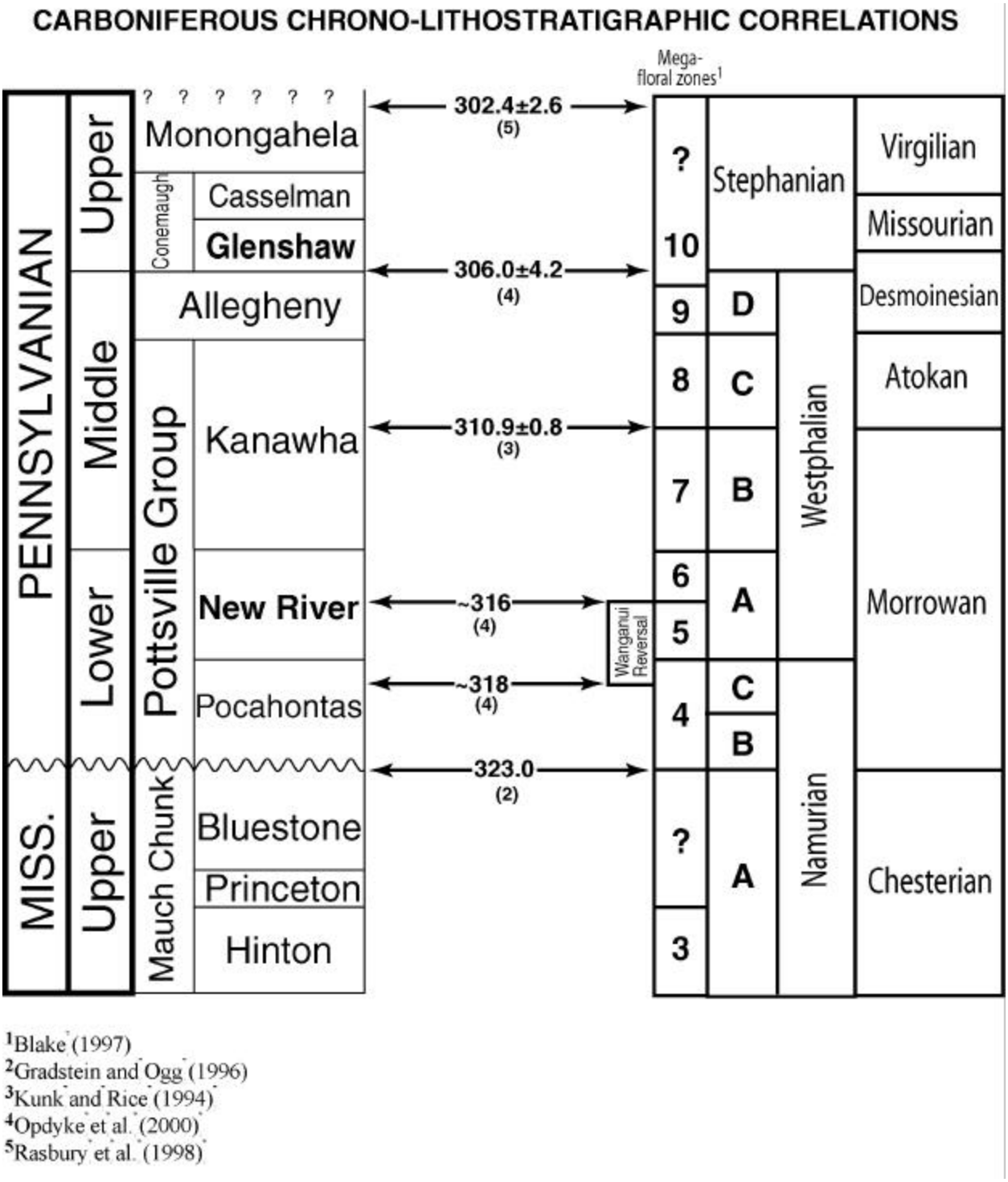

Figure 1.4 Estimated Carboniferous chrono-lithostratigraphic correlations for the central Appalachian basin. Values pertinent to this study are reported.

section of the Glenshaw Formation (Martino and Belt, 2001). Upper Pennsylvanian cycle duration of 143 ± 64 k.y. (~100 k.y. Milankovitch cyclicity) has been constrained using U-Pb dating of paleosols in the western United States (Rasbury et al., 1998). Based on the above thicknesses and age constraints, the average subsidence rate is estimated at 102-116 m/m.y. for all three Carboniferous intervals. In addition, Blackmer et al. (1994) used vitrinite reflectance (Levine and Davis, 1989) and the timing of remagnetization of Paleozoic rocks in the Appalachian basin (Miller and Kent, 1988) to estimate that it took approximately 40 Myr for maximum burial to occur in the central Appalachian basin. Therefore, based on subsidence and thermal calculations as well as the estimate from the timing of remagnetization, maximum burial for the New River and Glenshaw formations occurred at approximately 274 ± 4 and 263 ± 3 Ma, respectively. Using the estimated geothermal gradient cited above, vitrinite reflectance and fluid inclusion homogenization temperatures (Table 1.1) provide an independent means of constraining maximum burial depth and thereby subsidence rates. If maximum temperatures (~150 °C) correlate with maximum or near maximum depths (~4.4 km), then subsidence averaged 99 and 103 m/m.y. for the Lower and Upper Pennsylvanian, respectively (Fig. 1.5). Therefore rates calculated based on stratigraphic thicknesses and paleothermometry are comparable.

Exhumation rates were calculated using the estimated timing of maximum burial, AFT and (U-Th)/He ages (Fig. 1.5). (U-Th)/He ages within the New River (88 Ma) and Glenshaw (87 Ma) formations were averaged because our goal was to evaluate the overall behavior of the Upper and Lower Pennsylvanian intervals. Burial depths corresponding to AFT and (U-Th)/He ages were constrained using an annealing temperature of 100 ± 20 °C and closure temperature (T_c) of 60 °C, the interpolated paleogeothermal gradients cited above, an average surface

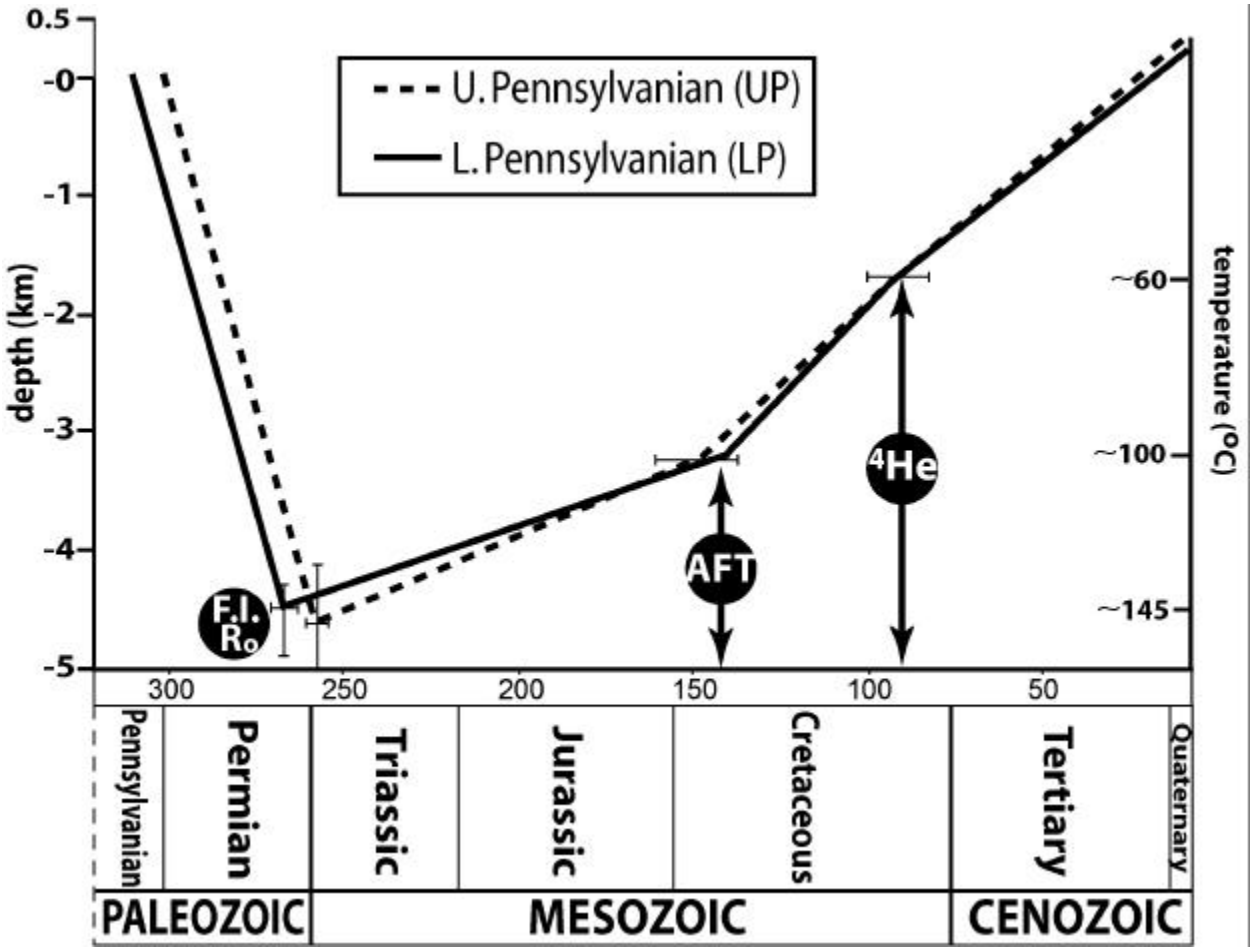

Figure 1.5 Summary of the burial and exhumation history of the central Appalachian basin inferred in this study. Reported rates are defined by mean paleothermometric and thermochronologic constraints. Error bars correspond to measured values reported in Table 1.1.

temperature of 15 °C and average present day formation temperature of ~19 °C (from present day depth and geotherm; Appendix G). The annealing temperature is based on previous AFT studies in the Appalachian Plateau (e.g., Roden and Miller, 1989) and T_c is a function of apatite grain size (Table 1.2; Farley, 2000).

Inferred exhumation histories of New River and Glenshaw formations are very similar and are based on calculations and assumptions discussed above (Fig. 1.5). The first phase of exhumation from ~4.4 to ~3.1 km burial depth, as constrained by AFT, was ~10 m/m.y. The second phase of exhumation from ~3.1 to ~1.7 km, as constrained by (U-Th)/He ages was ~30 m/m.y. whereas the final phase from ~1.7 km below the surface to 0.4 km above sea level (s.l.) occurred at approximately the same rate as the second phase.

The results of this study supplement existing knowledge concerning post-Alleghanian evolution of the central Appalachians (e.g., Poag and Sevon, 1989; Roden and Miller, 1989; Slingerland and Furlong, 1989; Pazzaglia and Gardner, 1994; Pazzaglia and Brandon, 1996) and are comparable to AFT studies involving upper Paleozoic strata in areas to the north and south of our sample locations. Mesozoic and Cenozoic exhumation rates for the Appalachian Plateau in central Pennsylvania range from ~10-15 m/m.y. (Blackmer et al., 1994) whereas average rates from the mid-Mesozoic to present for eastern Kentucky are ~29 m/m.y. (Boettcher and Milliken, 1994). Our study location and average exhumation rates for the equivalent time interval fall between the locations and results cited above.

DISCUSSION

Paleothermometric and thermochronologic results constrain the long-term burial and exhumation history of the Appalachian Plateau (Fig. 1.5). Paleothermometers are consistent and

	sample size(mg)	ave. grain radius (μm)	[He] pmols	[U] ppm	[Th] ppm	alpha corr.*	corrected age (Ma)
S-1	0.009	36	0.1065	20.5	60.8	0.64	See Table 1.1
M-1	0.008	32	0.1495	27.4	28.9	0.61	
M-2 (duplicate)	0.005	37	0.0272	15.3	27.5	0.65	
G-1	0.011	37	0.0936	16.2	72.4	0.65	
LR-1	0.014	35	0.1509	26.2	26.9	0.64	
LR-3 (duplicate)	0.013	36	0.0929	16.2	29.8	0.63	

Table 1.2 Summary of (U-Th)/He results. Sample labels correspond to those highlighted in Fig. 1.2. *according to Farley et al. (1996).

yield reasonable values of maximum burial depth and average rates of subsidence. In addition, burial indicators correlate well with apatite fission track results to constrain earliest exhumation. Thermochronometers appear to correlate well and provide reasonable rates of exhumation, although little is known about the relationship between AFT and (U-Th)/He dating techniques. The validity of combining these methods for basin studies would benefit from additional research.

Our results imply that the long-term burial history of the Carboniferous strata in the central Appalachian foreland baisn was remarkably uniform. No major differences in subsidence rates exist between samples collected near the Allegheny Front and those collected >60 km to the west of the front within the Appalachian Plateau. Only minor differences exist between the burial histories of Upper and Lower Pennsylvanian strata. Vitrinite reflectance indicates that Upper Pennsylvanian samples were buried deeper than Lower Pennsylvanian samples, although they are stratigraphically separated, by more than 500 meters. This paradox can be explained with respect to the location of the Upper Pennsylvanian samples which are closer to the depocenter (deeper portion) of the foreland basin than Lower Pennsylvanian samples.

The exhumation histories of the New River Formation of southern West Virginia and Glenshaw Formation of northern West Virginia are comparable and similarities of exhumation rates between regions, stratigraphic intervals and other studies are striking. If the difference between early and late exhumation rates is significant, tectonic, thermal and isostatic driving forces warrant consideration. The initial slow (~10-15 m/m.y.) exhumation phase of the Appalachian Plateau can be interpreted in two ways. The value could reflect isostatic rebound following thrust cessation and/or footwall uplift during Triassic rifting (e.g., Barr, 1987). Alternatively, the rate could be influenced by averaging late-stage burial with early exhumation,

because our calculations assume that exhumation occurred immediately following maximum burial. The second phase of exhumation defined by AFT and (U-Th)/He (~25-30 m/m.y.) is relatively high and reflects rapid denudation from the mid-Cretaceous onwards. Since major climatic changes are not recognized during this time, other possible explanations must be sought. Pazzaglia and Brandon (1996) have suggested magmatic activity deep in the crust drove uplift during the Cretaceous, perhaps related to migration of the Atlantic margin over hotspots (de Boer et al., 1988). The last phase of exhumation defined by (U-Th)/He ages and the present day depth (~20-25 m/m.y.) was probably driven, in part, by lithospheric flexure induced by increased sediment loading of the Atlantic passive margin during the late Cenozoic (Poag and Sevon, 1989; Pazzaglia and Gardner, 1994; Pazzaglia and Brandon, 1996).

CHAPTER 2: CONTROLS ON CARBONIFEROUS SANDSTONE DIAGENESIS, CENTRAL APPALACHIAN BASIN: A QUALITATIVE AND QUANTITATIVE ASSESSMENT

ABSTRACT

Carboniferous quartz, lithic and feldspar-rich sandstones from different stratigraphic intervals and locations within the central Appalachian Basin were sampled from core (95 %) and outcrop (5%) to evaluate sandstone diagenesis. A paragenesis was developed using petrographic, thermal and geochemical considerations including mineral chemistry and stable isotopes. Important eogenetic components include Fe-oxide/oxyhydroxide, siderite, kaolinite, chlorite and calcite whereas quartz, albite, illite, Fe-carbonate, and secondary porosity are the most important mesogenetic components.

A compositional multivariate data set compiled from point counts served as the basis for quantitative exploration of controls on sandstone diagenesis. Potential controls include framework grain composition, paleoclimate and depositional environment. *A priori groups* (independent variables) corresponding to the controls were compared using diagenetic products (dependent variables). The data set was reduced using Correspondence Analysis and Detrended Correspondence Analysis and compiled on ordination plots. Major conclusions of the quantitative analyses are, first, minerals that formed early appear to have been influenced by stratigraphic position. The distribution of siderite and iron-oxide/oxyhydroxide may reflect the second order paleoclimatic signature recognized throughout the Carboniferous, where siderite formed during everwet periods and iron-oxide/oxyhydroxide during semi-arid conditions, reflecting differences in redox. Second, framework grain composition controlled the distribution of diagenetic alterations in the burial environment. Despite the widespread recognition of lithic

grains as an important source of silica for quartz cementation, lithic arenites are deficient in authigenic quartz, yet have undergone various degrees of illitization. The quartz deficiency is attributed to compaction-related loss of primary porosity relatively early, that inhibited sufficient fluid flow to account for much higher concentrations of quartz cement in the more competent quartz arenites. Finally, no correlation can be demonstrated between depositional environment and diagenesis.

Keywords: diagenesis, sandstone, central Appalachian basin, multivariate statistics

INTRODUCTION

Sandstone diagenesis is a dynamic process that is influenced by factors inherent to the sediment source, depositional system and burial environment (e.g., Burley et al., 1985; Morad et al. 2000). The relationship between diagenesis and reservoir quality is well documented and much of our knowledge about sandstone diagenesis has benefited from studies involving reservoir property evaluation and quality prediction (e.g., Wilson, 1994; Primmer et al., 1997; Jeans, 2000). Therefore, reservoir quality assessment can benefit from a refined understanding of potential controls on diagenesis including framework grain composition/provenance (e.g., De Ros et al., 1994; Bloch, 1994; de Souza et al., 1995; Nentwich and Yole, 1997; Ramm, 2000), paleoclimate (e.g., Worden et al., 2000), and depositional environment (e.g., Fuchtbauer, 1983; Lowry and Jacobsen, 1993; Bloch and McGowen, 1994; McKay et al., 1995; Hamlin et al., 1996; Bailey et al., 1998; dos Anjos et al., 2000; Hiatt and Kyser, 2000; Rossi et al., 2001). The purpose of this study is to evaluate potential factors that have influenced Carboniferous sandstone diagenesis in the central Appalachian foreland basin (Fig. 2.1). In particular, goals of this project are to: 1) qualitatively assess sandstone diagenesis including their paragenesis, 2)

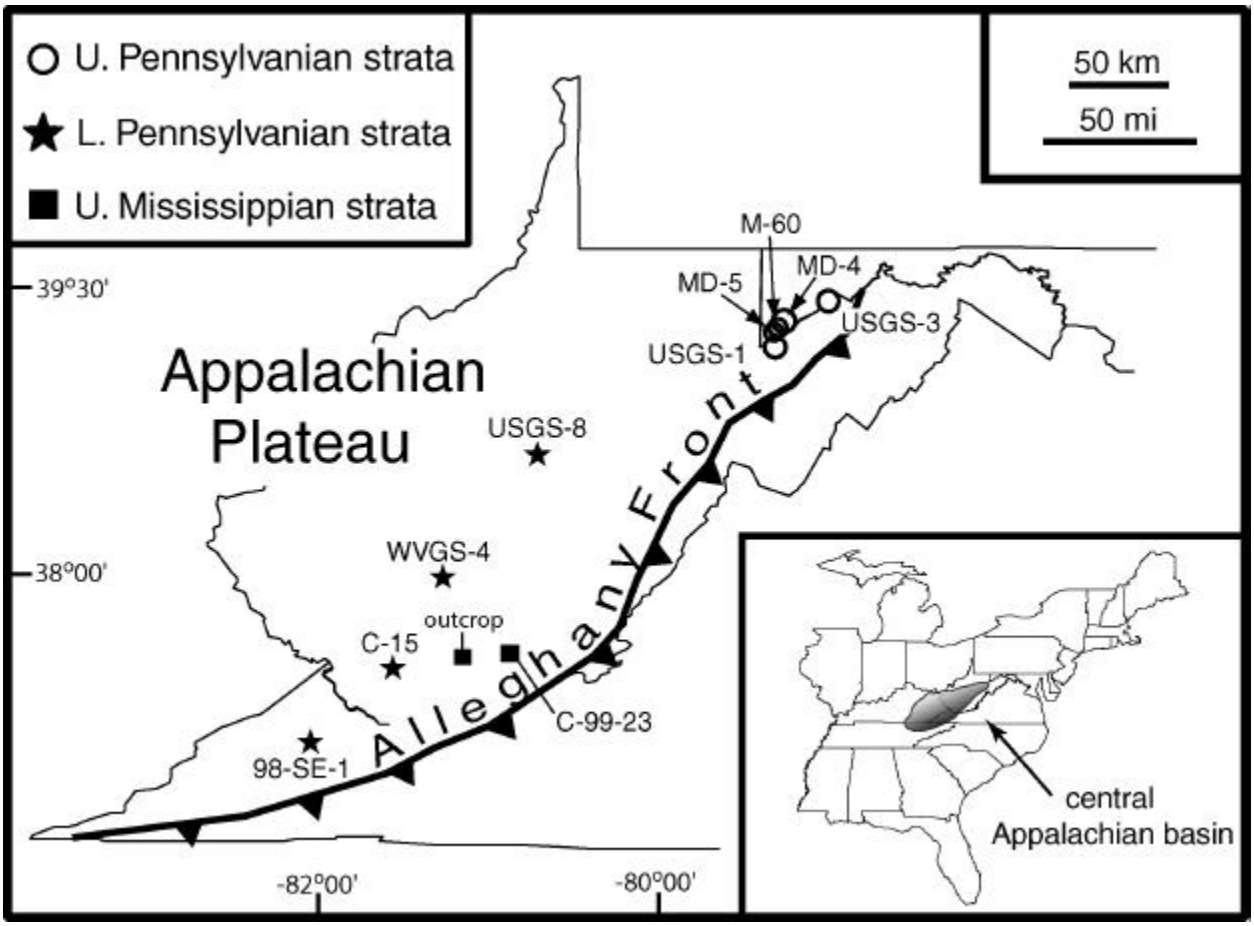

Figure 2.1 Core locations and structural setting map. All samples were collected within the Appalachian Plateau. Approximately 45% of the Mississippian samples were collected from outcrops in southern West Virginia.

supplement our current understanding of Carboniferous sandstone diagenesis in the central Appalachian basin, 3) demonstrate the value of multivariate statistics for resolving petrologic trends, and 4) quantitatively evaluate potential controls on sandstone diagenesis.

Carboniferous sandstones of the central Appalachian basin provide and ideal opportunity to evaluate controls on diagenesis because: 1) quartzose, lithic, and feldspathic sandstones are present, 2) paleoclimate varied from semi-arid to everwet (Cecil et al., 1985; Donaldson et al., 1985; Cecil, 1990), and 3) sequence stratigraphic studies within the Carboniferous of the central Appalachian basin have revealed that the sandstone bodies studied contain "fluvial-" and "marine-" influenced intervals that are characteristic of incised valley fill deposits (IVFs; Aitken and Flint, 1995; Greb and Chesnut, 1996; Miller and Eriksson, 2000; Martino and Belt, 2001; Korus and Eriksson, in review).

GEOLOGIC SETTING

The Appalachian foreland basin formed in response to three episodes of continental collision (Quinlan and Beaumont, 1984). Basin subsidence dynamics varied during each of the three major Paleozoic collisional events and the basin was wide and shallow during Alleghanian orogenesis (Tankard, 1986; Klein and Willard, 1989; Willard and Klein, 1990). This event produced highlands that served as an important source of sediment in the late Paleozoic. Basin geometry was primarily controlled by the long-term rheological response of the lithosphere to loading and a general thickening of the crust (Dickinson, 1974; Allen et al., 1986, 1991; Klein, 1991; Sinclair, 1997; Castle, 2001), although, short-term responses to loading have also been recognized (Tankard, 1986).

Upper Mississippian and Pennsylvanian basin fill is primarily composed of siliciclastic sedimentary rocks including sandstone, mudstone, conglomerate (rare), coal seams and subordinate limestone. Various stratigraphic markers subdivide the late Phanerozoic stratigraphic record. The Upper Mississippian Mauch Chunk Group is bound by the Stony Gap sandstone (base) and marine Bramwell Member (top), which marks the top of the Mississippian system in the central Appalachian basin (Miller and Eriksson, 2000). Coals and unconformities have been especially useful for regional correlations of Pennsylvanian strata in the central Appalachian basin (Fig. 2.2). The Lower Pennsylvanian New River Formation in southern West Virginia consists predominantly of nonmarine strata that filled the basin following the development of the early Pennsylvanian unconformity (Korus and Eriksson, in review). The Upper Pennsylvanian Glenshaw Formation (lower Conemaugh Group) in northeastern West Virginia and western Maryland also consists predominantly of siliciclastic units and subordinate carbonate rocks (caliche and minor marine units; Belt and Lyons, 1989). Both of the study intervals contain quartzose sandstones and carbonaceous rocks that are ideal for paleothermometric studies. More detailed discussion of the general tectonic and stratigraphic setting of the central Appalachian basin can be found in Milici and de Witt (1988).

Carboniferous sandstones in the central Appalachian basin vary in composition between quartzose and lithic with variable amounts of feldspar. In general, lower Pennsylvanian sandstones are quartzose whereas those from the upper Pennsylvanian are more lithic (Houseknecht, 1980; Donaldson et al., 1985; McDowell, 1986). However, lithic sandstones are locally developed in the lower Pennsylvanian of West Virginia whereas in southwestern Virginia correlative sandstones contain significant concentrations of feldspar (Davis and Ehrlich, 1974). Metamorphic rock fragments dominate the lithic fraction. Most workers relate the sandstone

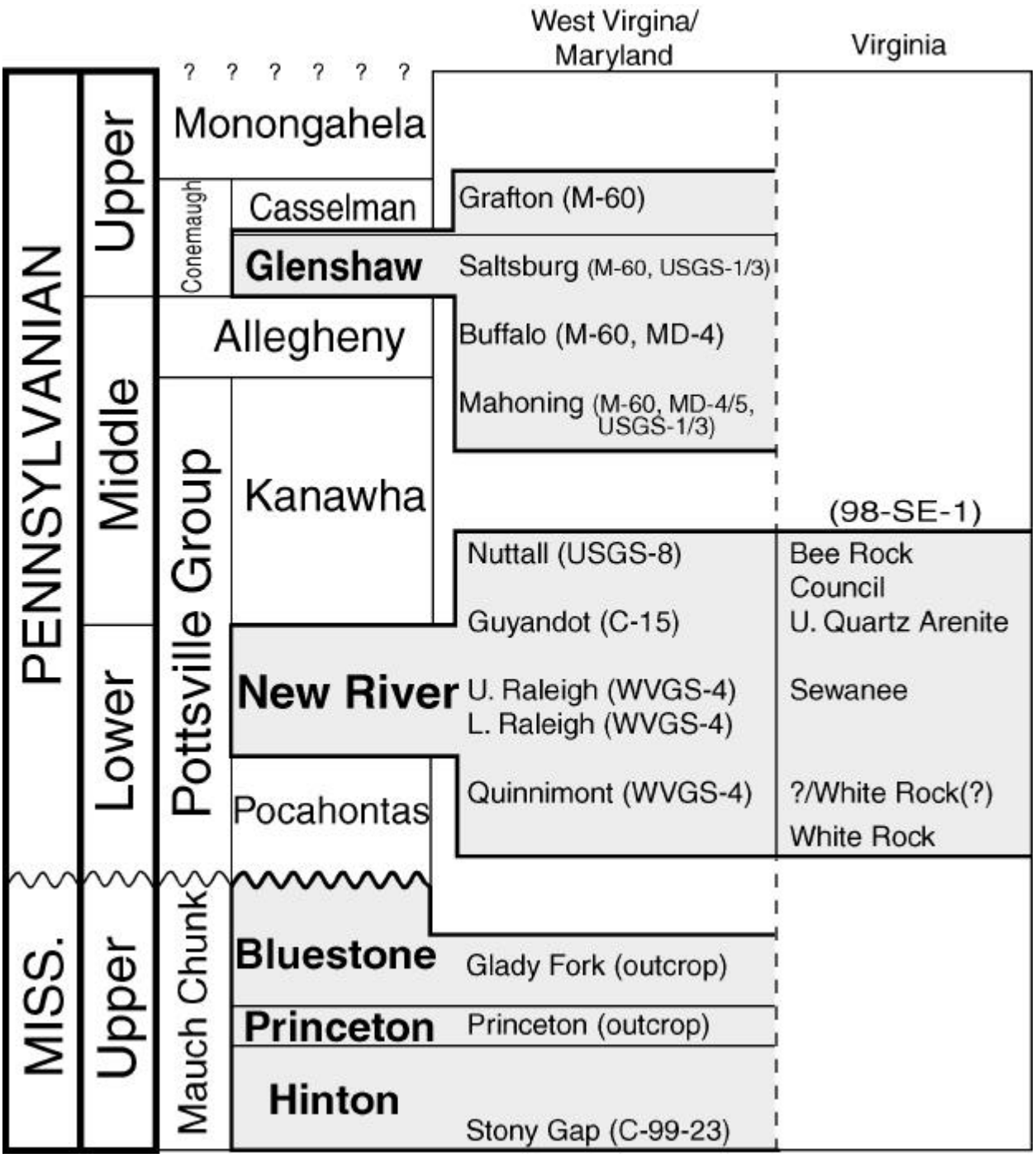

Figure 2.2 Generalized stratigraphy for the Carboniferous in the central Appalachian basin. Sandstones selected for this study are shown in relative stratigraphic order. Approximate correlations between sandstones of the New River Formation Virginia and West Virginia were constrained by coals. Well locations shown in Figure 1.1 are listed after corresponding sandstones (also see Appendix C).

compositions to recycling of Appalachian orogenic provenances (Houseknecht, 1980; Dickinson et al., 1983; Donaldson et al., 1985; McDowell, 1986), although cratonal sources have been inferred for correlative quartzose sandstones in Pennsylvania (Robinson and Prave, 1995). The higher concentration of feldspar in the southern part of our study area (southwestern Virginia) is attributed to dissection of the orogen down to a plutonic source (Davis and Ehrlich, 1974).

A second-order paleoclimatic curve has been proposed for the Carboniferous of the Appalachian basin on the basis of variations in geochemical signals recorded by lithology and coal swamp morphology (Cecil et al., 1985; Donaldson et al., 1985). Upper Mississippian and Upper Pennsylvanian strata contain abundant red beds that are considered to reflect "semi-arid/seasonal" paleoclimates. Late Pennsylvanian planar peat deposits were attributed to semi-arid conditions in which evaporation periodically exceeded rainfall. Lower Pennsylvanian intervals lack oxidized iron pigmentation that is attributed to more reducing, "everwet" conditions and the early Pennsylvanian swamps consisted of domed peat deposits that developed in everwet paleoclimates (Cecil et al., 1985). Additional evidence supporting a change from everwet conditions in the Lower and Middle Pennsylvanian to semi-arid/seasonal conditions in the Upper Pennsylvanian includes changes in floral assemblages (Kosanke and Cecil, 1996) and enriched $\delta^{18}O$ signatures in late Pennsylvanian and early Permian paleosols that developed in equatorial Pangea and are interpreted to indicate evaporation associated with more arid conditions (Tabor and Montañez, 2002).

Major sandstone bodies in the Upper Mississippian Mauch Chunk Formation, Lower Pennsylvanian New River Formation and Upper Pennsylvanian Glenshaw Formation are interpreted as incised–valley fill (IVF) deposits (Belt and Lyons, 1989; Miller and Eriksson, 2000; Martino and Belt, 2001; Korus and Eriksson, in review). Sampling of IVF sandstones

provides the means to test the hypothesis that depositional environment, and specifically early pore fluid chemistry influenced diagenesis.

METHODS

Data Collection

Sampling was determined by the accessibility of core that intersected stratigraphic intervals targeted in this study. Ninety-five percent of the sample set was collected from core and the remaining 5% are from Mississippian outcrops in southern West Virginia (Fig. 2.1). Core locations within the Appalachian Plateau range from southwestern Virginia to western Maryland (Fig. 2.1). Core sampling was desirable to minimize the influence of surface weathering of the sandstones and maximize preservation potential of diagenetic features.

Petrographic data were collected using a Nikon polarizing light microscope and an adapted Leitz mechanical stage. Standard point counting procedures were executed according to the Glagolev-Chayes (Glagolev, 1933; Chayes, 1949) method (for summary see Galehouse, 1971). Translation intervals (mm) were determined using the mean grain size for each sample estimated using c-length axis measurements of 20 detrital grains per thin-section. Framework grain composition and diagenetic features (e.g., authigenic minerals and pore space) were identified from 400 counts per thin-section on 186 samples and recorded into a data matrix (Appendix A). Data matrix construction facilitated variable grouping that could be easily pooled and evaluated using multivariate statistical methods discussed below. Samples containing high concentrations of detrital feldspar and authigenic carbonate were stained with Na-cobaltinitrite (K-feldspar) and K-ferricyanide and alizarin red (carbonate) stains to confirm mineralogy. Qualitative analysis of textural relationships between petrologic characteristics such as

cementation, replacement minerals and porosity was important to understanding the paragenesis and was used in combination with quantitative results to more accurately constrain the diagenetic history of these sandstones.

Geochemical analyses including mineral chemistry and stable isotope measurements on selected carbonates and feldspars were conducted to resolve mineralogy and better constrain pore fluid compositions. Mineral chemistry was determined using the CAMECA SX-50/SUN 3/160 electron probe microanalyzer at Virginia Tech. Acceleration potential and sample current were set at 15.0 kV and 10.0 nA, respectively for carbonate analyses. These settings were chosen to minimize sample damage to the potentially volatile carbonate minerals. Standards used were hematite (Fe), pyrolusite (Mn), apatite (Ca; Durango) and olivine (Mg; Marjalahti). Feldspar beam conditions for point analyses were 15.0 kV and 20.0 nA and the standards used were Na-feldspar (Si, Na; Amelia), kyanite (Al), orthoclase (K; Benson), apatite (Ca; Durango), hematite (Fe). Point analyses directed by elemental maps constrained the composition of albite. Carbon and oxygen isotopic measurements on siderite and Fe-dolomite were collected at the University of Tennessee, Knoxville using mass spectrometry. Individual mineral phases were measured from bulk samples using time and temperature controlled CO_2 extractions, which is possible due to differing solubility rates of siderite and dolomite.

Data Reduction

Exploratory multivariate methods were employed on the multivariate petrographic data set to identify patterns that could be related to potential controls on sandstone diagenesis. *A priori* groups (independent variables), corresponding to the potential "controls" described above, were separated according to framework grain composition, stratigraphic position (paleoclimate) and depositional environment. The multivariate data set compiled using the petrographic point-

counting methods consists of twenty-six petrologic characteristics including framework grain composition and porosity as well as cementation and replacement minerals (dependent variables).

Recently, von Eynatten et al. (2003) used discriminate analysis to suggest that petrographic point-count methods may not be the best technique to discriminate between sandstones from separate populations based on unbiased sampling. Alternatively, we conclude that any differences that can be discerned using the petrographic data set compiled here are statistically more conservative than results derived from alternative methods (e.g., bulk geochemical techniques; von Eynatten et al., 2003) used to evaluate differences between *a priori* sandstone populations.

Simple correspondence analysis (CA) was used to reduce the compositional data matrix because standard exploratory multivariate techniques such as principal component analysis (PCA) are subject to the unit-sum constraint, i.e., point counts for each sample sum to 400 or percentages sum to 100 and are inter-dependent (Aitkinson, 1986; Rollinson, 1992; Reyment and Savazzi, 1999). In addition, CA is not restricted by the presence of zero values that can inhibit the application of log-ratio corrections needed for other techniques (see Greenacre, 1984; Reyment and Savazzi, 1999). CA was executed using Statistical Analysis System (SAS) version 8.02 using SAS/STAT procedure with codes written using SAS/IML language (SAS Institute, 2001; Appendix B).

Detrended correspondence analysis (DCA; Hill and Gauch, 1980) was also used to reduce the multivariate data set, and in particular, to minimize the arch effect, which can be introduced by CA. DCA counteracts the arch effect by segmenting the first ordination axis and rescaling the second axis around zero. In addition, Miller et al. (2001) have shown that plotting

axis 1 scores from DCA output is an effective way to combine variables into one axis to analyze stratigraphic trends recorded by paleontologic data. We propose that this is a valuable technique for analyzing any stratigraphically controlled attributes including petrologic patterns related to the proposed qualitative second-order paleoclimate curve. Detrended Correspondence Analysis was executed using PC-ORD 4.10 (McCune and Mefford, 1999). Ordination plots of CA and DCA results provide a simple means to evaluate any potential population groupings (i.e., resolving similarities) that could be associated with a given control. All plots are based on the first two axes, which contain the greatest amount of variation between the chosen variables.

RESULTS

Petrography

Petrographic analysis of Upper Mississippian, and Lower and Upper Pennsylvanian sandstones reveals diverse petrologic characteristics. The sample set contains quartz, lithic and feldspathic arenites (Fig. 2.3; classification according to Dott, 1964) as well as an array of diagenetic products. The following discussion highlights the sandstone petrology with respect to framework grains, replacement minerals, cements and porosity. Paragenesis and quantitative considerations and analyses are discussed in subsequent sections.

Framework Grains.--- Sandstones vary in composition and include quartz, lithic and feldspathic arenites (Fig. 2.3). Framework grain composition is dominated by mono- and polycrystalline quartz, metamorphic and sedimentary rock fragments, potassium feldspar and accessory minerals including muscovite, heavy minerals and chert. Most quartz grains are well rounded, display undulatory extinction under cross-polarized light, and contain abundant fluid

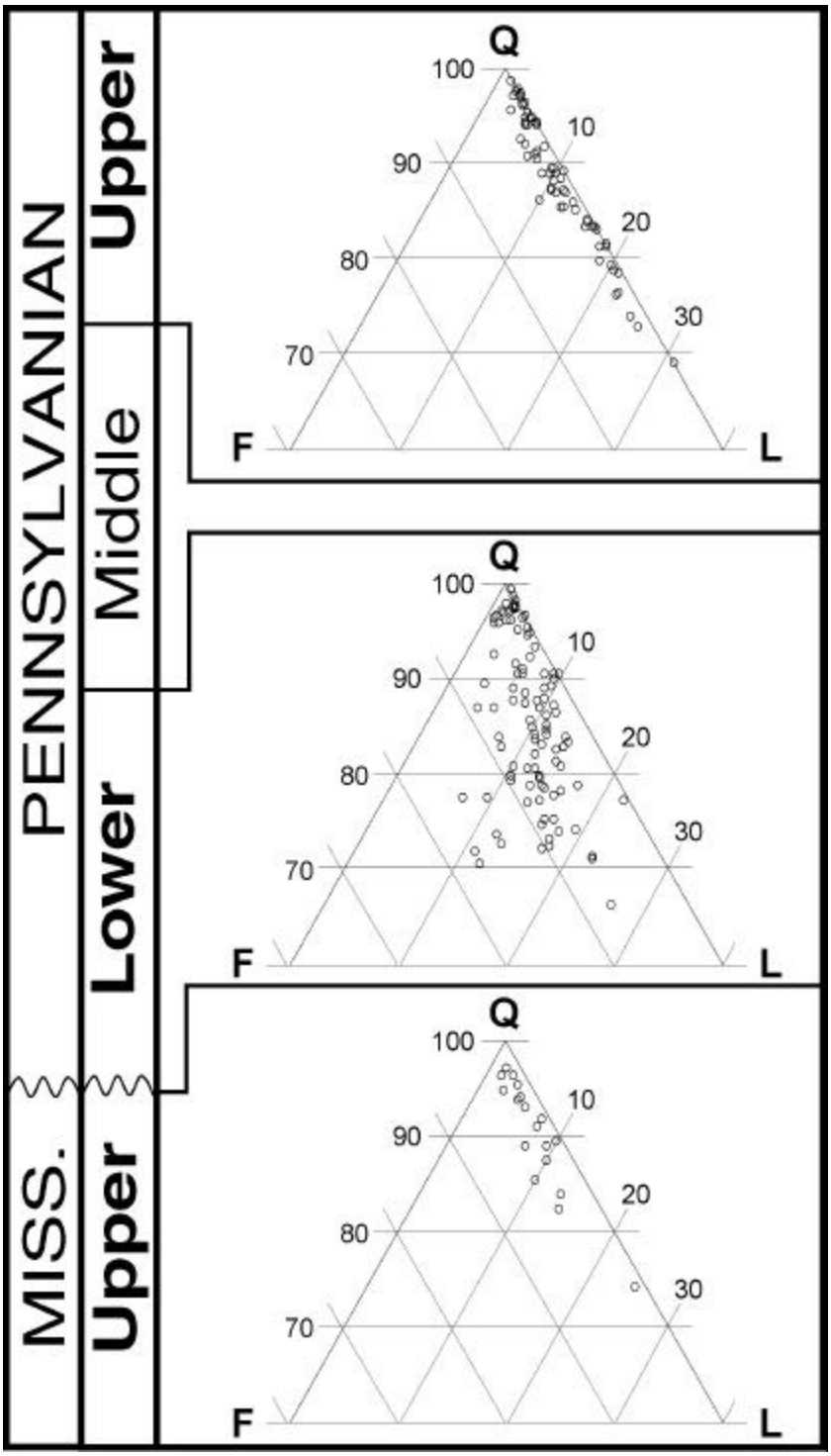

Figure 2.3 Proportions of quartz, feldspar and lithic framework grains illustrated in QFL diagrams for each study interval. Upper Pennsylvanian sandstones are generally lithic-rich, whereas Lower Pennsylvanian samples contain significant feldspathic and lithic components. Most Upper Mississippian samples are quartz-rich.

inclusions. The dominant lithic fragments are schistose. Quartz-mica schist grains are present throughout the study area, but are most abundant in sandstones from the northernmost (Upper Pennsylvanian samples) and southernmost (Lower Pennsylvanian samples, core 98-SE-1) portions of the study area. Minor amounts of sedimentary rock fragments (intraformational mudstone) are also present in Upper Pennsylvanian samples from northern West Virginia and western Maryland as well as in a few sandstones from southwestern Virginia. Potassium feldspar is easily identified by extensive sericitization (Fig. 4A) and is most abundant in samples from southwestern Virginia. Lesser amounts of detrital plagioclase feldspar and perthite are present in sandstones from southern West Virginia and southwestern Virginia. The most common accessory grain is muscovite. The highest concentrations of muscovite are generally present in the lithic-rich samples from Upper Pennsylvanian sandstones. Heavy minerals are rare and include apatite, zircon, tourmaline and ilmenite.

Replacement Minerals.--- Framework grain replacement is widespread and volumetrically significant in compositionally immature sandstones. Important replacement minerals include kaolinite, illite, calcite, dolomite and albite as well as minor amounts of Fe-oxide/oxyhydroxide (not differentiated) and chlorite. Fe-oxide/oxyhydroxide is associated with iron-bearing silicate, carbonate and sulfide mineral species and is most common in Upper Pennsylvanian sandstones. Authigenic kaolinite is present in some Upper and Lower Pennsylvanian sandstones. Host grains can be identified only in a few samples because kaolinitization is complete in most cases. Potassium feldspar and unstable, mica-bearing lithic, fragments are the most common identifiable precursors. Illite is the most abundant authigenic clay mineral and occurs extensively in lithic- and feldspar-rich sandstones. It completely replaces some framework

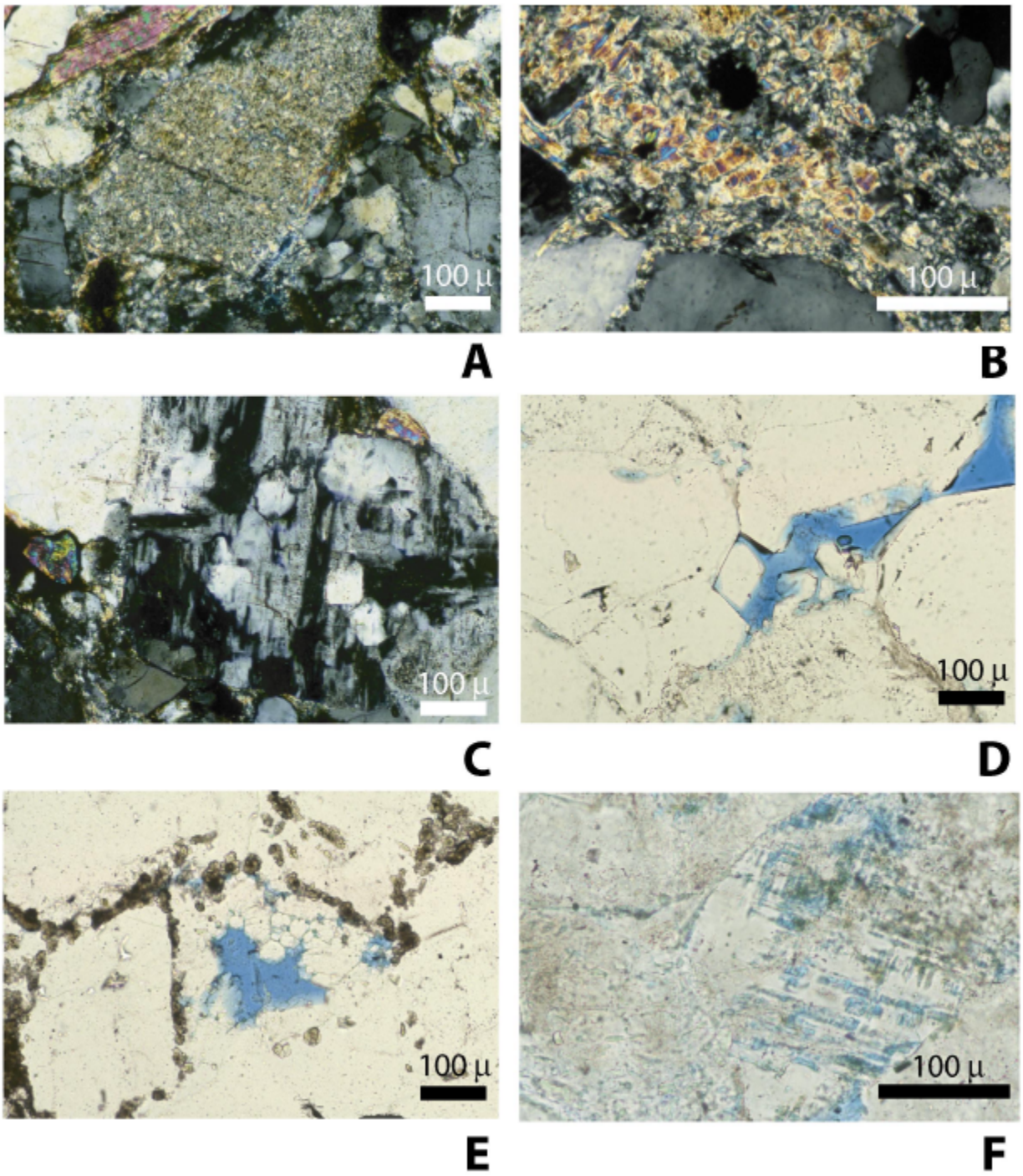

Figure 2.4 Photomicrographs of representative and volumetrically significant and other prominent petrologic features found within sandstones from this study: A. Illitized feldspar; B. Illitized kaolinite; C. Albitized domains and secondary porosity within K-feldspar; D. Syntaxial quartz overgrowths and prismatic quartz; E. Grain-rimming euhedral siderite and syntaxial quartz overgrowths; F. Secondary, intragranular porosity after K-feldspar.

grains including potassium feldspar (see Fig. 2.4A) as well as authigenic kaolinite (Fig. 2.4B), and is often associated with muscovite-bearing rock fragments. Chlorite is a minor constituent and is commonly associated with dust rims. Chlorite is also developed in association with other phyllosilicate-bearing components including schistose rock fragment as well as detrital biotite.

Calcite replacement is most extensive in feldspar-rich sandstones where it generally occurs as a partial replacement of potassium and plagioclase feldspar. Carbonate-rich (> 40% carbonate) intervals present at several stratigraphic levels in the New River Formation consist of Fe-dolomite of replacement origin. Electron probe microanalysis shows that this phase is ferruginous dolomite (Fig. 2.5) and confirms the petrographic identification of this distinctive mineral in other sandstones.

Albitization is common in feldspathic sandstones that occur only in southwestern Virginia. Albitized feldspar has a distinctive texture consisting of equant domains of untwinned albite surrounded by illitized K-feldspar. Petrographic observations were supplemented with electron microprobe analyses, which reveal that the albitized domains are pure albite (96-98% Ab) in coexistence with illitized K-feldspar (Fig. 2.6). The distribution and degree of albitization varies as illustrated in the grain maps in Figure 2.6. Elsewhere, equant albitized domains occur in K-feldspar hosts that have been partially dissolved (Fig. 2.4C). The presence of equant zones of albite within a feldspar host is easily distinguishable from linear intergrowths of K-feldspar and plagioclase that characterizes perthite. The anomalously low Ab/high potassium and calcium values for location 8 reported in Figure 2.6 indicates that the electron beam probably captured some host material and as well as calcite during the analysis.

Replacement fabrics observed in this study are common to sandstones throughout the Carboniferous of the central Appalachian basin. Fe-dolomite described by Milliken from a

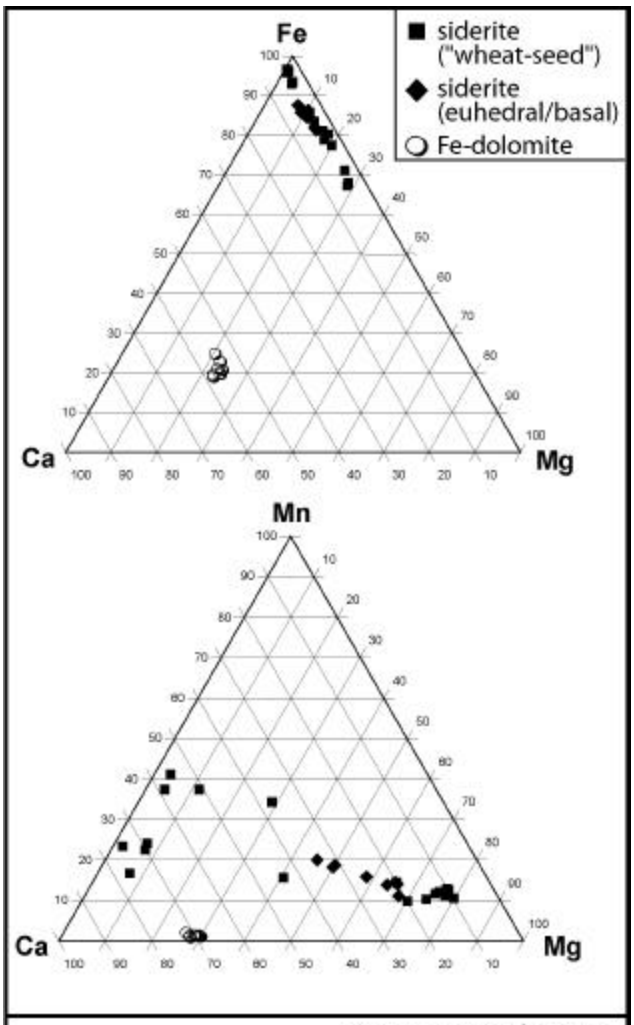

mineralogy		[mean values] Oxides (%)	Mole (%)	Molecular wt. %
Siderite ("wheat-seed")	Fe	54.03	84.4	87.2
	Ca	1.55	3.11	2.78
	Mn	1.48	2.33	2.39
	Mg	3.65	10.2	7.64
Siderite (euhedral/basal)	Fe	42.24	82.7	85.5
	Ca	1.77	4.44	3.97
	Mn	1.43	2.84	2.91
	Mg	2.89	10.1	7.58
Fe-dolomite	Fe	14.38	21.2	24.6
	Ca	29.20	55.2	55.2
	Mn	0.93	1.39	1.59
	Mg	8.41	22.1	18.6

Figure 2.5 Electron microprobe analyses of selected carbonate minerals from the New River Formation. "Wheat-seed" siderite was sampled from the middle of the Upper Raleigh sandstone and "euhedral" siderite came from the base of the same sandstone. Fe-dolomite is from the Lower Raleigh sandstone and predominantly occurs as a calcite replacement mineral.

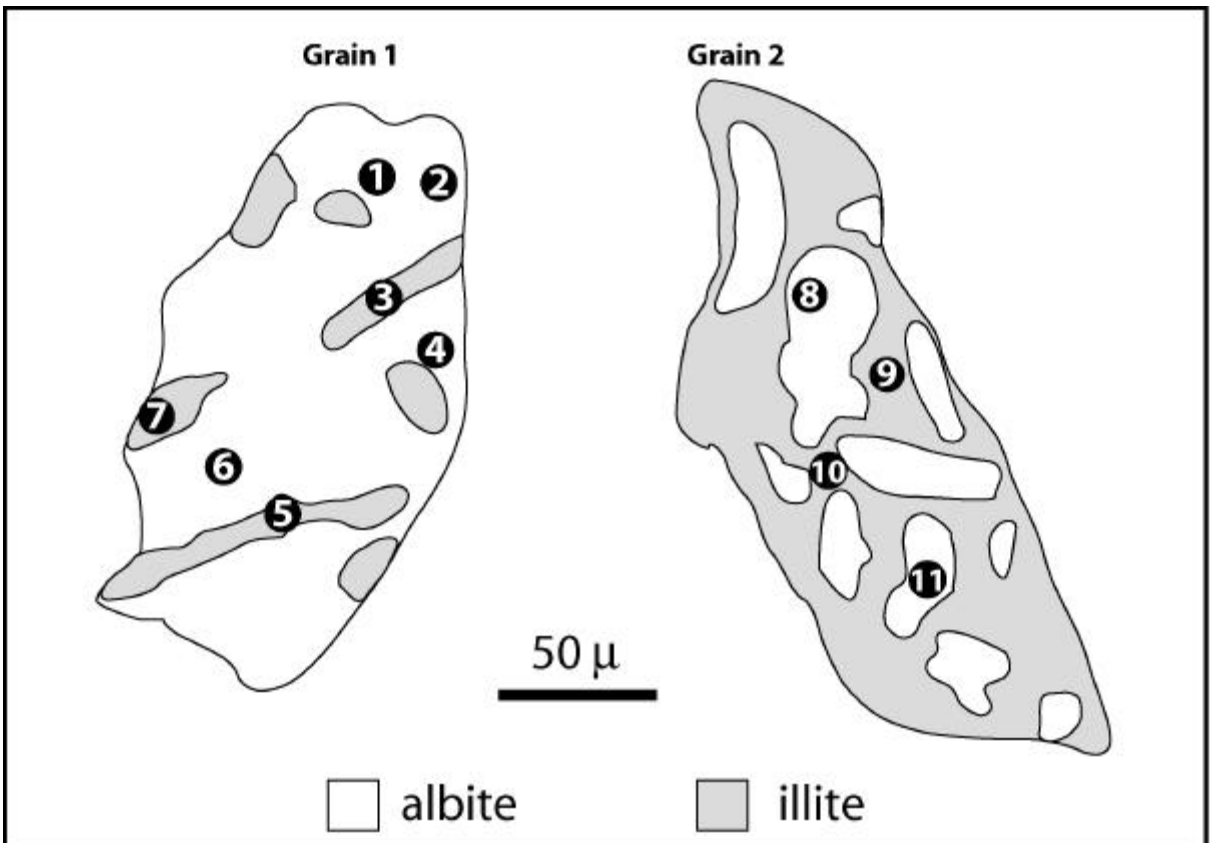

	loc.	SiO_2	Al_2O_3	CaO	FeO	Na_2O	K_2O	Total	%Ab
grain 1	**1**	66.77	19.80	0.36	0.04	11.24	0.11	98.33	**97.64**
	2	66.44	20.57	0.77	0.05	10.97	0.10	98.89	**95.71**
	3	47.40	37.28	0.07	0.28	0.00	10.18	95.21	(illitized feldspar)
	4	66.75	19.96	0.27	0.02	11.35	0.10	98.44	**98.14**
	5	45.71	34.13	0.15	0.84	0.17	9.82	90.81	(illitized feldspar)
	6	66.83	19.74	0.38	0.02	11.40	0.08	98.44	**97.75**
	7	46.89	35.76	0.11	0.28	0.83	9.65	93.52	(illitized feldspar)
grain 2	**8**	63.47	23.09	1.02	0.24	9.60	1.63	99.04	**85.44**
	9	48.97	29.64	0.02	2.31	0.20	9.56	90.70	(illitized feldspar)
	10	46.57	34.05	0.02	2.06	0.32	10.69	93.70	(illitized feldspar)
	11	65.37	19.70	0.07	0.04	10.72	0.33	96.24	**97.67**

Figure 2.6 Compositional map and mineral chemistries of albitized framework grains. The distribution of pure albite shown within these figures is typical of other observed occurrences. Electron probe microanalysis indicates that most of the host K-feldspar has been illitized. Mineral chemistry data reported corresponds to the locations highlighted on each grain. The single low Ab and relatively high potassium and calcium (possibly from calcite) value probably indicates that some host material was captured by the electron beam during the analysis.

comparable stratigraphic level near the southern portion of our study area (1998) is strikingly similar to the dolomite analyzed in this study. It generally occurs as a replacement of earlier calcite cements. Calcite is one of the most commonly cited replacement minerals in Carboniferous sandstones (Kamm and Heald 1983; Milliken 1998; Milliken 2001). Kaolinite has also been reported as an important mineral after feldspar (Heald 1965; Milliken 1998; Milliken 2001).

Cements.--- The most important cements in these sandstones are quartz , carbonates, oxides/oxyhydroxides and sulfides. Quartz is volumetrically the most important cement throughout the study interval, occurs in two distinctive forms, and is most common in quartz arenites. The first and most common morphology is as syntaxial overgrowths, which are easily distinguished from its detrital host by the occurrence of dust rims (Fig. 2.4D). Quartz also occurs less commonly as prismatic crystals (Fig. 2.4D) typically protruding into secondary pore spaces (Fig. 2.4E).

Carbonate minerals are the second most abundant cements, followed by small amounts of clay and pyrite. In addition to being a replacement mineral, calcite is also a relatively important cement that generally occurs as large inter-granular crystals that are most common in coarse-grained, compositionally mature samples, although smaller intra-granular crystals are present in less mature sandstones in association with labile grains such as metamorphic rock fragments and muscovite. Distinguishing between ferruginous dolomite cement and replacement is frequently equivocal because the highest concentrations of dolomite are associated with the replacement fabrics discussed above. However, as with calcite, some inter- and intra-granular dolomite is present in a few samples. Siderite is the third most common carbonate cement and is most

abundant in Lower Pennsylvanian sandstones (mineral chemistries presented in Figure 2.5). Siderite occurs in two distinctive crystal morphologies: 1) small (<20 microns) euhedral crystals surrounding detrital grains (predominantly quartz; Fig. 2.4E) that are most common at or near the base of sandstone bodies, and 2) "wheat-seed" siderite. Ankerite is present in small concentrations and generally occurs as small euhedral crystals lining secondary pore spaces. Chlorite exists as grain-rimming cement in a few isolated samples. Framboidal pyrite is present around detrital grains and larger subhedral crystals have been observed in primary pore spaces. Small amounts of clay minerals including illite occur around detrital grains, although distinguishing between illite cement and replacement is difficult.

Carbon and oxygen isotopic measurements were collected from carbonate-rich intervals in sandstones of the New River Formation. For "wheat-seed," and the euhedral grain-rimming siderite, $\delta^{18}O$ values range from –13 to –12 ‰ PDB and $\delta^{13}C$ from -0.7 to 3.0 ‰ PDB. For Fe-dolomite, $\delta^{18}O$ values are between –15 and –16 ‰ PDB and $\delta^{13}C$, -1.0 to –1.2 ‰ PDB.

Sandstone cements in other studies in the Appalachian basin are comparable to those discussed above. Quartz is cited as one of the most important cements present in Mississippian and Pennsylvanian sandstones (Heald, 1965; Kamm and Heald, 1983; Hohn et al., 1997; Milliken, 1998; Milliken, 2001) and may have formed in two stages within the Mississippian Berea sandstone according to Heald (1965). It also serves as one of the most important pore-occluding minerals (Hohn et al., 1997). Chlorite is reported as a grain-rimming constituent in Mississippian sandstones (Heald, 1965). Calcite cement is present in various concentrations throughout the Carboniferous (Heald, 1965; Kamm and Heald, 1983; Hohn et al., 1997; Milliken, 1998; Milliken, 2001). Siderite and dolomite are generally subordinate and isolated in most sandstones (Milliken, 1998; Milliken, 2001).

Porosity.--- Highest primary porosity is associated with quartz arenites, whereas secondary porosity is relatively evenly distributed throughout each type of sandstone. Primary pore spaces are small (typically <0.1 mm across) and are commonly preserved at termination points of quartz overgrowth cements (Fig. 2.4D). Intergranular secondary porosity is volumetrically significant and often retains the morphology of the pre-existing grain. Intragranular secondary porosity is also present and mainly occurs at the expense of unstable lithic and feldspar grains and less commonly, calcite (Fig. 2.4F). The maximum size of secondary pore space is often determined by the size of the host grain. Microporosity (<0.02 mm) associated with kaolinite is also present in minor amounts. In previous studies, secondary porosity is noted to be more abundant than primary porosity and to have formed after feldspar (Kamm and Heald, 1983), lithic fragments or both (Milliken, 2001).

PARAGENESIS

General paragenetic relationships between diagenetic products discussed above were constrained using textural evidence and geochemical considerations including published thermodynamic boundary conditions for certain diagenetic reactions, stable isotopes and redox (Fig. 2.7). Carboniferous sandstones record a variety of eogenetic, mesogenetic and possibly telogenetic reactions. Boundary conditions between these diagenetic realms are based on temperature and depth and we follow those outlined by Morad et al. (2000) and place maximum conditions of eogenesis at < 2km and <70 °C, where mesogenesis begins. The thermal framework for Carboniferous sandstones in the central Appalachian basin has been developed using paleothermometry and thermochronology (e.g., Roden et al., 1992; Blackmer et al., 1994; Boettcher and Milliken, 1994; Reed et al., a and b, in review).

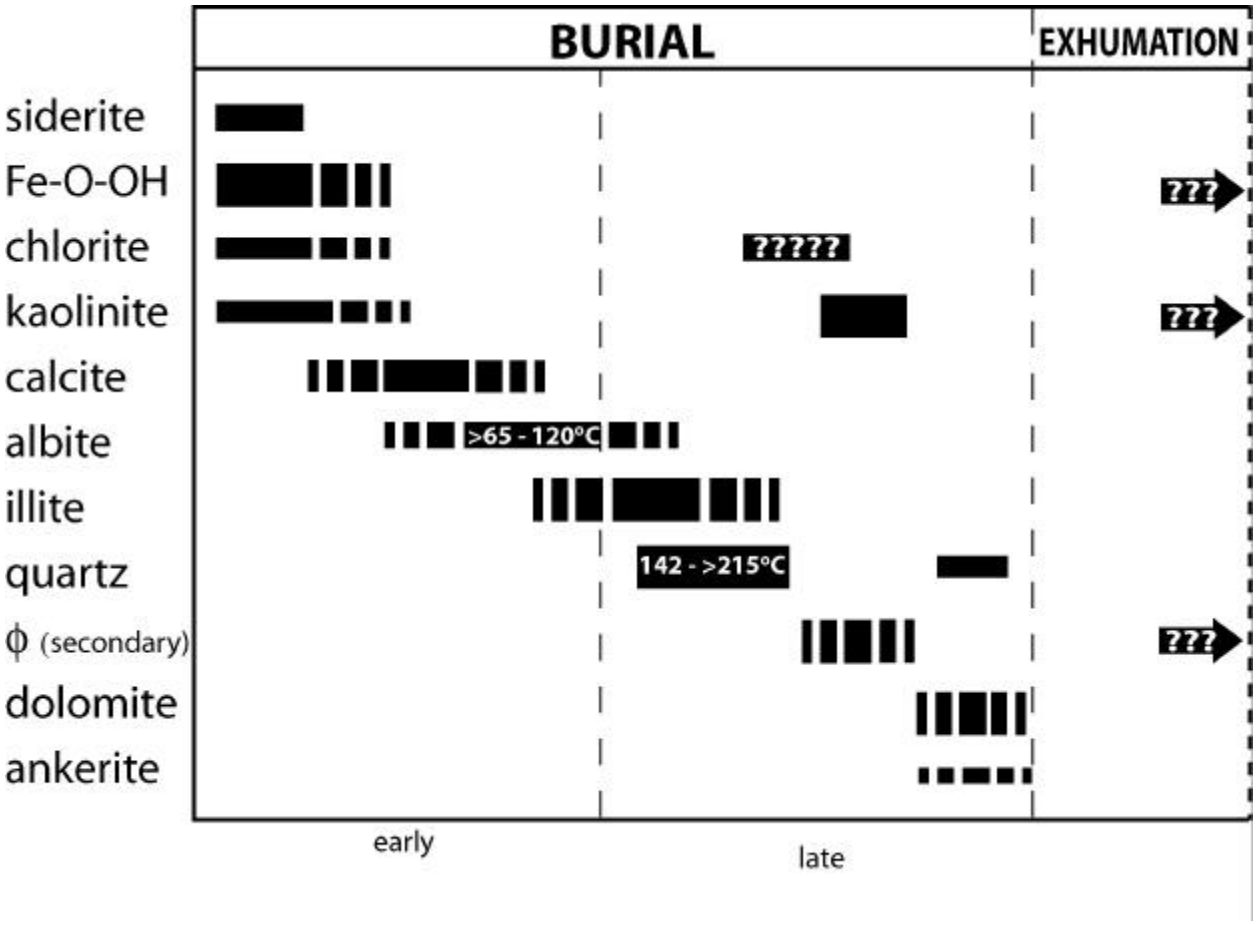

Figure 2.7 The proposed paragenesis is based on textural evidence and geochemical considerations including published thermodynamic boundary conditions, stable isotopes and redox. Dashed bars indicate degree of uncertainty. Well-constrained thermal boundaries are reported for some components and are discussed in the text. Line thickness defining the occurrence intervals represents the relative importance/abundance for each component.

Eogenesis

Grain coating minerals mark the earliest diagenetic events and include Fe-oxides/oxyhydroxides, siderite and chlorite. Fe-oxides/oxyhydroxides are most common in Upper Mississippian and Upper Pennsylvanian sandstones. We proposed that the presence of oxidized Fe-bearing minerals implies communication with atmospheric oxygen. In contrast, early siderite is most abundant in Lower Pennsylvanian sandstones and implies reducing pore fluids. Depleted $\delta^{18}O$ values (-12 to -13 ‰ PDB) from grain rimming siderite indicate a meteoric water influence and supports petrographic observations that it formed relatively early. Chlorite appears to have formed early in association with other grain-rimming minerals such as siderite and Fe-oxides/oxyhydroxides, although chloritization of grain-rimming clay minerals may also have occurred later in the paragenesis at elevated temperatures (cf. Hillier, 1994; Spötl et al., 1994). Constraining the timing of kaolinitization using textural evidence is difficult. However, some kaolinite formation is probably restricted to shallow burial depths because it generally forms after feldspar and mica in the presence of low pH meteoric water (e.g., Khanna et al., 1997; Lanson et al., 2002). Moreover, there is evidence in some samples that kaolinite predates illitization (Fig. 2.4B). Textural evidence suggests that calcite cementation post-dated grain coating minerals and was succeeded by the formation of secondary porosity.

Mesogenesis

The association of nearly pure albite with illitized feldspar grains suggests that the host grain was not significantly altered prior to albitization. Illitization of the remaining host ensued because of incomplete albitization of many grains (e.g., Fig. 2.6). Therefore, albitization must predate feldspar illitization placing it as one of the first important mesogenetic reactions. This

observation is further supported by interpretations presented in previous studies that suggest that the onset of K-feldspar albitization can occur at temperatures as low as 65 °C (Saigal et al., 1988), although higher temperatures (>90-120 °C) have been cited (Saigal et al., 1988; Kang-Min et al., 1997). In addition, kinetic modeling has shown that albitization of K-feldspar may occur between 120-150 °C (Baccar et al., 1993), although such high temperatures have not been widely reported in natural settings.

The timing of illitization is difficult to constrain based on textural evidence. However, significant illitization of feldspar and kaolinite in North Sea sandstones similar to that documented in this study has been inferred to take place at temperatures between 120 and 140 °C (Aagaard et al., 1990; Chuhan et al., 2000), although lower temperature replacement (90-95 °C) also has been invoked (Ehrenberg et al., 1993). Phase relationships between illite, muscovite and feldspar indicate that high potassium concentrations and low silica concentrations will promote illite formation after muscovite (Garrels, 1984), although kaolinite can potentially serve as an intermediate phase during this reaction (Bjorkum and Gjelsvik, 1988; Morad, 1990; Lanson et al., 2002).

Textural evidence indicates that illitization of feldspar (Fig. 2.4A pre-dated quartz cementation. Fluid inclusion paleothermometry of syntaxial quartz overgrowths complemented by vitrinite reflectance indicate that quartz cementation in Lower Pennsylvanian sandstones occurred near maximum burial conditions (~140-150 °C), whereas fluid inclusions in Upper Pennsylvanians samples indicate that precipitation of silica occurred at higher temperatures (>215°C; Reed et al., a, in review). We propose that the higher temperatures are related to the injection of warm, silica-rich fluids during Alleghanian thrusting (for further discussion see Reed et al., a, in review) and that the lower temperatures record maximum burial temperatures.

Furthermore, based on the progradational solubility of silica with respect to temperature, precipitation probably continued during cooling and exhumation (cf. Rimstidt, 1997).

Textural evidence constrains the relationship between secondary porosity and late-stage mineral phases. Microporosity and moldic porosity that developed as a consequence of feldspar dissolution and kaolinitization formed after syntaxial quartz overgrowths. The formation of kaolinite after feldspar during mesogenesis is possible where CO_2-rich fluids are present (e.g., Lanson et al., 2002). This scenario is feasible considering the abundance of organic-rich strata in this study interval. Textural evidence indicates that prismatic quartz was precipitated in secondary pores late in the diagenetic history (Fig. 4D).

Secondary pores also host dolomite/ankerite crystals in isolated locations suggesting that burial Fe-carbonates postdate secondary porosity. Fe-rich carbonate, especially dolomite that formed by replacement of calcite and to a lesser extent, detrital feldspar, was probably the latest mesogenetic mineral phase to form. The occurrence of burial Fe-carbonates in Mississippian and Pennsylvanian strata implies that late diagenetic fluids in the Appalachian basin were Fe-rich (Niemann and Read, 1988; Nelson and Read, 1990; Milliken, 1998). Proposed sources for late diagenetic Fe in the Appalachian basin are clay mineral transformation in surrounding shales (Milliken, 1998) and topographically driven Fe-rich fluids introduced from tectonic highlands (Deming and Nunn, 1991; Montanez, 1994). The timing of Fe-dolomite formation and sources of Fe can be estimated using multiple lines of evidence. If the smectite to illite transformation reaction served as an important source of Fe, this would constrain dolomite formation temperatures to greater than 100 °C (cf. Boles and Franks, 1979; Kantorowicz, 1985). Textural observations imply that Fe-carbonates formed during deep burial, after secondary porosity and the depleted $\delta^{18}O$ values (-15 to –16 ‰ PDB) displayed by the Fe-dolomites likely represent

isotopic fractionation influenced by elevated temperatures. Ankerite from Upper Jurassic sedimentary rocks of the North Sea with similarly depleted $\delta^{18}O$ and $\delta^{13}C$ values have been attributed to high temperature (>140 °C) pore fluids with an organic source of carbon (Hendry et al. 2000). Similarly, depleted Fe-carbonate $\delta^{18}O$ and $\delta^{13}C$ signatures in Lower Pennsylvanian sandstones of the Appalachian basin have also been ascribed to relatively high temperatures and the influence of organic material (Milliken, 1998). Depleted $\delta^{18}O$ values from Fe-dolomite in this study could also reflect the isotopic composition of topographically driven fluids that migrated from the late Paleozoic highlands (cf. Deming and Nunn, 1991; Montanez, 1994).

Telogenesis

The central Appalachian basin as been inverted, uplifting the studied sandstones to shallow depths (< 400 meters present depth). Therefore, Carboniferous strata were potentially subjected to telogenetic processes. It is difficult to discern what processes associated with leaching can be attributed to eogenesis or telogenesis because both occur near the surface. For example, secondary porosity likely formed during burial but may have further developed during exhumation, especially due to the introduction of meteoric water late in the exhumation history. Similarly, we cannot exclude the possibility that some kaolinite may have formed during exhumation by the hydrolysis of K-feldspar grains that were preserved or partially preserved during burial. It is clear that the oxidation of Fe-bearing carbonates that formed in the deep-burial environment, and framework, Fe-bearing silicate grains is a result of near-surface oxidation.

STATISTICAL ANALYSIS

In this analysis, potential controls on sandstone diagenesis including framework grain composition, paleoclimate and depositional environment are defined as *a priori* groups. Variable selection and definitions of *a priori* groups were based on sampling intensity and geologic assumptions related to the analysis of each potential control. For example, components that we interpret to have formed early during diagenesis and are relatively abundant were pooled to evaluate if they were influenced by paleoclimate and/or depositional environment. Diagenetic products (i.e., variables) within each group were analyzed using correspondence analysis and detrended correspondence analysis.

Framework Grain Composition

A priori groups for the analysis of framework grain composition are based on a simple sandstone classification scheme and include quartz ($Q_{>90}F_{<10}L_{<10}$), feldspathic ($Q_{<90}F_{>10}L_{<10}$) and lithic ($Q_{<90}F_{<10}L_{>10}$) arenites (Dott, 1965). Quartz cement, clay replacement and primary and secondary porosity were the variables chosen to evaluate the influence of framework grain composition on diagenesis because these components are abundant and can influence reservoir quality. The data matrix was reduced using correspondence and detrended correspondence analysis to compare the results between methods and determine whether correspondence analysis results are influenced by the arch effect. Each point on Figure 2.8 represents an individual sample and the larger symbols are the variables that were used for this analysis. Samples with similar scores indicate that they are more related to each other than samples with dissimilar scores. Variables that plot within specific groupings defined by similar samples indicate that some dependence exists between the *a priori* group and the variable. Ordination plots indicate

that a strong correlation exists between quartz arenites and quartz cement (Fig. 2.8). In addition, clay replacement minerals, especially illite, plot within feldspathic and lithic arenite clusters (Fig. 2.8). Correlation between porosity and framework grain composition is less apparent, although some correspondence exists between primary porosity and quartz-rich sandstones, which is especially evident in the CA ordination plot. There is no clear correlation between secondary porosity and lithology.

Paleoclimate

Paleoclimate evaluation involved testing the hypothesis that early diagenesis (eogenesis) varied as a function of climate. Cecil et al. (1985) generated a qualitative second-order paleoclimate curve based on gross lithologic changes, geochemical signatures, and coal swamp geometry. According to Cecil et al. (1985) the Upper Mississippian and Pennsylvanian times were marked by semi-arid/seasonal climates whereas Lower Pennsylvanian strata record evidence of everwet conditions. Variables chosen for the analysis reflect predicted redox conditions present during the semi-arid and everwet time periods as predicted by the paleoclimatic curve (Fig. 2.9). Semi-arid conditions should be reflected by more oxidized mineral species such as Fe-oxides/oxyhydroxides (e.g., Weibel, 1998), whereas everwet times should contains higher concentrations of reduced mineral species such as siderite.

Fe-oxide/oxyhydroxides and siderite were pooled and dimensions were reduced using detrended correspondence analysis. Axis 1 scores, which account for the greatest amount of variance in the data set, were plotted for each time interval. DCA was used because two or more variables can be plotted on the same axis, which enables direct comparisons between the qualitative curve generated by Cecil et al. (1985) and the quantitative curve generated in this

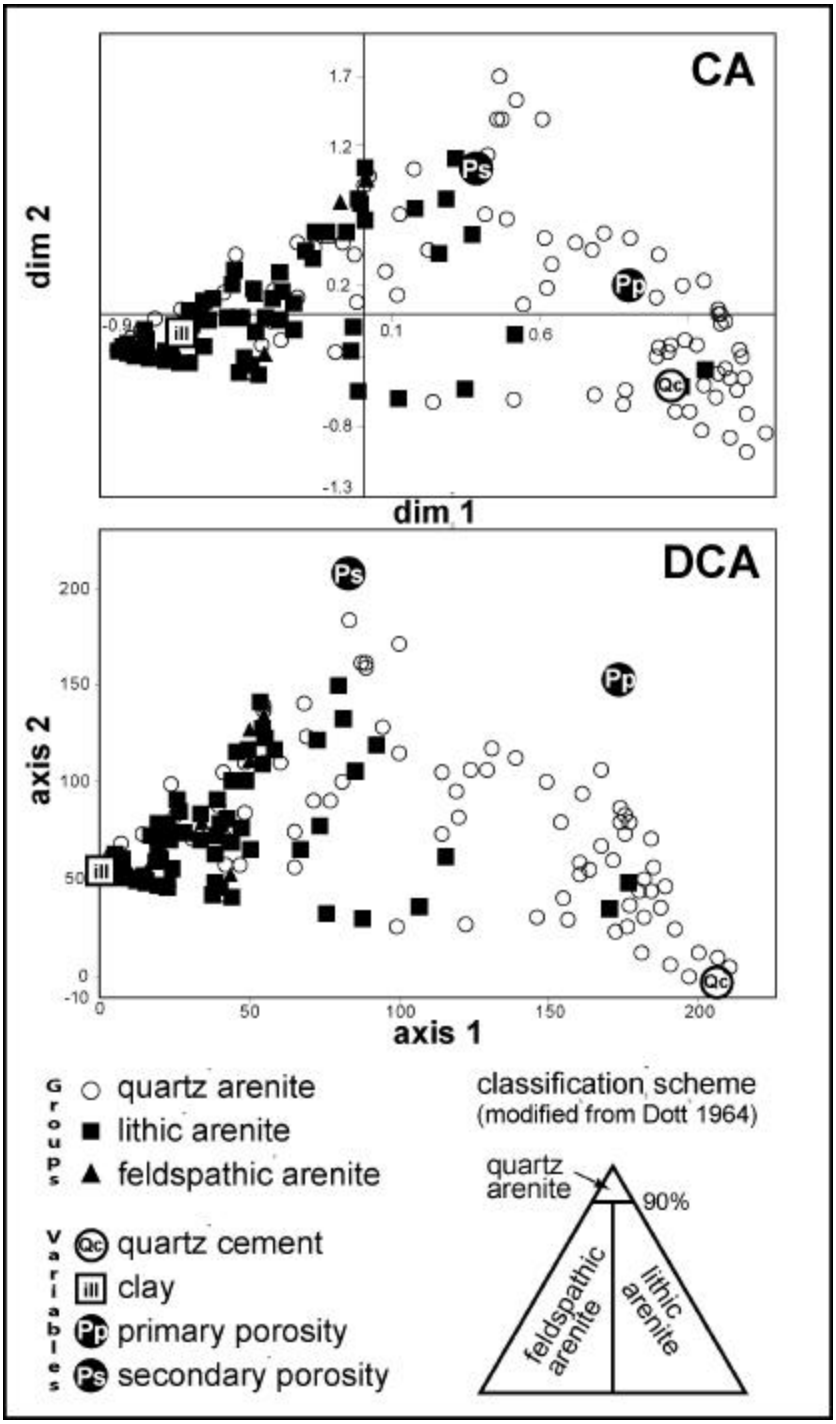

Figure 2.8 Ordination plots evaluating the influence of framework grain composition on sandstone diagenesis. Axes labeled dim 1 and dim 2, and axis 1 and axis 2 correspond to the highest and second highest components of variance obtained in Correspondence Analyses (CA) and Detrended Correspondence Analysis (DCA), respectively. Diagenetic products are plotted to show correlations between independent variables (lithologic groups) and dependent variables (diagenetic products). Each point corresponds to a single sample. Larger symbols correspond to the variables that were included in the analysis.

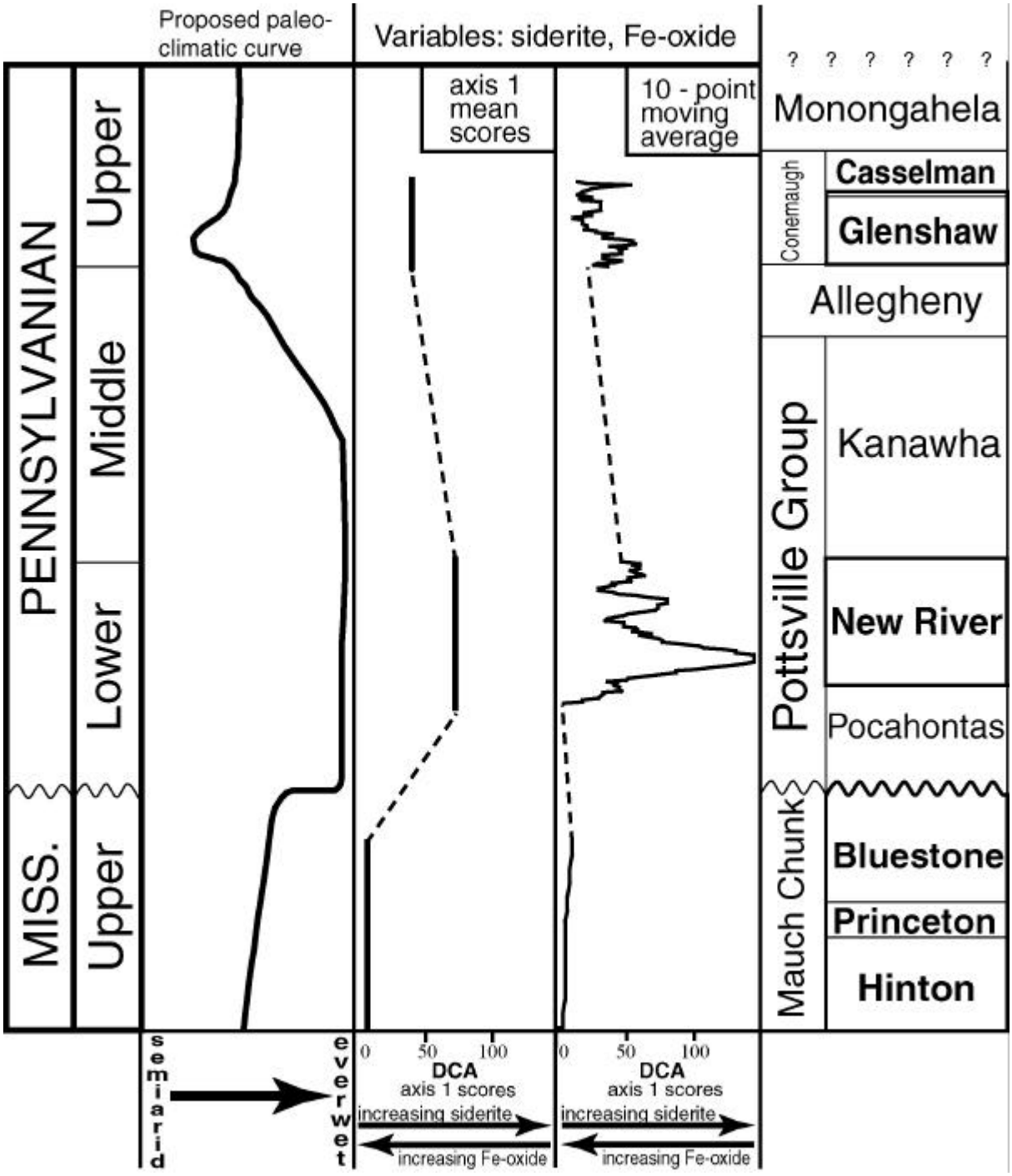

Figure 2.9 Plot illustrating paleoclimatic influences on sandstone diagenesis. Inferred paleoclimatic curve are based on (Cecil et al. 1985). Dashed lines represent intervals that were not sampled for this study. Variables used in the analysis were siderite and Fe-oxide/ oxyhydroxide. DCA scores serve as a proxy for paleoclimate, i.e. point-counts and Spearman correlation coefficients confirm that low scores correlate to high concentrations of Fe-oxide/oxyhydroxide (proxy for semi-arid conditions) and high scores to high concentrations or siderite (proxy for everwet conditions).

study. Variable pooling was necessary to reduce noise because: 1) Fe-oxide/oxyhydroxides and siderite are absent from some samples, and 2) we are only interested in the long-term diagenetic trends recorded in Upper Mississippian, Lower Pennsylvanian and Upper Pennsylvanian strata. DCA scores reflect how well samples correlate based on the presence and concentrations of Fe-oxide/oxyhydroxides and siderite, where low scores correspond to samples and intervals rich in Fe-oxide/oxyhydroxides and high scores reflect relative concentrations of siderite. Relative concentrations and correspondence between mineralogy and the proposed paleoclimate are confirmed by point-count data and Spearman correlation coefficients (r). DCA scores and siderite have a positive *r* value (0.92) whereas DCA scores and Fe-oxide/oxyhydroxide have a negative r value (-0.51), which indicates that high DCA scores correlate to relatively high counts of siderite and low scores to relatively high counts of Fe-oxide/oxyhydroxides and vise versa. Therefore, based on the assumptions between the chosen variables and paleoclimate, the DCA scores serve as a proxy for paleoclimate, i.e. low scores correlate to semi-arid and high scores to everwet conditions. Direct comparisons summarized in Figure 2.9 can be made between the qualitative and two quantitative curves. First, axis 1 mean scores for each stratigraphic interval are plotted and dashed lines represent time intervals that were not sampled and analyzed. Second, a 10-point moving average of axis 1 scores presents a higher resolution view of the results. Results from both methods mimic the qualitative curve proposed by Cecil et al. (1985).

Depositional Environment

Fe-oxide/oxyhydroxide, siderite, calcite, kaolinite and primary porosity were used to evaluate depositional environment, in particular, the influence of early poor fluid chemistry on diagenesis. Fe-oxide/oxyhydroxide and kaolinite were chosen because the occurrence of Fe-oxide/oxyhydroxide should reflect oxidizing conditions typical of fluvial environment and

kaolinitization commonly forms from the leaching of feldspar by meteoric water. Calcite could reflect the introduction of Ca^{+2} by marine pore fluids and the formation of siderite with compositions of < 90 mol % $FeCO_3$ (Fig. 2.5) has been attributed to marine environments (e.g., Mozley, 1989) and therefore should have formed in reducing environments associated with marine flooding. Sandstones were divided into "marine" and "fluvial" facies based on field observations and facies analysis (Fig. 2.10). The analyses are based on ratios of estimated values of marine:fluvial facies intervals of approximately 20:80 for Lower and Upper Pennsylvanian strata. Upper Mississippian samples were collected from only fluvial deposystems and are therefore present only in the fluvial group.

Three methods were used to analyze results from correspondence analysis. First, all Carboniferous samples were pooled into "marine" and "fluvial" groups. Ordination plots from this analysis do not suggest any clear groupings of samples from the "marine" and "fluvial" groups. Second, results from the first analysis were tested further by including only samples located within the top and bottom 20 percents of the sandstones (i.e., samples within the middle 60% were omitted prior to running correspondence analysis). As observed with the first analysis, no patterns were observed and significant overlap exists between "marine" and "fluvial" samples. The final analysis omitted samples and scores after CA and results were again equivocal. Therefore, there is no apparent dependence between facies within IVFs and diagenetic products for the pooled variables.

DISCUSSION

Controls on Sandstone Diagenesis

Exploratory multivariate statistical methods employed in this study provide an effective means to rigorously test hypotheses concerning potential controls on sandstone diagenesis, and

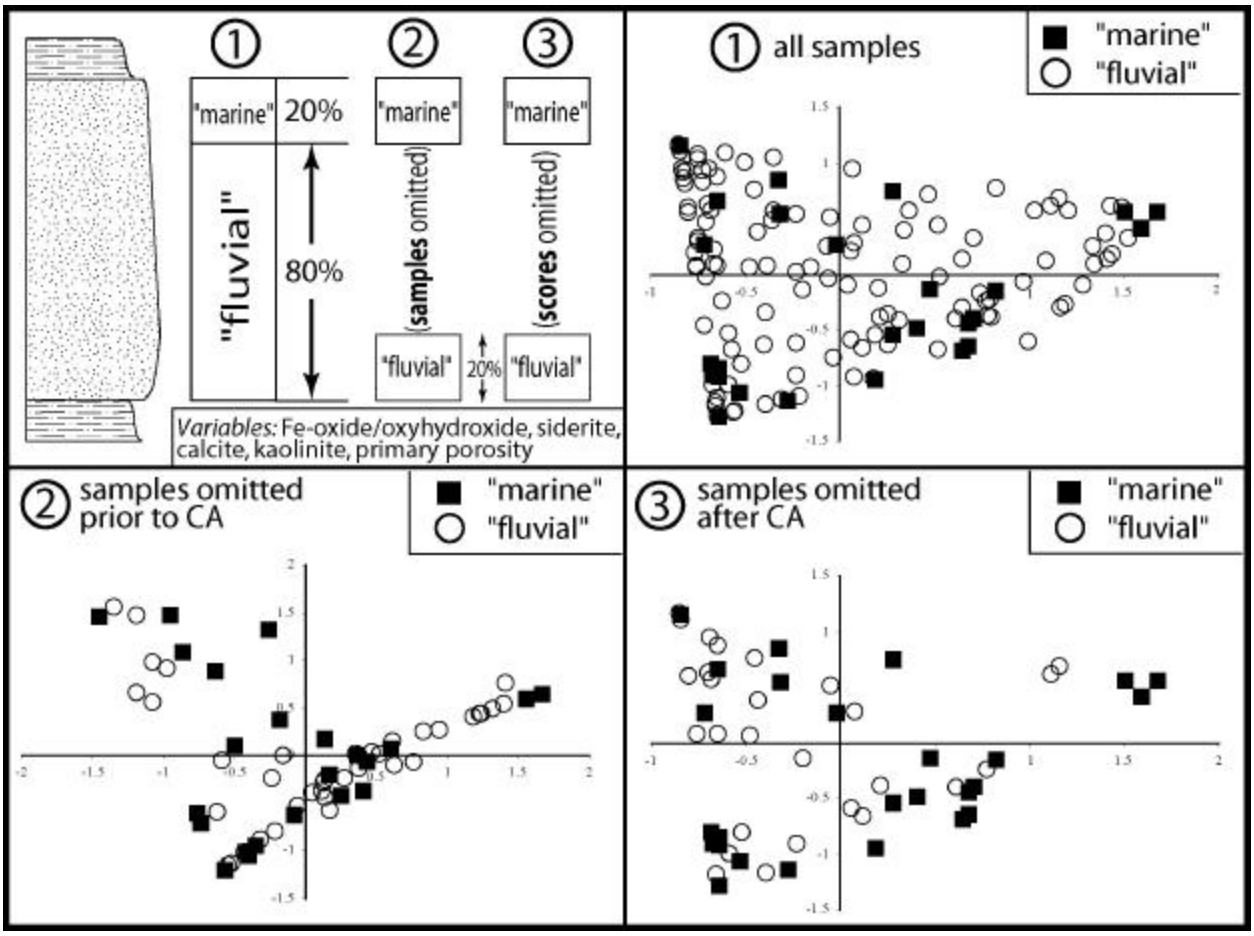

Figure 2.10 Ordination plots evaluating the influence of depositional environment on sandstone diagenesis. Variable scores were omitted from the ordination plots since no dependence on depositional environment can be discerned. Correspondence analysis dim 1 and dim 2 are plotted for each analysis. Variables included in the analysis were Fe-oxide/oxyhydroxide, siderite, calcite, kaolinite and primary porosity.

supplements similar quantitative approaches that have been applied to sandstone petrology (e.g., Dyman et al., 1988; Ehrenberg, 1997; Giles, 1997; von Eynatten et al,. 2003). Visual examination of ordination plots simplifies interpretations involving large multi-component data sets. Correspondence and detrended correspondence analyses effectively manage problems associated with compositional data sets, which are common in petrologic studies.

Framework grain composition appears to have had the greatest influence on Carboniferous sandstone diagenesis in the central Appalachian basin. The significant correlation between quartz cement and quartz arenites is likely related to the preservation of primary porosity during burial (Fig. 2.8). This can be attributed to the competency of the quartz framework grains. As textural and fluid inclusion evidence show, silica precipitation occurred relatively late, near maximum burial. Therefore, sufficient permeability must have been preserved during burial to accommodate silica-bearing fluids that were being introduced from the Alleghany Front (Reed et al., a, in review). However, additional sources of silica including clay mineral reactions and pressure dissolution of quartz framework grains cannot be dismissed. The correlation between illite and low concentrations of syntaxial quartz overgrowths within lithic and feldspathic sandstones indicates that a decrease in primary porosity occurred relatively early and that feldspar and lithic framework grains provided the necessary chemical components for the formation of illite.

Quantitative results from this study support the observations made by Cecil et al. (1985) and Donaldson et al. (1985) concerning long-term paleoclimatic influences on lithologic characteristics from the Upper Mississippian, Lower Pennsylvanian and Upper Pennsylvanian in the central Appalachian basin (Fig. 2.9). Low DCA scores corresponding to the Upper Mississippian and Pennsylvanian indicate correlation between Fe-oxide/oxyhydroxide and the

inferred semi-arid paleoclimatic conditions. Lower scores associated with Upper Mississippian sandstones could reflect the lower number of samples than the Upper Pennsylvanian. The Lower Pennsylvanian is marked by higher scores and higher concentrations of siderite, which correspond to everwet conditions as discussed above. The correlation between semi-arid conditions and Fe-oxide/oxyhydroxide is a reflection of oxidizing settings, whereas that between everwet conditions and abundance of siderite reflects availability of Fe reducers. If we assume that terrestrial systems such as soils and streams are the main source of Fe, then it will most likely be transported in as Fe^{+3} (Langmuir, 1997). Therefore, everwet conditions of the Lower Pennsylvanian were more likely to have harbored Fe reducing microbes than depositional environments indicative of semi-arid conditions.

There appears to be no correlation between early diagenesis and depositional environment defined by fluvial and marine facies identified within IVFs. We predicted that eogenetic mineral species such as kaolinite and Fe-oxide/oxyhydroxide would correlate to the fluvial facies that may have been characterized initially by low salinity pore fluids and higher pO_2. Communication with atmospheric oxygen (open system) during turbulent flow associated with fluvial processes creates an oxidized environment (Langmuir, 1997). In addition, pore fluids with a meteoric affinity promote feldspar hydrolysis, producing kaolinite. Alternatively, we hypothesized that calcite should correlate to the introduction of Ca^{+2} and Mg^{+2} associated with “marine” pore fluids and based on evidence cited above, siderite should reflect lower redox potential during marine flooding of the IVF. The results (Fig. 2.10) indicate that significant communication existed between “fluvial” and “marine” facies of the IVFs and facilitated pore fluid mixing.

Primary and Secondary Porosity

The distribution of primary and secondary porosity within the studied sandstones is primarily controlled by framework grain composition. Primary porosity is low throughout the study interval and can be attributed to two important processes. First, the compaction of labile framework grains including metamorphic and sedimentary rock fragments minimizes the preservation potential of primary porosity. Second, the preservation of primary porosity in quartz arenites sandstones during burial must have been long-lived because pores serve as conduits for silica-rich fluids that produced quartz cement late in the burial history (Fig. 2.7). Secondary porosity is associated with both compositionally mature and immature sandstones (Fig. 2.8). Textural evidence indicates that most secondary porosity developed after syntaxial quartz cementation and before prismatic quartz. Thus, avenues for fluid migration were present during burial and may have facilitated the dissolution of chemically unstable detrital and authigenic minerals within the quartz arenites. Secondary porosity associated with lithic and feldspathic arenites probably formed prior to significant compaction or during telogenesis.

Sandstone Diagenesis in the Appalachian Basin: Further Considerations

This study supplements our understanding of Carboniferous sandstone diagenesis in the central Appalachian basin. Specifically, we have provided further documentation of important diagenetic products including Fe-carbonate (Milliken, 1998; Milliken, 2001), calcite (Kamm and Heald, 1983; Milliken, 1998; Milliken, 2001), kaolinite (Heald, 1965; Milliken, 1998; Milliken, 2001), quartz (Heald, 1965; Kamm and Heald, 1983; Hohn et al., 1997; Milliken, 1998; Milliken, 2001), chlorite (Heald, 1965), and secondary porosity (Kamm and Heald, 1983; Milliken, 2001). In addition, results from this study have allowed us to speculate on parameters

that are poorly understood including paragenesis and factors that influenced sandstone diagenesis.

The paragenesis presented here relies on: 1) the textural evidence resolved using petrography geochemical considerations, and 2) our current understanding of proposed thermodynamics of diagenetic mineral reactions. It also includes additional observations and interpretations for some important minerals reactions (e.g., albitization and widespread illitization), although additional stratigraphic levels and core locations within the Appalachian Plateau need to be evaluated to refine our understanding of Carboniferous sandstone diagenesis. We have assumed that thermal constraints on diagenetic mineral reactions presented in other studies, primarily from the North Sea, are broadly applicable to the central Appalachian basin. The thermodynamics should remain constant within any sedimentary basin, but kinetic considerations may vary. For example, basin subsidence and exhumation rates will control the residence time of certain stratigraphic horizons within important thermal windows. This variation could potentially control authigenic mineral species and porosity formation. Therefore, diagenetic studies in the central Appalachian basin would benefit from refined thermal calibration of the basin (e.g., Roden et al., 1992; Blackmer et al., 1994; Boettcher and Milliken, 1994; Reed et al., a and b, in review) that is tied closely to various diagenetic reactions.

SUMMARY AND CONCLUSIONS

Carboniferous sandstones in the central Appalachian basin have provided an excellent setting to evaluate diagenesis. Important observations and conclusions from this study include:

1) Multivariate statistical techniques provide a rigorous means to evaluate potential controls on sandstone diagenesis. We proposed that other petrologic studies that primarily rely on qualitative observations could potentially benefit from a similar objective approach.
2) The development of Carboniferous sandstone paragenesis has benefited from combining textural observations, an understanding of mineral thermal stability fields of diagenetic minerals, and established thermal constraints within sedimentary basins.
3) Framework grain composition appears to be the most significant control on Carboniferous sandstone diagenesis in the central Appalachian basin. The relationship between the proposed second-order paleoclimate curve for the Carboniferous in the Appalachian basin and early diagenesis has been further justified using quantitative methods outlined in this study. No relationship between depositional environment and diagenesis is evident in these samples indicating that pore fluid communication occurred between fluvial and marine portions of these incised valley fill deposits.
4) Important directions of future work in the Appalachian basin include developing a more refined thermal history in concert with further constraining the timing of important diagenetic reactions.

CHAPTER 3: PALEOTHERMOMETRY AND QUARTZ AUTHIGENESIS IN PENNSYLVANIAN SANDSTONES, CENTRAL APPALACHIAN BASIN: APPLICATION OF FLUID INCLUSIONS AND VITRINITE REFLECTANCE

ABSTRACT

Fluid inclusion microthermometry and vitrinite reflectance are used to constrain burial and quartz authigenesis histories for Pennsylvanian sandstones in the central Appalachian basin. Paleotemperatures indicate that the Pennsylvanian strata in the Appalachian Plateau were buried to greater than 4.5 kilometers (based on an estimated geothermal gradient of ~30 °C/km). While only seven fluid inclusions were found that were large enough to provide microthermometric data, all of these inclusions are definitely in authigenic quartz and, therefore, represent fluids associated with quartz precipitation during burial. Homogenization temperatures of four fluid inclusions in quartz overgrowths in the lower Pennsylvanian New River Formation sandstones were 143.5±1.5°C, 145±2°C, 148°C and 163°C. Paleotemperatures from vitrinite reflectance (138 – 177 °C; n=22; mean = 151 °C) are consistent with the fluid inclusion results. Fluid inclusions in upper Pennsylvanian sandstones indicate temperatures that are somewhat higher than vitrinite reflectance paleotemperatures from surrounding organic-rich units. Homogenization temperatures of three fluid inclusions from the upper Pennsylvanian Glenshaw Formation are 217°C and 237±7°C (2 inclusions), whereas vitrinite reflectance paleotemperatures from the same interval are much lower (132 – 171 °C; n = 4; mean = 150 °C).

The paleotemperature results indicate that tectonic setting played an important role in quartz authigenesis. The location of upper Pennsylvanian samples adjacent to the Allegheny front and the discrepancy between the fluid inclusion and vitrinite reflectance data imply that warm silica-bearing fluids, likely sourced from low-grade metamorphic reactions, were injected into upper Pennsylvanian sandstone aquifers during thrust loading associated with the

Alleghanian orogeny. Local, short-lived temperature gradients (extending < 90 meters) exceeding 500 °C/km facilitated silica precipitation. Differences between fluid inclusion and vitrinite reflectance paleotemperatures in lower Pennsylvanian strata are negligible. Calculations based on silica solubility show that the advective fluid flow model inferred for quartz cementation in upper Pennsylvanian sandstones may also apply to units further from the thrust front, but owing to smaller temperature differences between the host and fluid, twice the volume of fluid would have been required to precipitate the same amount of quartz.

Keywords: fluid inclusions, quartz cement, Appalachian basin, paleothermometry, Pennsylvanian, burial history, foreland basin, vitrinite reflectance

INTRODUCTION

Constraining the thermal evolution of sedimentary basins is important for understanding basin dynamics, diagenesis, and hydrocarbon genesis and maturation. The use of fluid inclusions in carbonate and siliciclastic rocks is well documented (e.g., Fishman, 1997; Konnerup-Madsen and Dypvik, 1988; McDonald and Skilbeck, 1996; Walderhaug, 1994a, 1994b), and combined fluid inclusion microthermometry and vitrinite reflectance data have been applied to reconstruct thermal histories of sedimentary basins (e.g., Barker and Goldstein, 1990; Tobin and Claxton, 2000). Fluid inclusions trapped in diagenetic minerals constrain paleotemperatures (c.f. Burruss, 1989), and inclusions may provide the only direct link to basin fluid compositions, in particular, the salinity of the fluids (e.g., Roedder, 1984; Guscott and Burley, 1993; Goldstein and Reynolds 1994). Moreover, temperature information can help to constrain the timing of diagenetic events if the strata were buried under normal burial conditions. Vitrinite reflectance supplements

microthermometric data and serves as an independent means to further constrain burial histories (Barker and Goldstein, 1990; Tobin and Claxton, 2000; Rowan et al., 2002).

Quartz cement is widely recognized as volumetrically one of the most significant components in sandstones (Worden and Morad, 2000), but conflicting models have been proposed for the origin of such cements. An important focus of the debate is whether silica is sourced within the host sandstone, outside the host sandstone, or both (see Worden and Morad, 2000 for detailed discussion). It is also well documented that quartz cements often form during burial at temperatures greater than 80 °C (Worden and Morad, 2000). Therefore, thermal conditions during burial can be assessed using fluid inclusions within quartz cement.

Fluid inclusions are a valuable tool for studying sedimentary systems but few studies have been conducted in the Appalachian basin (see for example Evans and Battles, 1999). The Appalachian basin provides an opportunity to study the thermal and diagenetic evolution of a foreland basin associated with different tectonic provinces. Specifically, comparison of quartz-rich samples within the Appalachian Plateau with those adjacent to the Allegheny thrust front may permit identification of potential differences in sources and transport mechanisms of silica (Fig. 3.1). Carboniferous sandstones are well suited to address this question because many contain relatively large quantities of quartz cement, and core samples are available within the plateau and along the thrust front. Thus, the purpose of this study is to: 1) constrain the thermal history of Pennsylvanian strata in the Appalachian plateau and in the footwall of the thrust front, from deposition to maximum burial using paleothermometric techniques, and 2) establish a thermal framework that can be applied to understanding sandstone diagenesis, especially quartz authigenesis.

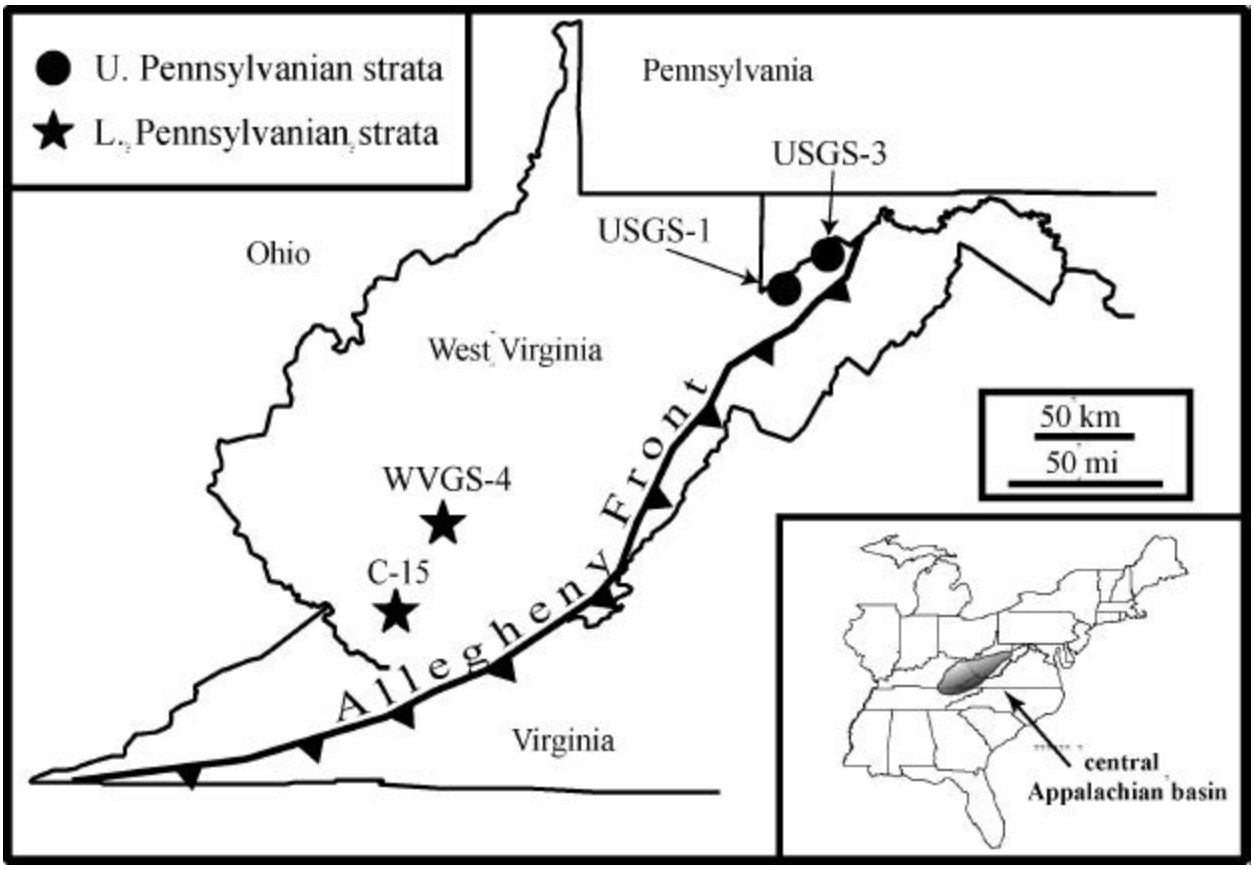

Figure 3.1 Location map showing locations of the drill holes relative to the Allegheny Front. Cores intersecting lower Pennsylvanian New River Formation strata are located in southern West Virginia (wells C-15 and WVGS-4). The Upper Pennsylvanian Glenshaw Formation was sampled in wells USGS-1 and USGS-3 in northeastern West Virginia.

GEOLOGIC SETTING

The Appalachian foreland basin formed in response to three episodes of continental collision (Quinlan and Beaumont, 1984). The final episode of widespread subsidence was caused by the Alleghanian orogeny. This event produced highlands that served as an important source of sediment in the late Paleozoic. Basin subsidence dynamics varied during each of the three major Paleozoic collisional events and the basin was wide and shallow during the Alleghanian event (Tankard, 1986; Klein and Willard, 1989; Willard and Klein, 1990). Basin geometry was primarily controlled by the long-term rheological response of the lithosphere to loading and a general thickening of the crust (Dickinson, 1974; Allen et al., 1986, 1991; Klein, 1991; Sinclair, 1997; Castle, 2001), although, short-term responses to loading have also been recognized (Tankard, 1986). Upper Carboniferous basin fill is primarily composed of siliciclastic sedimentary rocks including sandstone, mudstone, conglomerate (rare), coal seams and subordinate limestone.

Various stratigraphic markers subdivide the late Phanerozoic stratigraphic record. Coals and unconformities have been especially useful for regional correlations of Carboniferous strata in the central Appalachian basin (Fig. 3.2). Upper and lower Pennsylvanian sections used in this study are commonly defined and identified by such markers. The New River Formation in southern West Virginia consists predominantly of nonmarine strata that filled the basin following the development of the early Pennsylvanian unconformity (Korus, 2002). The Upper Pennsylvanian Glenshaw Formation (lower Conemaugh Group) in northeastern West Virginia and western Maryland also consists predominantly of siliciclastic units and subordinate carbonate rocks (caliche and minor marine units; Belt and Lyons, 1989). Both of the study intervals contain quartz arenites and carbonaceous rocks that are ideal for paleothermometric

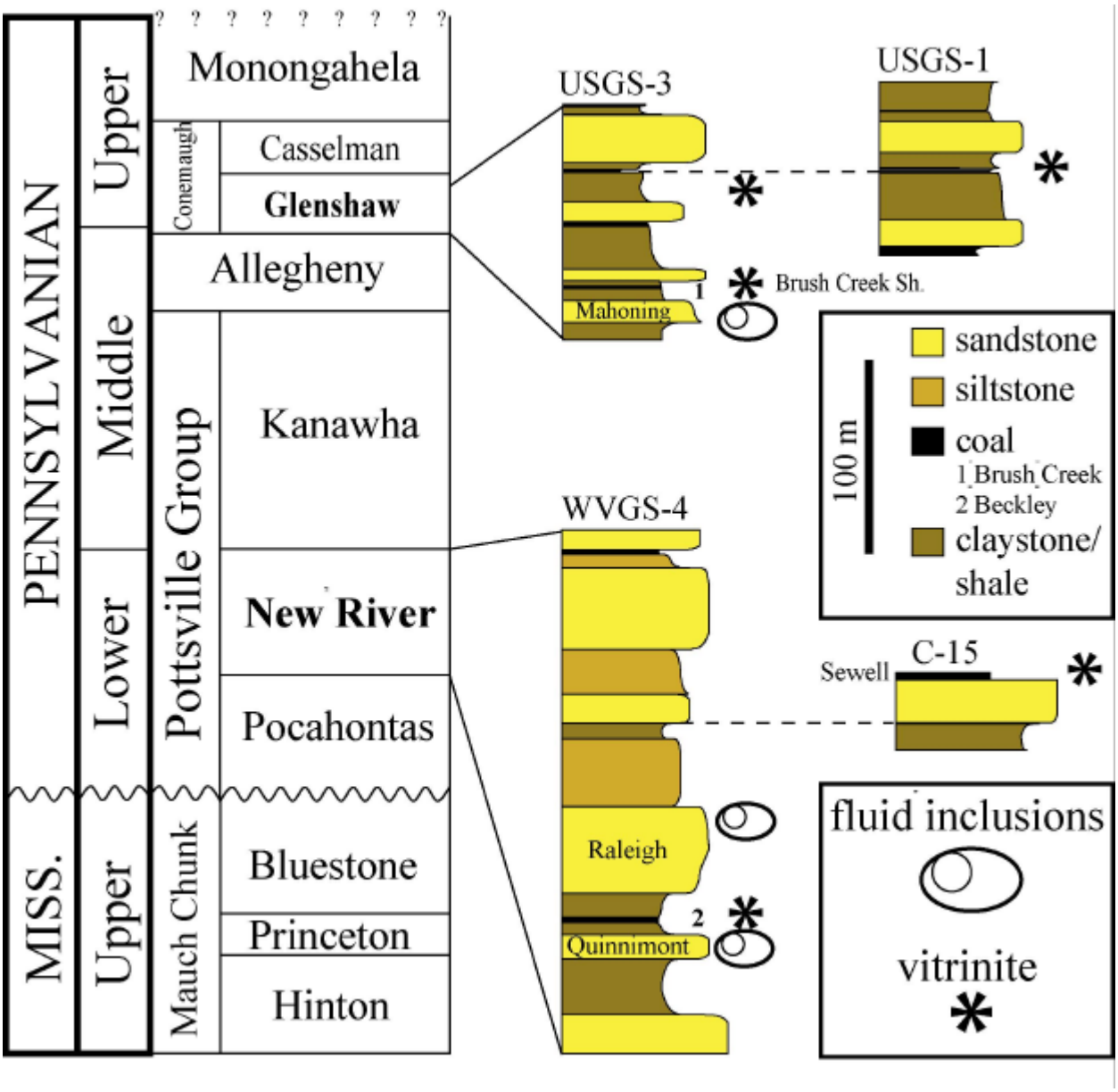

Figure 3.2 Generalized stratigraphy of the Upper Carboniferous, central Appalachian basin showing fluid inclusion and vitrinite reflectance sample locations. Lithostratigraphic correlations between wells are denoted with a dashed line.

studies. More detailed discussion of the general tectonic and stratigraphic setting of the central Appalachian basin can be found in Milici and de Witt (1988).

Petrologic characteristics of Pennsylvanian sandstones in the central Appalachian basin reflect the changing tectonic setting during the late Paleozoic. Much of the sediment was likely sourced from the Alleghanian orogenic belt, shedding quartz- and lithic-rich sediment into the basin, but quartz-rich sediment was probably also derived from the stable craton (Dickinson *et al.* 1983). Quartz-rich samples are generally clean and many contain the highest concentration of quartz cement. The lithic-rich fraction of New River and Glenshaw formation sandstones is predominantly metamorphic rock fragments, reflecting dissection of the mountain belt.

METHODS

Sandstones and organic-rich strata used for this study were obtained from core at two locations representing different stratigraphic levels within the central Appalachian basin (Figs. 3.1 and 3.2). Lower Pennsylvanian samples were recovered from 300-400 meters present depth in south-central West Virginia in the Appalachian Plateau. Upper Pennsylvanian samples are from depths of 50-300 meters below the surface were obtained from drill holes in northeastern West Virginia, adjacent to the Allegheny front.

Fluid Inclusion Techniques

Detailed petrographic examination of 170 thin-sections from the study interval reveals that syntaxial quartz overgrowths occurred relatively late in the paragenesis. Of these 170 sections, 10 representative sections were selected for fluid inclusion studies because they contained abundant quartz overgrowths. In the selected sandstones, authigenic quartz is abundant, comprising an estimated 5-14 % volume percent of the rock. Fluid inclusion

petrography of the authigenic quartz was conducted at high magnification (> 800x) because inclusions in the quartz overgrowths are small (≤ 4 microns) and rare (Fig. 3.3). Most samples contained only one measurable inclusion.

The search for inclusions was restricted to overgrowths. However, owing to the three-dimensional nature of the samples, it was not always obvious whether a given inclusion was in the overgrowth or in the detrital grain. Cathodoluminescence has been used successfully by other workers to distinguish between authigenic and detrital quartz (Sippel 1968), but was not used to verify the locations of the fluid inclusions in this study before microthermometric analysis because of potential thermal damage to the sample. Instead, the location of the "dust rim" relative to the quartz overgrowth and fluid inclusion was used. Most detrital grains in the studied sandstones have well defined dust rims characterized by abundant clays, organic matter, fluid and other inclusions. Focusing through the sample and noting the migration of the grain boundary with depth in the sample usually identified the location of a given fluid inclusion relative to the grain boundary. Using this approach, it was possible to determine whether the inclusion was in the detrital grain or in the overgrowth. Dust rim inclusions have been studied by many workers (e.g., Fishman, 1997; Konnerup-Madsen and Dypvik, 1988; McDonald and Skilbeck, 1996; Walderhaug, 1994a, 1994b) because they are abundant and relatively large but were avoided here because inclusions trapped along the relatively weak and porous grain boundary may reequilibrate (Osborne and Haszeldine, 1993).

Ideally, one would prefer to study fluid inclusion assemblages (FIAs, Goldstein and Reynolds, 1994) comprised of several tens of inclusions to be confident that the inclusions have not leaked or otherwise reequilibrated after trapping, or during microthermometric analysis.

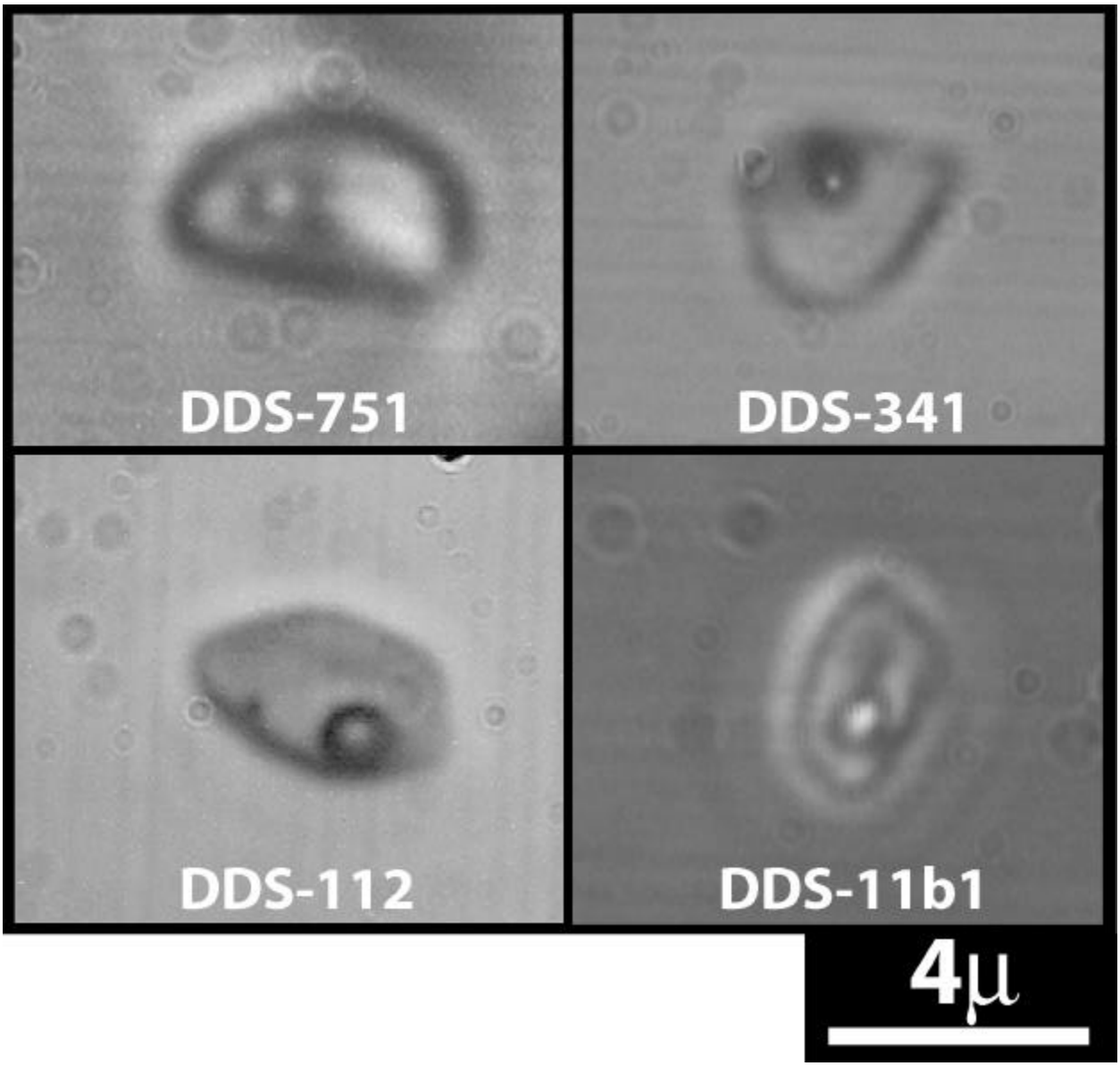

Figure 3.3 Images of selected liquid-rich aqueous fluid inclusions measured in this study. Vapor bubbles are visible in each image.

Despite countless laboratory hours spent searching for fluid inclusions in quartz cement, only seven measurable inclusions, from three sandstones, were found in authigenic quartz from the study interval. Each inclusion represents an FIA according to the terminology of Goldstein and Reynolds (1994). Thus, while the total number of inclusions measured is small compared to most other studies, they nevertheless provide important information concerning the thermal evolution of the study area. Each of the seven FIAs is unarguably in authigenic quartz, and each provides information on the temperature during quartz precipitation at that stratigraphic and geographic location.

Fluid inclusion microthermometric measurements were made using a Linkam THMSG 600 heating and cooling stage attached to an Olympus BX60 petrographic microscope and using magnifications of 1600x and 2000x. Cycling, similar to that described by Goldstein and Reynolds (1994) for heating runs, was necessary to constrain the homogenization temperatures of small inclusions. This method relies on the reappearance and the position of the vapor bubble during cooling after it is no longer visible in the inclusion. At relatively high temperatures, the optics were further degraded and homogenization was often equivocal. During the initial heating run, the sample was heated until the inclusion appeared to homogenize, and then cooled. The behavior of the bubble during cooling was carefully observed. In some inclusions, the bubble would either pop back or appear at a position within the inclusion that was different from that where it was last observed, indicating that homogenization had occurred during the heating run. This temperature was recorded as the homogenization temperature for those inclusions where the bubble popped back during cooling. In some cases the vapor bubble would slowly grow in the same location during cooling, regardless of the temperature. The homogenization temperature for

these inclusions was estimated based on the highest temperature at which the bubble was clearly visible, and on the rate of shrinkage of the vapor bubble during heating.

Vitrinite Reflectance

Carbonaceous intervals were sampled above and below the targeted sandstones within each core. Vitrinite macerals were extracted from shale and coal and then mounted in epoxy and polished. A high degree of maceral dispersion for many of the shales limited the number of measurements that could be made. Reflectance measurements (see Appendix D) were made using a McCrone MPA1 photometer. Mean maximum reflectance values were recorded and calibrated using glass standards. Sample quality and size limited the number of macerals that could be extracted per sample, but reproducible values were collected from both black shale and coal.

Temperatures estimated based on reflectance values were calibrated using SIMPLE-R_o (Suzuki et al., 1993). This method is an equation-based kinetic model that uses fewer steps than other kinetic models proposed for vitrinite reflectance data reduction. Heating rates used for thermal reconstructions were ~ 2 °C/m.y. and were estimated based on stratigraphic thickness, known chronostratigraphic markers, and an estimated average geothermal gradient. Supplementary reflectance values for coal compiled from various sources (see below) were used to increase our data set. These values are reported for stratigraphic intervals and locations near the sandstones and core locations collected for this study. These data were compiled from three sources: Pennsylvania State University Coal Database (PSUCD), West Virginia Geological and Economic Survey (WVGES) and Hower (1978). Temperatures for the supplementary reflectance data were also estimated using SIMPLE-R_o so that direct comparisons between the two data sets could be made.

RESULTS

Petrography

Fluid inclusion assemblages (FIAs) were identified in many of the overgrowths, although most inclusions were too small for microthermometric analysis (< 4 microns). The seven FIAs that contained measurable inclusions (≥ 4 microns are all two-phase (liquid > vapor). Other inclusions were sometimes observed within the FIA but were too small to be measured. Many of the inclusions had an inactive vapor bubble, perhaps resulting from the size and/or shape of the fluid inclusion (Roedder, 1971). All inclusions studied appear to be primary. They are generally randomly distributed and lack any apparent preferred alignment that would suggest an association with fractures.

Microthermometry

Microthermometric data were obtained from three sandstones (Table 3.1). Homogenization temperatures were obtained for each sample, and first and last melting temperatures were recorded for four of seven inclusions. Salinity estimates were made according to Bodnar (1993). The accuracy of the measurements was influenced by size and optical quality limitations discussed above, although measurements were reproducible. Homogenization temperatures of three inclusions from the upper Pennsylvanian Mahoning sandstone were 217°C, 230-245°C, and 230-244°. Only homogenization temperature ranges could be determined for the latter two inclusions owing to the small size of the inclusions and the fact that the bubble grew back slowly, rather than popping back, during cooling following homogenization. Lower Pennsylvanian samples homogenized at much lower temperatures. Three inclusions in the Raleigh sandstone homogenized at 148°C, 163°C, and 143-147°C. A single inclusion in the Quinnimont sample homogenized in the range 142-145°C. Freezing runs indicate that the fluids

MICROTHERMOMETRY SUMMARY

Sandstone	*sample*	*Th*	*estimated fluid system*	*salinity (wt. % NaCl)**
			Upper Pennsylvanian (Glenshaw Formation)	
Mahoning				
	DDS-751	217°C	(Ca-Na-Mg)Cl_x	13.5
	DDS-75b3	230-245°C	*first and last melt temperatures undeterminable*	
	DDS-755	230-244°C	*first and last melt temperatures undeterminable*	
			Lower Pennsylvanian (New River Formation)	
Upper Raleigh				
	DDS-112	148°C	(Ca-Na-Mg)Cl_x	1.7-3.3
	DDS-11b1	163°C	(Ca-Na-Mg)Cl_x	5.0
	DDS-11b2	143-147°C	(Ca-Na-Mg)Cl_x	3.3-6.5
Quinnimont				
	DDS-341	142-145°C	*first and last melt temperatures undeterminable*	

*Bodnar (1993)

Table 3.1 Summary of fluid inclusion microthermometric data. Samples correspond to stratigraphic locations shown on Figure 3.2.

present in the Mahoning, Raleigh and Quinnimont sandstones are probably Ca-Na-Mg-rich chlorides base on first melting temperatures below the H_2O-NaCl eutectic. Salinities for the Upper Pennsylvanian Mahoning sandstone are ~13.5 weight % NaCl (final melting temperature ≈ -9.8 to –9.3 °C), whereas salinities for the Lower Pennsylvanian Raleigh sandstone range from 1.7-6.5 weight % NaCl (final melting temperatures ≈ -4.0 to –1.0 °C). Ice melting temperatures for the Lower Pennsylvanian Quinnimont sandstone could not be determined due to the poor optics and small size of the inclusions.

Vitrinite Reflectance

Vitrinite reflectance data are summarized in Table 3.2. Values from this study and supplementary data range from 0.97-1.51 for the New River Formation and 0.85-1.39 for the Glenshaw Formation. Standard deviations for our measurements range from 0.02-0.07 R_o and are relatively consistent with values collected from other sources cited in Table 3.2. Paleotemperature estimations using SIMPLE-R_o yielded values ranging from ~ 138-177 °C (mean = 151 °C) for the New River Formation samples. Glenshaw Formation paleotemperatures range from 132-171 °C (mean = 150 °C).

DISCUSSION

Burial Conditions and Quartz Cementation, New River Formation

Homogenization temperatures measured in quartz overgrowths constrain temperatures of silica precipitation and serve as a proxy for burial conditions for upper Carboniferous strata in the Appalachian Plateau. The presence of methane in the fluid inclusions must be considered

VITRINITE REFLECTANCE VALUES

Ro	*est. T*[1]	*lithology*	*interval*	*Reference*
		UPPER PENNSYLVANIAN (GLENSHAW FORMATION)		
0.85	132 °C	black shale	unnamed	this study
1.03	143	black shale	unnamed	this study
1.39	171	black shale	Brush Creek sh.	this study
1.17	154	coal	Brush Creek	PSUCD
		Lower Pennsylvanian (New River Formation)		
1.03	143	coal	Sewell B	PSUCD
0.99	140	coal	Sewell B	PSUCD
1.01	142	coal	Sewell B	PSUCD
1.07	147	coal	Sewell	this study
1.14	152	coal	Sewell	PSUCD
1.15	153	coal	Sewell	PSUCD
1.21	160	coal	Sewell	PSUCD
1.28	165	coal	Sewell	PSUCD
1.35	170	coal	Sewell	PSUCD
1.08	148	coal	Sewell	Hower (1978)
1.01	142	coal	Sewell	Hower (1978)
0.97	138	coal	Sewell	Hower (1978)
0.99	140	coal	Sewell	Hower (1978)
1.11	151	coal	Sewell	WVGES
1.15	153	coal	Sewell	WVGES
1.30	166	coal	Sewell	WVGES
1.51	177	coal	Sewell	WVGES
1.04	144	black shale	unnamed	this study
1.00	141	black shale	unnamed	this study
0.98	139	black shale	unnamed	this study
1.17	154	coal	Beckley	WVGES
1.19	155	coal	Beckley	WVGES

[1]Suzuki et al. (1993) SIMPLE-Ro
Sources: Pennsylvania State University Coal Database (PSUCD); West Virginia Geological and Economic Survey (WVGES)

Table 3.2 Vitrinite reflectance temperatures from the study area. All temperatures were estimated using SIMPLE-R_o so that direct comparisons could be made between data from this study and supplementary data.

when studying Carboniferous age fluid inclusions within the Appalachian Plateau even though microthermometric analysis failed to show evidence for methane. Raman analyses, to test for the presence of methane, could not be conducted owing to the strong fluorescence from epoxy used to prepare the sample. Small quantities of methane can affect the interpretation of aqueous fluid inclusion measurements because it increases the vapor pressure at the homogenization temperature (Fig. 3.4), yielding homogenization temperatures that may be near or equal to trapping temperatures (Tt). The minimum concentration of methane required for Th=Tt is relatively low (4450 ppm). This concentration is the minimum value required to increase the methane bubble point curve to the pressure along the hydrostatic gradient at the measured homogenization temperature. Although methane cannot be detected in these small fluid inclusions, the presence of methane in the fluids is probable based on the widespread occurrence of coal in the central Appalachian basin as well as other potential source beds such as the underlying Devonian black shale. The good agreement between the vitrinite reflectance temperatures and fluid inclusion homogenization temperatures would suggest that the homogenization temperature is approximately equal to the trapping temperature, thus requiring no pressure correction.

Fluid inclusions measured from samples collected in southern West Virginia indicate that burial and heating of New River Formation strata is compatible with normal geothermal conditions. Except for sample DDS-11b1 (163 °C), homogenization temperatures range from 142-148 °C for Upper Raleigh and Quinnimont sandstones, resulting in burial depths greater than 4.5 kilometers for an estimated geothermal gradient of 30 °C/km. Note that we are assuming that inclusion trapping temperatures are approximately equal to formation temperatures, i.e., the measured Th does not require a pressure correction. This assumption is

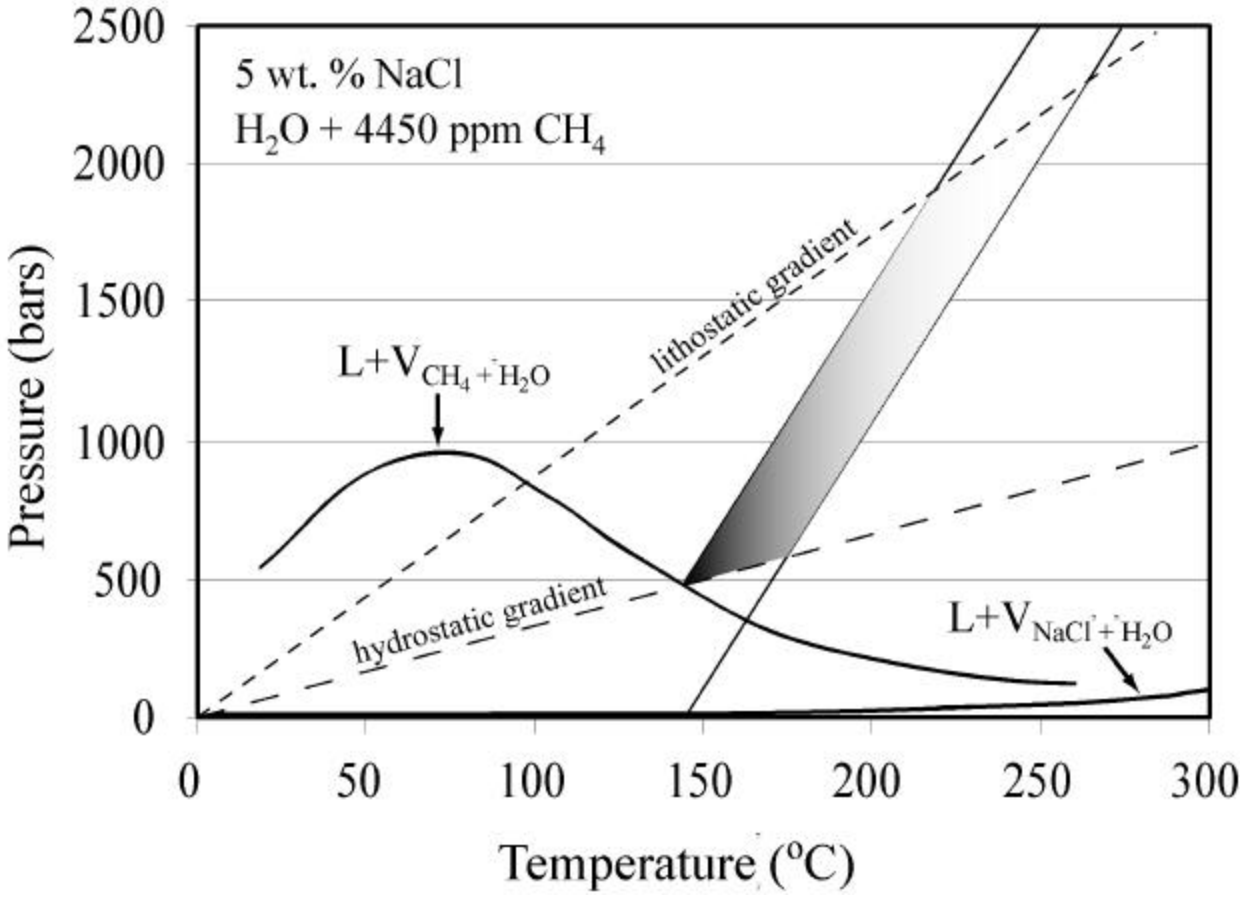

Figure 3.4 Diagenetic conditions for normal burial in the central Appalachian Basin. Shown are the isochores for an H_2O-NaCl inclusion containing 5 wt.% NaCl, and for a 5 wt.% NaCl aqueous inclusion containing 4450 ppm CH_4, both of which homogenize at 145°C. The shaded region represents inferred burial conditions for the studied sandstones, defined by the two isochores. Shading intensity represents the paleocondition probability; the darkest regions reflect the most probable conditions. Sodium chloride and methane isochore slopes = 19 bars/^{o}C. Maximum lithostatic pressure is 1.2 kilobars (4.5 km @ 2.65g/cc). Litho- and hydrostatic gradients are 8.7 bars/^{o}C and 3.3 bars/^{o}C, respectively.

supported by the effects of methane on the pressure in the inclusion at Th, as discussed below. Temperatures estimated from vitrinite reflectance data collected adjacent to Upper Raleigh and Quinnimont sandstones range from 139-147 °C (see Table 3.2) and independently support burial temperatures established by fluid inclusion microthermometry. These data are also consistent with geodynamic models that have estimated subsidence histories for Pennsylvanian strata in the Appalachian basin (Beaumont et al., 1987). In addition, conodont alteration indices (CAI) for Upper Mississippian strata in southern West Virginia range from 2 to 2.5 (Epstein et al., 1977) and are consistent with our vitrinite reflectance results.

Several sources of silica are possible for lower Pennsylvanian sandstones. Detailed petrography reveals minor pressure dissolution between detrital quartz grains. Estimating the contribution of pressure-dissolved quartz to total quartz cement is problematic (Borlykke and Egeberg, 1993; Worden and Morad, 2000) because of the three dimensional nature of the sample. Minor amounts can be observed petrographically, but the relatively large volume of quartz cement present cannot be attributed entirely to pressure dissolution. Therefore, other potential sources must be considered. Alteration of rock fragments may have contributed silica for quartz cementation (Land et al., 1987). In addition, the New River Formation contains large amounts of mudrock, suggesting that clay mineral transformations could have introduced additional silica into the system (e.g., Boles and Franks, 1979; McBride, 1989). Petrographic observations and X-ray diffraction studies of lower Pennsylvanian mudstones (Lessing and Thomson, 1973; Larese et al., 1977) reveal that illite is the predominant clay mineral. Estimated burial temperatures are in the range where smectite would be converted to illite. Although the above sources of silica are possible, the most likely source for the required large volumes of

silica is low-grade metamorphism, tectonism and related regional fluid flow during Alleghanian orogenesis. This potential source is discussed in detail in the following sections.

Burial Conditions and Quartz Cementation, Glenshaw Formation

In comparison with the New River Formation, homogenization temperatures of fluid inclusions in the Mahoning sandstone, Glenshaw Formation, appear to be anomalously high (Table 3.1). Moreover, they are *not* consistent with temperatures estimated using vitrinite reflectance from the same interval. Homogenization temperatures range from 217-245 °C, whereas vitrinite reflectance yields temperatures from 132-171 °C. This discrepancy is likely related to differences in paleohydrogeologic conditions between the organic-rich strata used for vitrinite reflectance measurements and sandstone strata used for fluid inclusion analyses. Fluid inclusion data suggest that the Mahoning sandstone served as a conduit for warm, silica-bearing fluids. Evans and Battles (1999) found evidence for warm fluids in the Valley and Ridge province, but could not find evidence for these fluids across the Allegheny Front. Our data indicate that the warm fluids may have migrated to a stratigraphic level higher than that studied by Evans and Battles (1999). Therefore, fluid expulsion into Upper Pennsylvanian sandstone aquifers from the Allegheny thrust front was likely tectonically induced. All vitrinite reflectance values reported in this study were from shale, with one supplementary value from coal. Such low permeability units would help compartmentalize the injected fluids and would not be in direct contact with the warm fluids.

Tectonically driven fluids have been proposed for various settings outside (e.g., Bradbury and Woodell, 1987; Ge and Garven, 1989; Bethke and Marshak, 1990; Wojcik et al., 1997; Travé et al., 1998; Machel and Cavell, 1999; Rossi et al., 2000) and within the Appalachians (Oliver, 1986; Dorobek, 1989; Barnaby and Read, 1992; Schedl et al., 1992; Montañez, 1994;

Evans and Battles, 1999; Kirkwood et al., 2000). More recently, studies of the Illinois Basin have recognized evidence for regional fluid migration (Fishman, 1997; Chen et al., 2001). Rowan et al. (2002) used vitrinite reflectance and fluid inclusions to decipher the thermal history of Pennsylvanian strata in the Illinois Basin. Computer modeling of the thermal evolution of the Illinois Basin indicates that observations made from fluid inclusion and vitrinite reflectance required both heating due to burial and heating from the introduction of hotter fluids (Rowan et al., 2002).

Low-grade metamorphic reactions involving pelitic rocks likely introduced relatively large volumes of silica into the system during thrust loading in the hinterland (Schedl et al., 1992; Evans and Battles, 1999), but other local sources of silica cannot be dismissed. As proposed for the New River Formation, possible sources include minor pressure dissolution, clay mineral reactions, and dissolution of rock fragments. Stratigraphic, petrologic, hydrogeologic and tectonic conditions are favorable for all four potential sources, but determining which of these processes was most important is problematic.

Silica Precipitation and Thermal Considerations

The elevated temperatures recorded by fluid inclusions in the Mahoning sandstone, compared to vitrinite reflectance values from surrounding strata, indicate that the host rock was much cooler than the injected fluid. This scenario is ideal for promoting silica precipitation. Advective fluid transport across steep isotherms will cause warm, silica-saturated fluids to become supersaturated with respect to silica as they lose heat to a much cooler host (Wood, 1986). Figure 3.5 illustrates the amount of silica (moles/kg-fluid) that will precipitate for a given fluid and host rock temperature over the temperature range that encompasses burial diagenesis and low-grade metamorphism (100 to 300 °C). The results document that a significant amount

of silica can be precipitated when warm fluids enter a cooler host rock, as has been documented above for the Glenshaw Formation.

When applied to New River Formation sandstones, it appears that only limited amounts of silica can be precipitated from the fluids migrating from the Allegheny Front into the Appalachian Plateau, but relatively large volumes of quartz cement are present in the Raleigh and Quinnimont sandstones. This observation can be explained by considering the temperature derivative of quartz-solubility as a function of temperature (Rimstidt, 1997). Figure 3.6 shows the temperature ranges for the New River and Glenshaw formation fluids and corresponding rates of silica precipitation (moles/kg-fluid) as a function of temperature. The results demonstrate that either twice as much fluid, or twice as much time, or some combination of the two, is required to produce the same amount of quartz cement in the New River Formation sandstones as in the Glenshaw Formation sandstones. Therefore, it is reasonable to conclude that much of the quartz cement observed in the New River Formation sandstones was sourced from the hinterland, assuming sufficient fluid volumes were available. In addition, our results imply that high fluxes of fluid are not required, suggesting that external, advective driven fluids are capable of generating the observed quartz cement.

If fluids 70-80 degrees Celsius warmer than surrounding rock were injected into the Mahoning sandstone, then surrounding strata should show evidence of this thermal event. The limited vitrinite reflectance data suggest that units stratigraphically near the sandstone recorded a relatively high temperature event(s). The highest reflectance value (171 °C) was collected from shale located approximately 16 meters above the Mahoning sandstone in core USGS-3, whereas a second sample from the same core located 80 meters above the Mahoning yielded a temperature of only 143 °C. Vitrinite reflectance data from a comparable stratigraphic interval

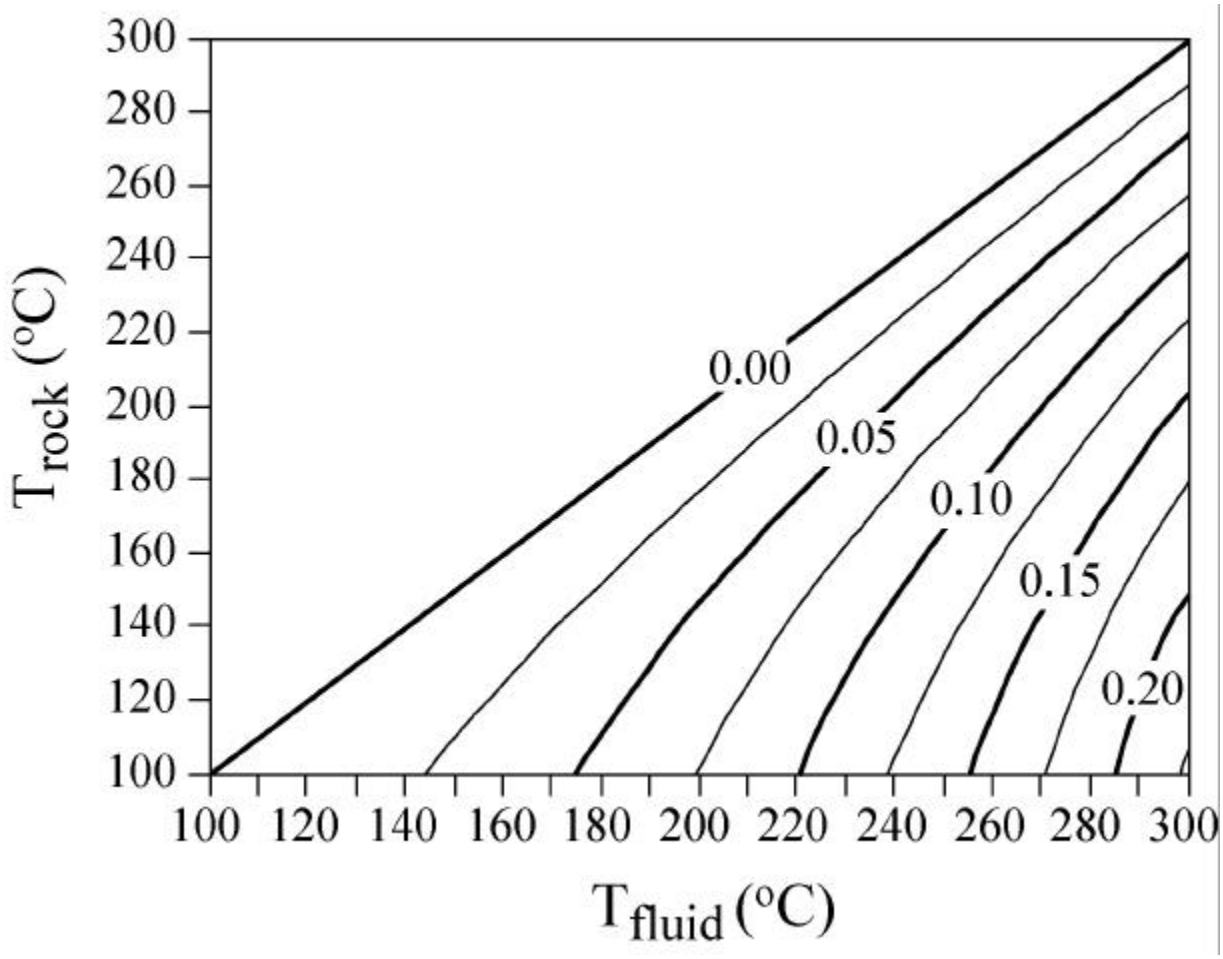

Figure 3.5 Isopleths showing the amount of silica (moles/kg-fluid) that will precipitate as a result of decreasing temperature when a fluid at temperature T_{fluid} enters a rock with temperature T_{rock}. Isopleths calculated using data from Rimstidt (1997).

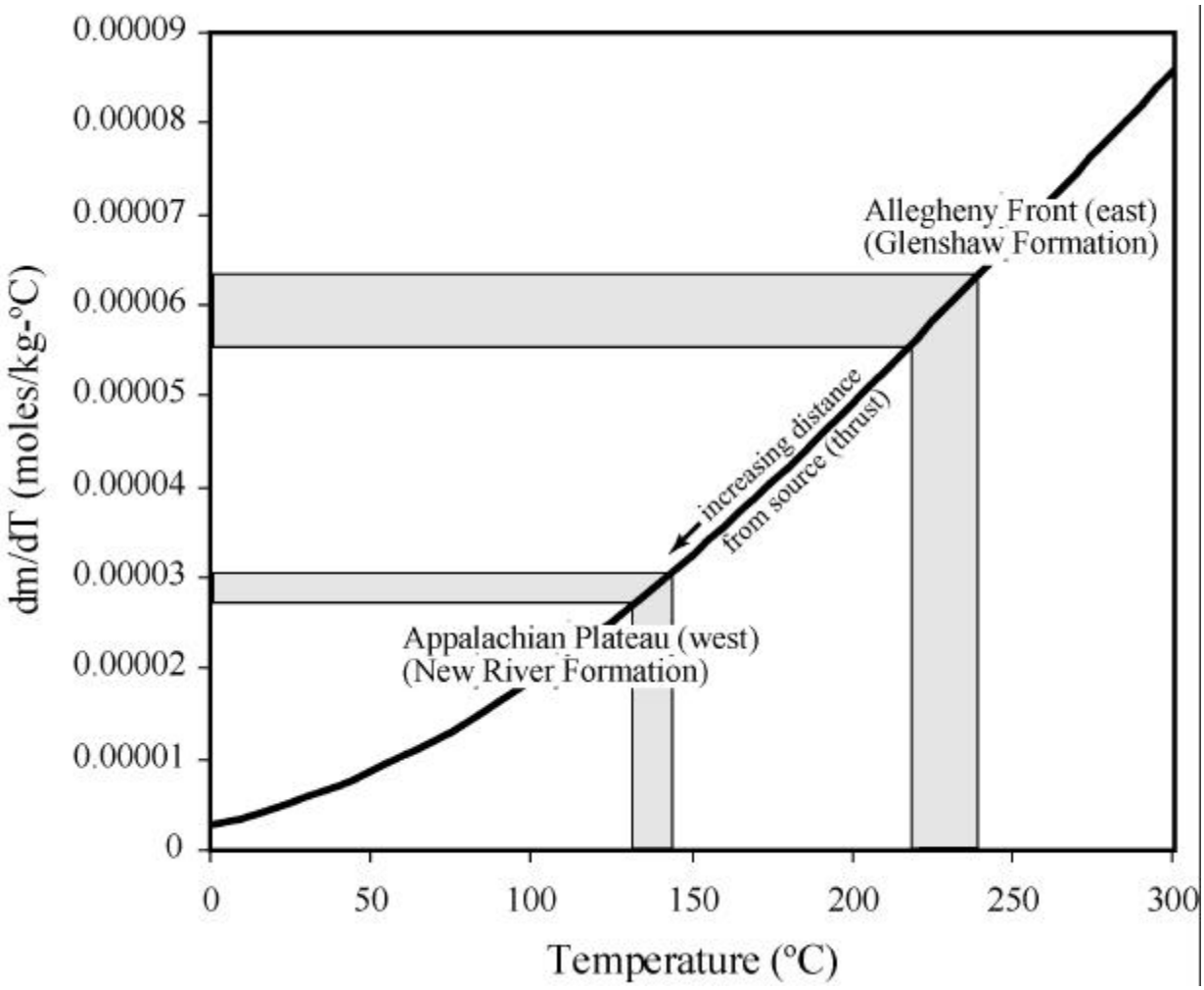

Figure 3.6 The derivative of the solubility function of quartz plotted versus temperature (Rimstidt, 1997). The results predict the amount of silica that will precipitate as a result of incremental decreases in temperature. The two temperature regimes of interest for this study are shaded. The results indicate that the amount of silica that will be precipitated as a result of temperature decrease decreases as a function of distance from the Allegheny front.

(approximately 10 meters above the previous sample) in USGS-1 yielded a temperature of 132 °C. This suggests that the Mahoning sandstone may have served as the main conduit for the high temperature fluid, and that thermal communication between it and surrounding strata decreased as a function of distance from the heat source. The local temperature gradient calculated from these conditions is greater than 500°C/km although a gradient of this magnitude was probably short-lived. Additional sampling in this area would be required to better constrain this elevated, transient geotherm.

CONCLUSIONS

Fluid inclusion microthermometry and vitrinite reflectance data indicate that Pennsylvanian strata in the central Appalachian basin were buried to depths exceeding 4.5 kilometers. The consistency between fluid inclusion and vitrinite reflectance data from within the Appalachian Plateau, and away from the thrust front, suggest that temperatures of sandstones and surrounding rocks were defined by a geothermal gradient of 30 °C/km. In contrast, only vitrinite reflectance data can be used to estimate burial depths for upper Pennsylvanian strata adjacent to the Allegheny front since fluid inclusion data record an anomalously high transient thermal gradient, resulting from the introduction of warm fluid during thrusting. Paleotemperatures from vitrinite reflectance measurements on upper Pennsylvanian samples indicate that burial depths were comparable to those further from the thrust front.

Advective flow of silica-rich fluids from the Allegheny thrust front served as a significant source of quartz cement for lower and upper Pennsylvanian sandstones. Fluid inclusions indicate that warm fluids were injected into upper Pennsylvanian sandstone aquifers during active thrusting. Differences in homogenization temperatures and temperatures determined from vitrinite reflectance measurements reveal that a steep thermal gradient existed during deep burial

diagenesis of the Glenshaw Formation adjacent to the thrust front. Data from vitrinite reflectance show that the host rock was probably greater than 70 degrees Celsius cooler than the low-grade metamorphic fluids being introduced from beneath the thrust front. These conditions promoted significant quartz precipitation, although other sources including pressure dissolution, clay mineral reactions and alteration of other detrital silicates cannot be discounted. Lower Pennsylvanian sandstones located more than 70 kilometers from the thrust were subjected to different thermal conditions. Paleotemperatures from fluid inclusions and vitrinite reflectance show no significant difference in the temperature between the host rock and the silica-bearing fluids. Regardless, calculations involving silica solubility and precipitation indicate that the same fluids that were derived from the hinterland and were responsible for cementation of the sandstones adjacent to the thrust front (Glenshaw Formation) may have contributed to the total quartz cement observed in New River Formation sandstones.

The formation of quartz cement in sandstones remains controversial, and it is important to consider driving mechanisms for fluid flow in different tectonic settings. Integrated methods are required to understand the origin of diagenetic fluids. Additional applications and future avenues for research include: 1) incremental core sampling away from the Allegheny front to test if a decrease in temperature is recorded by the quartz cement, and 2) the use of $\delta^{18}O$ as a tracer across the thrust front, for example, whether $\delta^{18}O$ values of vein quartz from the hinterland are comparable to those observed in quartz cements in foreland sandstones.

REFERENCES

Aagaard, P., Egeberg, P.K., Saigal, G.C., Morad, S., and Bjørlykke, K., 1990, Diagenetic albitization of detrital K-feldspars in Jurassic, Lower Cretaceous and Tertiary clastic reservoir rocks from offshore Norway, II. Formation water chemistry and kinetic considerations: Journal of Sedimentary Petrology, v. 60, no. 4, p. 575-581.

Aitken, J.F., and Flint, S.S., 1995, The application of high-resolution sequence stratigraphy to fluvial systems: a case study from the Upper Carboniferous Breathitt Group, eastern Kentucky, USA: Sedimentology, v. 42, p. 3-30.

Aitkinson, J., 1986, The statistical analysis of compositional data: London, Chapman, 416 p.

Allen, P.A., Crampton, S.L., and Sinclair, H.D., 1991, The inception and early evolution of the North Alpine foreland basin, Switzerland: Basin Research, v. 3, p. 143-163.

Allen, P.A., Homewood, P. and Williams, G.D., 1986, Foreland basins: An introduction, *in* Allen, P.A., and Homewood, P., eds., Foreland Basins: Special Publication, International Association of Sedimentologists 8, p. 3-12.

Arne, D., and Zentilli, M., 1994, Apatite fission track thermochronology integrated with vitrinite reflectance, *in* Mukhopadhyay, P.K., and Dow, W.G., eds., Vitrinite Reflectance as a Maturity Parameter: Applications and Limitations: American Chemical Society Symposium Series 570, p. 249-268.

Baccar, M. B., Fritz, B., and Madé, B., 1993, Diagenetic albitization of K-feldspar and plagioclase in sandstone reservoirs: thermodynamic and kinetic modeling: Journal of Sedimentary Petrology, v. 63, no. 6, p. 1100-1109.

Bachu, S., Ramon, J.C., Villegas, M.E., and Underschultz, J.R., Geothermal regime and thermal history of the Llanos Basin, Columbia: American Association of Petroleum Geologists Bulletin, v. 79, no. 1, p. 116-129.

Bailey, A.M., Roberts, H.H., and Blackson, J.H., 1998, Early diagenetic minerals and variables influencing their distributions in two long cores, Mississippi River delta plain: Journal of Sedimentary Research, v. 68, no. 1, p. 185-197.

Barker, C.E., and Goldstein, R.H., 1990, Fluid-inclusion technique for determining maximum temperature in calcite and its comparison to the vitrinite reflectance geothermometers: Geology v. 18, p. 1003-1006.

Barnaby, R.J., and Read, J.F., 1992, Dolomitization of a carbonate platform during late burial: Lower to Middle Cambrian Shady Dolomite, Virginia Appalachians: Journal of Sedimentary Petrology, v. 62, no. 6, p. 1023-104.

Barr, D., 1987, Lithospheric stretching, detached normal faulting and footwall uplift, *in* Coward, M.P., Dewey, J.F., and Hancock, P.L., eds., Continental Extensional Tectonics: Geological Society Special Publication 28, p. 75-94.

Beaumont, C., Quinlan, G.M., and Hamilton, J., 1987, The Alleghanian orogeny and its relationship to the evolution of the eastern interior, North America, *in* Beaumont, C., and Tankard, A.J., eds., Sedimentary Basins and Basin-forming Mechanisms: Canadian Society of Petroleum Geologists, Memoirs 12, p. 425-445.

Belt, E.S., and Lyons, P.C., 1989, A thrust-ridge paleodepositional model for the Upper Freeport coal bed and associated clastic facies, Upper Potomac coal field, Appalachian basin, U.S.A: International Journal of Coal Geology, v. 12, p. 293-328.

Bethke, C.M. and Marshak, S., 1990, Brine migrations across North America – The plate tectonics of groundwater: Annual Review of Earth and Planetary Sciences v. 18, p. 287-315.

Bjørkum, P.A., and Gjelsvik, N., 1988, An isochemical model for formation of authigenic kaolinite, K-feldspar and illite in sediments: Journal of Sedimentary Petrology: v. 58, no. 3, p. 506-511.

Bjørkum, P.A., Walderhaug, O., and Aase, N.E., 1993, A model for the effect of illitization on porosity and quartz cementation of sandstones: Journal of Sedimentary Petrology, v. 63, no. 6, p. 1089-1091.

Bjorlykke, K. and Egeberg, P.K., 1993, Quartz cementation in sedimentary basins: American Association of Petroleum Geologists v. 77, no. 9, p. 1538-1548.

Blackmer, G.C., Omar, G.I., and Gold, D.P., 1994, Post-Alleghanian unroofing history of the Appalachian Basin, Pennsylvania, from apatite fission track analysis and thermal models: Tectonics, v. 13, no. 5, p. 1259-1276.

Blackwell, D.D., Steele, J.L., and Carter, L.S., 1989, Heat flow database for the United States, *in* Kinsfather, O.J., and Meyers, H., eds., Geophysics of North America, CD-ROM. National Oceanographic and Atmospheric Administration, National Geophysical Data Center.

Blake, B.M., 1997, Revised lithostratigraphy and megafloral biostratigraphy of the New River and Kanawha formations (Pottsville Group: Lower and Middle Pennsylvanian) in southern West Virginia [M.S. Thesis]: Morgantown, West Virginia University, 159 p.

Bloch, S., 1994, Effect of detrital mineral composition on reservoir quality, *in* Wilson, M.D., ed., Reservoir Quality Assessment and Prediction in Clastic Rocks: SEPM, Short Course 30, p. 161-182.

Bloch, S., and McGowen, J.H., 1994, Influence of depositional environment on reservoir quality prediction, *in* Wilson, M.D., ed., Reservoir Quality Assessment and Prediction in Clastic Rocks: SEPM, Short Course 30, p. 41-57.

Bodnar, R. J., 1993, Revised equation and table for determining the freezing point depression of H_2O-NaCl solutions: Geochimica et Cosmochimica Acta, v. 57, no. 3, p. 683-684.

Boettcher, S.S., and Milliken, K.L., 1994, Mesozoic-Cenozoic unroofing of the southern Appalachian basin: apatite fission track evidence from Middle Pennsylvanian sandstones: Journal of Geology, v. 102, p. 655-663.

Boles, J.R., and Franks, S.G., 1979, Clay diagenesis in Wilcox sandstones of southwest Texas: implications of smectite diagenesis on sandstone cementation: Journal of Sedimentary Petrology, v. 49, no. 1, p. 55-70.

Bone, Y., and Russel, N.J., 1988, Correlation of vitrinite reflectance reflectivity with fluid inclusion microthermometry: assessment of the technique in the Cooper/Eromanga Basins, South Australia: Australian Journal of Earth Sciences, v. 35, p. 567-570.

Bradbury, H.J., and Woodwell, G.R., 1987, Ancient fluid flow within foreland terrains, *in* Fluid Flow in Sedimentary Basins and Aquifers, Goff, J.C., and Williams, B.P.J, eds., Geological Society Special Publication 34, p. 87-102.

Burley, S.D., Kantorowicz, J.D., Waugh, B., 1985, Clastic diagenesis, *in* Brenchley, P.J., and Williams, B.P.J., eds., Sedimentology: Recent developments and applied aspects: The Geological Society of London Special Publication 18, p. 189-226.

Burruss, R.C., 1989, Paleotemperatures from fluid inclusions: advances in theory and technique, *in* Naeser, N.D. and McCulloh, T.H., eds., Thermal History of Sedimentary Basins: Methods and Case Histories, Springer-Verlag, New York, NY, p. 119-131.

Castle, J.W., 2001, Appalachian basin stratigraphic response to convergent-margin structural evolution: Basin Research, v. 13, p. 397-418.

Cecil, C.B., 1985, Paleoclimate controls on late Paleozoic sedimentation and peat formation in the central Appalachian basin: International Journal of Coal Geology, v. 5, p. 195-230.

Cecil, C.B., 1990, Paleoclimate controls on stratigraphic repetition of chemical and siliciclastic rocks: Geology, v. 18, p. 533-536.

Chayes, F., 1949, A simple point counter for thin-section analysis: American Mineralogist, v. 34, p. 1-11.

Chen, Z., Riciputi, L.R., Mora, C.I., and Fishman, N.S., 2001, Regional fluid migration in the Illinois basin: Evidence from insitu oxygen isotope analysis of authigenic K-feldspar and quartz from the Mount Simon Sandstone: Geology v. 29, no. 12, p. 1067-1070.

Chesnut, D.R., 1994, Eustatic and tectonic control of deposition of the lower and middle Pennsylvanian strata of the central Appalachian basin, *in* Dennison, J.M., and Ettensohn, F.R., eds., Tectonic and Eustatic Controls on Sedimentary Cycles: SEPM Concepts in Sedimentology and Paleontology, Volume 4, p. 51-64.

Chuhan, F.A., Bjørlykke, K., and Lowery, C., 2000, The role of provenance in illitization of deeply buried reservoir sandstones from Haltenbanken and North Viking Graben, offshore Norway: Marine and Petroleum Geology, v. 17, no. 6, p. 673-689.

Chyi, L.L., Barnett, R.G., Burford, A.E., Quick, T.J., and Gray, R.J., 1987, Coalification patterns of the Pittsburgh coal: their origin and bearing on hydrocarbon maturation: International Journal of Coal Geology, v. 7, p. 69-83.

Crowhurst, P.V., Green, P.F., and Kamp, P.J.J., 2002, Appraisal of (U-Th)/He apatite thermochronology as a thermal history tool for hydrocarbon exploration: an example from the Taranaki basin, New Zealand: American Association of Petroleum Geologists Bulletin, v. 86, no. 10, p. 1801-1819.

Davis, M.W., and Ehrlich, R., 1974, Late Paleozoic crustal composition and dynamics in the southeastern United States, *in* Briggs, G., ed., Carboniferous of the Southeastern United States: Geological Society of America, Special Paper 148, p. 171-185.

de Boer, J.Z., McHone, J.G., Puffer, J.H., Ragland, P.C., and Whittington, D., 1988, Mesozoic and Cenozoic magmatism, *in* Sheridan, R.E., and Grow, J.A., eds., The Geology of North America, Volume I-2, The Atlantic Continental Margin, U.S., p. 217-241.

De Ros, L.F., Morad, S., and Paim, P.S.G., 1994, The role of detrital composition and climate on the diagenetic evolution of continental molasses: evidence from the Cambro-Ordovician Guaritas Sequence, southern Brazil: Sedimentary Geology, v. 92, p. 197-228.

de Souza, R.S., De Ros, L.F., and Morad, S., 1995, Dolomite diagenesis and porosity preservation in lithic reservoirs: Carmópolis Member, Sergipe-Alagoas Basin, northeastern Brazil: American Association of Petroleum Geologists, Bulletin, v. 79, no. 5, p. 725-748.

Deming, D., and Nunn, J.A., 1991, Numerical simulations of brine migration by topographically driven recharge: Journal of Geophysical Research, v. 96, no. B2, p. 2485-2499.

Deng, X., Sun, Y., Lei, X., and Lu, Q., 1996, Illite/smectite diagenesis in the NanXiang, Yitong, and North China Permian-Carboniferous basins: application to petroleum exploration in China: American Association of Petroleum Geologists, Bulletin, v. 80, no. 2, p. 157-173.

Dickinson, W.R, Beard, L.S., Brakenridge, G.R., Erjavec, J.L., Ferguson, R.C., Inman, K.F., Knepp, R.A., Lindberg, F.A. and Ryberg, P.T., 1983, Provenance of North American

Phanerozoic sandstones in relation to tectonic setting: Geological Society of America Bulletin, v. 94, no. 2, p. 222-235.

Dickinson, W.R., 1974, Plate tectonics and sedimentation, *in* Dickinson, W.R., ed., Tectonics and Sedimentation: Special Publication Society of Economic Paleontologist and Mineralogists 22, p. 1-27.

Donaldson, A.C., Renton, J.J., and Presley, M.W., Pennsylvanian deposystems and paleoclimates of the Appalachians: International Journal of Coal Geology, v. 5, p. 167-193.

Dorobek, S., 1989, Migration of orogenic fluids through the Siluro-Devonian Helderberg Group during late Paleozoic deformation: constraints on fluid sources and implications for thermal histories of sedimentary basins: Tectonophysics, v. 159, no. 1-2, p. 25-45.

dos Anjos, S.M.C., De Ros, L.F., de Souza, R.S., de Assis Silva, C .M., and Sombra, C.L., 2000, Depositional and diagenetic controls on the reservoir quality of Lower Cretaceous Penência rift basin, Brazil: American Association of Petroleum Geologists, v. 84, no. 11, p. 1719-1742.

Dott, R.H., 1964, Wacke, graywacke and matrix; what approach to immature sandstone classification?: Journal of Sedimentary Petrology, v.34, no.3, p.625-632.

Dyman, T.S., Krystinik, K.B., and Takahashi, K.I., 1988, Quantitative petrographic analysis of mid-Cretaceous sandstones, southwestern Montana: U. S. Geological Survey, Bulletin 1830, 22 p.

Ehrenberg, S.N., 1997, Influence of depositional sand quality and diagenesis on porosity and permeability: examples from Brent Group reservoirs, northern North Sea: Journal of Sedimentary Research, v. 67, no. 1, p. 197-211.

Ehrenberg, S.N., Aagaard, P., Wilson, M.J., Faser, A.R., and Duthie, D.M.L., 1993, Depth-dependent transformation of kaolinite to dickite in sandstones of the Norwegian continental shelf: Clay Minerals, v. 28, p. 325-352.

Evans, M.A., and Battles, D.A., 1999, Fluid inclusion and stable isotope analyses of veins from central Appalachian Valley and Ridge province: implications for regional synorogenic hydrologic structure and fluid migration: Geological Society of America Bulletin, v. 111, no. 12, p. 1841-1860.

Farley, K.A., 2000, Helium diffusion from apatite: General behavior as illustrated by Durango fluorapatite: Journal of Geophysical Research, v. 105, no. B2, p. 2903-2914.

Farley, K.A., Rusmore, M.E., and Bogue, S.W., 2001, Post-10 Ma uplift and exhumation of the northern Coast Mountains, British Columbia: Geology, v.29, no.2, p. 99-102.

Farley, K.A., Wolf, R.A., and Silver, L.T., 1996, The effects of long alpha-stopping distances on (U-Th)/He ages: Geochimica et Cosmochimica Acta, v. 60, no. 21, p. 4223-4229.

Feinstein, S., Kohn, B.P., and Eyal, M., 1989, Significance of combined vitrinite reflectance and fission-track studies in evaluating thermal history of sedimentary basins: an example from southern Israel, *in* Naeser, N.D. and McCulloh, T.H., eds., Thermal History of Sedimentary Basins: Methods and Case Histories, Springer-Verlag, New York, NY, p. 197-216.

Fishman, N.S., 1997, Basin-wide fluid movement in a Cambrian paleoaquifer: Evidence from the Mt. Simon sandstone, Illinois and Indiana, i*n* Basin-wide Diagenetic Patterns: Integrated Petrologic, Geochemical, and Hydrologic Considerations, Montanez, I.P., Gregg, J.M., and Shelton, K.L., eds., SEPM Special Publication 57, p. 221-234.

Fuchtbauer, H., 1983, Facies controls on sandstone diagenesis, *in* Parker, A., and Sellwood, B.W., eds., Sediment Diagenesis, NATA ASI Series, D. Reidel Publishing Company, p. 269-288.

Galehouse, J.S., 1971, Point Counting, *in* Carver, R.E., ed., Procedures in Sedimentary Petrology: New York, Wiley-Interscience, p. 385-407.

Garrels, R.M., 1984, Montmorillonite/illite stability diagrams: Clays and Clay Minerals, v. 32, p. 161-166.

Ge, S., and Garven, G., 1989, Tectonically induced transient groundwater flow in foreland basin, *in* The Origin and Evolution of Sedimentary Basins and their Energy and Mineral Resources, Price, R.A., ed., American Geophysical Union, p. 145-157.

Giles, M.R., 1997, Diagenesis: A Quantitative Perspective: Boston, MA, Kluwer Academic Publishers, 526 p.

Gillespie, W.H., and Pfefferkorn, H.W., 1979, Distribution of commonly occurring plant megafossils in the proposed Pennsylvanian system stratotype, *in* Englund, K.J., Arndt, H.H., and Henry, T.W., eds., Proposed Pennsylvanian System Stratotype, Virginia and West Virginia, AGI Selected Guidebook Series No. 1, p. 87-96.

Glagolev, A.A., 1933, On the geometrical methods of quantitative mineralogical analysis of rocks (in Russian): Transactions of the Institute of Economic Mineralogy, v. 59, p. 1-47.

Goldstein, R.H., and Reynolds, T.J., 1994, Systematics of fluid inclusions in diagenetic minerals, Society of Economic Paleontologists and Mineralogists, Short Course 31, 199 p.

Gradstein, F.M., and Ogg, J., 1996, A Phanerozoic time scale: Episodes, v. 19, p. 3-5.

Greb, S.F., and Chesnut, D.R., 1996, Lower and lower Middle Pennsylvanian fluvial to estuarine deposition, central Appalachian basin: Effects of eustasy, tectonics, and climate: Geological Society of America, Bulletin, v. 108, no. 3, p. 303-317.

Greenacre, M.J., 1984, Theory and applications of correspondence analysis: London, Academic Press, 364 p.

Guscott, S.C., and Burley, S.D., 1993, A systematic approach to reconstructing paleofluid evolution from fluid inclusions in authigenic quartz overgrowths, *in* Proceedings of Geofluids 93, Parnell, J., ed., p. 323-328.

Hamlin, H.S., Dutton, S.P., Seggie, R.J., and Tyler, N., 1996, Depositional controls on reservoir properties in a braided delta sandstone, Tirrawarra Oil Field, South Australia: American Association of Petroleum Geologists, Bulletin, v. 80, no. 2, p. 139-156.

Heald, M.T., 1965, Lithification of sandstones in West Virginia: West Virginia Geological and Economic Survey, Bulletin 30, 28 p.

Hendry, J.P., Wilkinson, M., Fallick, A.E., and Haszeldine, R.S., 2000, Ankerite cementation in deeply buried Jurassic sandstone reservoirs of the central North Sea: Journal of Sedimentary Research, v. 70, no. 1, p. 227-239.

Hiatt, E., and Kyser, K., 2000, Links between depositional and diagenetic processes in basin analysis: porosity and permeability in sedimentary rocks, *in* Kyser, K., ed., Fluids and Basin Evolution: Mineralogical Association of Canada, Short Course Series 28, p. 63-92.

Hill, M.O., and Gauch, H.G., 1980, Detrended correspondence analysis, an improved ordination technique: Vegetatio, v. 42, p. 47-58.

Hillier, S., 1994, Pore-lining chlorites in siliciclastic reservoir sandstones: electron microprobe, SEM and XRD data, and implications for their origin: Clay Minerals, v. 29, p. 665-679.

Hohn, M.E., McDowell, R.R., Matchen, D.L., and Vargo, A.G., 1997, Heterogeneity of fluvial-deltaic reservoirs in the Appalachian basin: a case study from a Lower Mississippian oil field in central West Virginia: American Association of Petroleum Geologists, Bulletin, v. 81, no. 6, p. 918-936.

House, M.A., Kohn, B.P., Farley, K.A., and Raza, A., 2002, Evaluating thermal history models for the Otway basin, southeastern Australia, using (U-Th)/He and fission-track data from borehole apatites: Tectonophysics, v. 349, p. 277-295.

Houseknecht, D.W., 1980, Comparative anatomy of a Pottsville lithic arenite and quartz arenite of the Pocahontas basin, southern West Virginia: petrogenetic, depositional, and stratigraphic implications: Journal of Sedimentary Petrology, v. 50, no. 1, p. 3-20.

Hower, J.C., 1978, Anisotropy of Vitrinite Reflectance in Relation to Coal Metamorphism for Selected United States Coals [Ph.D. thesis]: University Park, Pennsylvania; Pennsylvania State University, 356 p.

Hower, J.C., and Rimmer, S.M., 1991, Coal rank trends in the Central Appalachian coalfield: Virginia, West Virginia, and Kentucky: Organic Geochemistry, v. 17, no. 2, p. 161-173.

Hulver, M.L., 1997, Post-orogenic Evolution of the Appalachian Mountain System and its Foreland [Ph.D. Thesis]: Chicago, University of Chicago, 1055 p.

Jeans, C.V., 2000, Mineral diagenesis and reservoir quality – the way forward: an introduction: Clay Minerals, v. 35, p. 3-4.

Kamm, M.W., and Heald, M.T., 1983, Petrology and diagenesis of the Ravencliff Sandstone in West Virginia: Southeastern Geology, v. 24, no. 1, p. 1-12.

Kamp, P.J.J., Webster, K.S., and Nathan, S., 1996, Thermal history analysis by integrated modeling of apatite fission track and vitrinite reflectance data: application to an inverted basin (Buller Coalfield, New Zealand): Basin Research, v. 8, p. 383-402.

Kang-Min, Y., Boggs, S., Seyedolali, A., and Jaehong, K., 1997, Albitization of feldspars in sandstones from the Gohan (Permian) and Donggo (Permo-Triassic) formations, Gohan area, Kangwondo, Korea: Geoscience Journal (Seoul), v. 1, no. 1, p. 26-31.

Kantorowicz, J.D., 1985, The origin of authigenic ankerite from the Ninian Field, UK North Sea: Nature, v. 315, p. 214-216.

Khanna, M., Saigal, G.C., and Bølykke, K., 1997, Kaolinitization of Upper Triassic-Lower Jurassic sandstones of the Tampen Spur area, North Sea: Implications for early diagenesis and fluid flow, *in* Montañez, I.P., Gregg, J.M., and Shelton, K.L., eds., Basin-wide diagenetic patterns: integrated petrologic, geochemical, and hydrologic considerations: SEPM, Special Publication, No. 57, p. 253-268.

Kirby, E., Reiners, P.W., Krol, M.A., Whipple, K.X., Hodges, K.V., Farley, K.A., Tang, W., and Chen, Z., 2002, Late Cenozoic evolution of the eastern margin of the Tibetan Plateau: inferences from 40Ar/39Ar and (U-Th)/He thermochronology: Tectonics, v. 21, no. 1, p. 1-20.

Kirkwood, D., Ayt-Ougougdal, M., Gayot, T., Beaudoin, G., and Pironon, J., 2000, Paleofluid-flow in a foreland basin, Northern Appalachians: From syntectonic flexural extension to Taconian overthrusting: Journal of Geochemical Exploration, v. 69-70, p. 269-273.

Klein, G. deV., 1991, Geodynamics and geochemical aspects of sedimentary basin classification: Journal of African Earth Sciences, v. 13, no. 1, p. 1-11.

Klein, G.deV., and Willard, D.A., 1989, Origin of the Pennsylvanian bearing cyclothems of North America: Geology v. 17, no. 2, p. 152-155.

Konnerup-Madsen, J., and Dypvik, H., 1988, Fluid inclusions and quartz cementation in Jurassic sandstones from Haltenbanken, offshore Mid-Norway: Bulletin de Mineralogie, vol.111, no.3-4, p. 401-411.

Korus, J.T., 2002, The Lower Pennsylvanian New River Formation: A nonmarine record of glacioeustacy in a foreland basin [M.S. thesis]: Blacksburg, Virginia Tech 55 p.

Korus, J.T., and Eriksson, K.A., in review, Paleogeomorphology and facies architecture of a trunk-tributary paleovalley system: Lower Pennsylvanian New River Formation, West Virginia: Journal of Sedimentary Research.

Kosanke, R.M., and Cecil, C.B., 1996, Late Pennsylvanian climate changes and palynomorph extinctions: Review of Palaeobotany and Palynology, v. 90, p. 113-140.

Kunk, M.J., and Rice, C.L., 1994, High-precision $^{40}Ar/^{39}Ar$ age spectrum dating of sanidine from the Middle Pennsylvanian Fire Clay tonstein of the Appalachian basin, *in* Rice, C.L., ed., Elements of Pennsylvanian Stratigraphy, Central Appalachian Basin, Geological Society of America Special Paper 294, 105-113.

Land, L.S., Milliken, K.L., and McBride, E.F., 1987, Diagenetic evolution of Cenozoic sandstones, Gulf of Mexico sedimentary basin: Sedimentary Geology v. 50, no. 1-3, p. 195-225.

Langmuir, D., 1997, Aqueous Environmental Geochemistry: Prentice Hall, Upper Saddle River, New Jersey, 600 p.

Lanson, B., Beaufort, D., Berger, G., Bauer, A., Cassagnabère, A., and Meunier, A., 2002, Authigenic kaolin and illitic minerals during burial diagenesis of sandstones: a review: Clay Minerals, v. 37, p. 1-22.

Larese, R.E., Lessing, P., Seckel, J.A., and VanWie, W.A., 1977, Clays of West Virginia Part II. Open-File Report, West Virginia Geological and Economic Survey 109 p.

Law, B.E., Shah, S.H.A., and Malik, M.A., 1998, Abnormally high formation pressures, Potwar Plateau, Pakistan, *in* Law, B.E., Ulmishek, G.F., and Slavin, V.I., eds., Abnormal pressures in hydrocarbon environments: American Association of Petroleum Geologists, Memoir 70, p. 247-258.

Leischer, K., Welte, D.H., and Littke, R., 1993, Fluid inclusions and organic maturity parameters as calibration tools in basin modeling, *in* Basin Modeling: Advances and Applications, Doré, A.G., Augustson, J. H., Hermanrud, C., Stewart, D. J., Sylta, O., eds., 161-172.

Lessing, P. and Thomson, R.D. (1973): Clays of West Virginia Part 1. Mineral Resources Series 3, West Virginia Geological and Economic Survey, 190 p.

Levine, J.R., and Davis, A., 1989, The relationship of coal optical fabrics to Alleghanian tectonic deformation in the central Appalachian fold-and-thrust belt, Pennsylvania: Geological Society of America Bulletin, v. 101, no. 10, p. 1333-1347.

Lowry, P. and Jacobsen, T., 1993, Sedimentological and reservoir characteristics of a fluvial-dominated delta-front sequence: Ferron Sandstone Member (Turonian), east central Utah, USA, *in* Ashton, M., ed., Advances in Reservoir Geology: Geological Society, Special Publication No. 69, p. 81-103

Machel, H.G., and Cavell, P.A., 1999, Low-flux, tectonically-induced squeegee fluid flow ("hot flash") into the Rocky Mountain Foreland Basin: Bulletin of Canadian Petroleum Geology v. 47, no. 4, p. 510-533.

Martino, R.L., and Belt, E.S., 2001, Facies architecture and allocycles in the Glenshaw Formation (Upper Pennsylvanian), upper Potomac basin, Maryland/West Virginia: Abstracts with Programs – Geological Society of America, v. 33, no. 6, p. 78.

McBride, E.F., 1989, Quartz cement in sandstones: a review: Earth-Science Reviews v. 26, p. 69-112.

McCune, B., and Mefford, M.J., 1999, PC-ORD: multivariate analysis of ecological data. Version 4.10. Gleneden Beach, Oregon, MjM Software Design.

McDonald, S.J. and Skilbeck, C.G., 1996, Authigenic fluid inclusions in lithic sandstone: a case study from the Permo-Triassic Gunnedah Basin, New South Wales: Australian Journal of Earth Sciences, v. 43, no. 2, p. 217-228.

McDowell, R.J., 1986, An interpretation of the Grafton sandstone and its implications for Pennsylvanian paleohydraulics, climate, provenance, and tectonics: Compass of Sigma Gamma Epsilon, v. 63, no. 2, p. 48-57.

McKay, J.L., Longstaffe, F.J., and Plint, A.G., 1995, Early diagenesis and its relationship to depositional environment and relative sea-level fluctuations (Upper Cretaceous Marshybank Formation, Alberta and British Columbia): Sedimentology, v. 42, p. 161-190.

Milici, R.C., and de Witt, W., 1988, The Appalachian Basin, i*n* Sedimentary Cover – North American Craton: U.S., Sloss, L.L., ed., p. 427-469.

Miller, A.I., Holland, S.M., Meyer, D.L., and Dattilo, B.F., 2001, The use of faunal gradient analysis for intraregional correlation and assessment of changes in sea-floor topography in the type Cincinnatian: Journal of Geology, v. 109, p. 603-613.

Miller, D.J., and Eriksson, K.A., 2000, Sequence stratigraphy of Upper Mississippian strata in the central Appalachians: a record of glacioeustacy and tectonoeustacy in a foreland basin setting: American Association of Petroleum Geologists, Bulletin, v. 84, no. 2, p. 210-233.

Miller, J.D., and Kent, D.V., 1988, Regional trends in the timing of Alleghanian remagnetization in the Appalachians: Geology, v. 16, no. 7, p. 588-591.

Milliken, K.L., 1998, Carbonate diagenesis in non-marine foreland sandstones at the western edge of the Alleghanian overthrust belt, southern Appalachians, *in* Morad, S., ed., Carbonate Cementation in Sandstones: International Association of Sedimentologists, Special Publication 26, p. 87-105.

Milliken, K.L., 2001, Diagenetic heterogeneity in sandstone at the outcrop scale, Breathitt Formation (Pennsylvanian), eastern Kentucky: American Association of Petroleum Geologists, Bulletin, v. 85, no. 5, p. 795-815.

Montanez, I.P., 1994, Late diagenetic dolomitization of Lower Ordovician Upper Knox carbonates: a record of the hydrodynamic evolution of the southern Appalachian basin: American Association of Petroleum Geologists, v. 78, no. 8, p. 1210-1239.

Morad, S., 1990, Mica alteration reactions in Jurassic reservoir sandstones from the Haltenbanken area, offshore Norway: Clays and Clay Minerals, v. 38, no. 6, 584-590.

Morad, S., Ketzer, J.M., and De Ros, L.F., 2000, Spatial and temporal distribution of diagenetic alterations in siliciclastic rocks: implications for mass transfer in sedimentary basins: Sedimentology, v. 47, p. 95-120.

Nadon, G.C., 1998, Magnitude and timing of peat-to-coal compaction: Geology, v. 26, no. 8, p. 727-730.

Nadon, G.C., and Issler, D.A., 1997, The timing and magnitude of floodplain compaction: Geoscience Canada, v. 24, no. 1, p. 37-43

Naeser, N.D., Naeser, C.W., and McCulloh, T.H., 1989, The application of fission-track dating to the depositional and thermal history of rocks in sedimentary basins, *in* Naeser, N.D. and McCulloh, T.H., eds., Thermal History of Sedimentary Basins: Methods and Case Histories, Springer-Verlag, New York, NY, p. 157-180.

Nelson, W.A., and Read, J.F., 1990, Updip to downdip cementation and dolomitization patterns in a Mississippian aquifer, Appalachians: Journal of Sedimentary Petrology, v. 60, no. 3, p. 379-396.

Nentwich, F.W., and Yole, R.W., 1997, Petrology and diagenetic history of deltaic litharenites, Oligocene Kugmallit Sequence, Beaufort-Mackenzie Basin, Arctic Canada: Bulletin of Canadian Petroleum Geology, v. 45, no. 3, p. 339-355.

Net, L.I., Alonso, M.S., and Limarino, C.O., 2002, Source rock and environmental control on clay mineral associations, Lower Section of Paganzo Group (Carboniferous), northwest Argentina: Sedimentary Geology, v. 152, no. 3-4, p. 183-199.

Niemann, J.C., and Read, J.F., 1988, Regional cementation from unconformity-recharged aquifer and burial fluids, Mississippian Newman Limestone, Kentucky: Journal of Sedimentary Petrology, v. 58, no. 4, p. 688-705.

O'Sullivan, P.B., 1999, Thermochronology, denudation and variations in palaeosurface temperature: a case study from the North Slope foreland basin, Alaska: Basin Research, v. 11, p. 191-204.

Oliver, J., 1986, Fluids expelled tectonically from orogenic belts: Their role in hydrocarbon migration and other geologic phenomena: Geology, v. 14, no. 2, p. 99-102.

Opdyke, N.D., Roberts, J., Claoué-Long, J., Irving, E., and Jones, P.J., 2000, Base of Kiaman: Its definition and global stratigraphic significance: Geological Society of America Bulletin, v. 112, no. 9, p. 1315-1341.

Osborne, M., and Haszeldine, S., 1993, Evidence for resetting of fluid inclusion temperatures from quartz cements in oilfields: Marine and Petroleum Geology, v. 10, no. 3, p. 271-278.

Pazzaglia, F.J., and Brandon, M.T., 1996, Macrogeomorphic evolution of the post-Triassic Appalachian mountains determined by the deconvolution of the offshore basin sedimentary record: Basin Research, v. 8, p. 255-278.

Pazzaglia, F.J., and Gardner, T.W., 1994, Late Cenozoic flexural deformation of the middle U.S. Atlantic passive margin: Journal of Geophysical Research, v. 99, no. B6, p. 12,143-12,157.

Pennsylvania State University Coal Database (http://www.ems.psu.edu/COPL/coal.html).

Poag, C.W., and Sevon, W.D., 1989, A record of Appalachian denudation in postrift Mesozoic and Cenozoic sedimentary deposits of the U.S. middle Atlantic continental margin: Geomorphology, v. 2, p. 119-157.

Primmer, T.J., Cade, C.A., Evans, J., Gluyas, J.G., Hopkins, M.S., Oxtoby, N.H., Smalley, P.C., Warren, E.A., and Worden, R.H., 1997, Global patterns in sandstone diagenesis: their application to reservoir quality prediction for petroleum exploration, *in* Kupecz, J.A., Gluyas, J., and Bloch, S., eds., Reservoir quality prediction in sandstones and carbonates: American Association of Petroleum Geologists, Memoir 69, p. 61-77.

Pytte, A.M., and Reynolds, R.C., 1989, The thermal transformation of smectite to illite, *in* Naeser, N.D, and McCulloh, T.H., eds., Thermal History of Sedimentary Basins: Methods and Case Histories: Springer-Verlag, New York, p. 133-140.

Quinlan, G.M., and Beaumont, C., 1984, Appalachian thrusting, lithospheric flexure, and Paleozoic stratigraphy of the Eastern Interior of North America: Canadian Journal of Earth Sciences v. 21, p. 973-996.

Ramm, M., 2000, Reservoir quality and its relationship to facies and provenance in Middle to Upper Jurassic sequences, northeastern North Sea: Clay Minerals, v. 35, p. 77-94.

Rasbury, E.T., Hanson, G.N., Meyers, W.J., Holt, W.E., Goldstein, R.H., and Saller, A.H., 1998, U-Pb dates of paleosols: Constraints on late Paleozoic cycle durations and boundary ages: Geology, v. 26, no. 5, p. 403-406.

Reed, J.S., Bodnar, R.J, Eriksson, K.A., and Rimstidt, J.D., in prep (a), Paleothermometry and quartz authigenesis in Pennsylvanian sandstones, central Appalachian basin: application of fluid inclusions and vitrinite reflectance: Canadian Mineralogist.

Reed, J.S., Spotila, J.A., Eriksson, K.A., and Bodnar, R.J., in review (b), The downs and ups of Pennsylvanian strata: central Appalachian basin: Geology.

Reiners, P.W., Brady, R., Farley, K.A., Fryxell, J.E., Wernicke, B.P., and Lux, D., 2000, Helium and argon thermochronometry of the Gold Butte block, South Virgin Mountains, Nevada: Earth and Planetary Science Letters, v. 178, p. 315-326.

Reyment, R.A., and Savazzi, E., 1999, Aspects of multivariate statistical analysis in geology: Amsterdam, Elsevier, 285 p.

Rimstidt, J.D., 1997, Quartz solubility at low temperatures: Geochimica et Cosmochimica Acta, v. 61, no. 13, p. 2553-2558.

Robinson, R.A.J., and Prave, A.R. 1995, Cratonal contributions to a “classic” molasses: the Carboniferous Pottsville Formation of eastern Pennsylvania revisited: Geology, v. 23, no. 4, p. 369-372.

Roden, M.K., 1990, Apatite fission-track thermochronology of the southern Appalachian basin: Maryland, West Virginia, and Virginia: Journal of Geology, v. 99, p. 41-53.

Roden, M.K., and Miller, D.S., 1989, Apatite fission-track thermochronology of the Pennsylvania Appalachian basin: Geomorphology, v. 2, p. 39-51.

Roden, M.K., Cerveny, P.F., and Bergman, S.C., 1992, Apatite fission track thermochronology of the Appalachian foreland basin from the Virginia piedmont to eastern Ohio: Geological Society of America Abstracts with Programs, v. 24, p. A237.

Roden, M.K., Cerveny, P.F., and Bergman, S.C., 1992, Apatite fission track thermochronology of the Appalachian foreland basin from the Virginia piedmont to eastern Ohio: Geological Society of America Abstracts with Programs, v. 24, p. A237.

Roedder, E., 1971, Metastability in fluid inclusions: Society of Mining Geology, Japan, Special Issue 3, p. 327-334.

Roedder, E., 1984, Fluid inclusions: Reviews in Mineralogy 12.

Rollinson, H.R., 1992, Another look at the constant sum problem in geochemistry: Mineralogical Magazine, v. 56, p. 469-475.

Rossi, C., Goldstein, R.H., and Marfil, R., 2000, Pore fluid evolution and quartz diagenesis in the Khatatba Formation, Western Desert, Egypt: Journal of Geochemical Exploration, v. 69-70, p. 91-96.

Rossi, C., Marfil, R., Ramseyer, K., and Permanyer, A., 2001, Facies-related diagenesis and multiphase siderite cementation and dissolution in the reservoir sandstones of the Khatatba Formation, Egypt's western desert: Journal of Sedimentary Research, v. 71, no. 3, p. 459-472.

Rowan, E.L., Goldhaber, M.B. and Hatch, J.R., 2002, Regional fluid flow as a factor in the thermal history of the Illinois basin: Constraints from fluid inclusions and the maturity of Pennsylvanian coals: American Association of Petroleum Geologists, v. 86, no. 2, p. 257-277.

Saigal, G.C., Morad, S., Bjørlykke, K., Egeberg, P. K., and Aagaard, P., 1988, Diagenetic albitization of detrital K-feldspar in Jurassic, Lower Cretaceous, and Tertiary clastic reservoir rocks from offshore Norway, I. Textures and origin: Journal of Sedimentary Petrology, v. 58, no. 6, p. 1003-1013.

SAS Institute, 2001, SAS/IML software, version 8.02: Cary, North Carolina, SAS Institute.

Sinclair, H.D., 1997, Tectonostratigraphic model for underfilled peripheral basins: An alpine perspective: Geological Society of America Bulletin, v. 109, no. 3, p. 324-346.

Sippel, R.F., 1968, Sandstone petrology, evidence from luminescence petrography: Journal of Sedimentary Petrology v. 38, no. 2, p. 530-554.

Slingerland, R., and Furlong, K.P., 1989, Geodynamic and geomorphic evolution of the Permo-Triassic Appalachian Mountains: Geomorphology, v. 2, p. 23-37.

Spotila, J.A., Bank, G.C., Reiners, P.W., Naeser, C.W., and Henika, W.S., in review, Origin of the Blue Ridge escarpment along the passive margin of North America: Basin Research.

Spotila, J.A., Farley, K., and Sieh, K.E., 1998, Uplift and erosion of the San Bernardino Mountains associated with transpression along the San Andreas fault, California, as constrained by radiogenic helium thermochronometry: Tectonics, v. 17, p. 360-378.

Spötl, C., Houseknecht, D.W., and Longstaffe, F.J., 1994, Authigenic chlorites in sandstones as indicators of high-temperature diagenesis, Arkoma foreland basin, USA: Journal of Sedimentary Research, v. A64, no. 3, p. 553-566.

Suzuki, N., Matsubayashi, H., and Waples, D.W., 1993, A simpler kinetic model of vitrinite reflectance: American Association of Petroleum Geologists Bulletin, v. 77, p. 1502-1508.

Tabor, N.J., and Montañez, I.P., 2002, Shifts in late Paleozoic atmospheric circulation over western equatorial Pangea: insights from mineral $\delta^{18}O$ compositions: Geology, v. 30, no. 12, p. 1127-1130.

Tankard, A., 1986, Depositional response to foreland deformation in the Carboniferous of eastern Kentucky: American Association of Petroleum Geologists, Bulletin, v. 70, no. 7, p. 853-868.

Tobin, R.C., and Claxton, B.L., 2000, Multidisciplinary thermal maturity studies using vitrinite reflectance and fluid inclusion microthermometry: A new calibration of old techniques: American Association of Petroleum Geologist Bulletin v. 84, p. 1647-1665.

Travé, A., Labaume, P., Calvet, F., Soler, A., Tritlla, J., Buatier, M., Potdevin, J.-L., Séguret, M., Raynaud, S., and Briqueu, L., 1998, Fluid migration during Eocene thrust emplacement in the south Pyrenean foreland basin (Spain): An integrated structural, mineralogical and geochemical approach, *in* Cenozoic Foreland Basins of Western Europe, Mascle, A., Puigdefàbregas, C., Luterbacher, H.P., and Fernàndez, M.,eds., Geological Society Special Publication 134, p. 163-188.

Vitorello, I., and Pollack, H.N., 1980, On the variation of continental heat flow with age and thermal evolution of continents: Journal of Geophysical Research, v. 85, no. B2, p. 983-995.

von Eynatten, H., Barcelo-Vidal, C., and Pawlowsky-Glahn, V., 2003, Composition and discrimination of sandstones: a statistical evaluation of different analytical methods: Journal of Sedimentary Research, v. 73, no. 1, p. 47-57.

Walderhaug, O., 1994a, Precipitation rates for quartz cement in sandstones determined by fluid-inclusion microthermometry and temperature-history modeling: Journal of Sedimentary Research, v. A64, no. 2, p. 324-333.

Walderhaug, O., 1994 b, Temperatures of quartz cementation in Jurassic sandstones from the Norwegian continental shelf – evidence from fluid inclusions: Journal of Sedimentary Research, v. A64, no. 2, p. 311-323.

Weibel, R., 1998, Diagenesis in oxidizing and locally reducing conditions – an example form the Triassic Skagerrak Formation, Denmark: Sedimentary Geology, v. 121, p. 259-276

Willard, D.A., and Klein, G.deV., 1990, Tectonic subsidence history of the central Appalachian basin and its influence on Pennsylvanian coal deposition: Southeastern Geology, v. 30, no. 4, p. 217-239.

Wilson, M.D., ed., 1994, Reservoir Quality Assessment and Prediction in Clastic Reservoirs: SEPM Short Course 30, 432 p.

Wojcik, K.M., Goldstein, R.H. and Walton, A.W., 1997, Regional and local controls of diagenesis driven by basin-wide flow system: Pennsylvanian sandstones and limestones, Cherokee Basin, Southeastern Kansas, *in* Basin-wide Diagenetic Patterns: Integrated Petrologic, Geochemical, and Hydrologic Considerations, Montanez, I.P., Gregg, J.M., and Shelton, K.L., eds., SEPM Special Publication 57, p. 235-252.

Wojcik, K.M., Goldstein, R.H., and Walton, A.W., 1997, History of diagenetic fluids in a distant foreland area, Middle and Upper Pennsylvanian Cherokee basin, Kansas, USA: Fluid inclusion evidence: Geochimica et Cosmochimica Acta, v. 58, no. 3, p. 1175-1191.

Wolf, R.A., Farley, K.A., and Silver, L.T., 1996, Helium diffusion and low-temperature thermochronometry of apatite: Geochimica et Cosmochimica Acta, v. 60, no. 21, p. 4231-4240.

Wood, J.R., 1986, Thermal transfer in systems containing quartz and calcite, i*n* Roles of Organic Matter in Sedimentary Diagenesis, Gautier, D.L., ed., SEPM Special Publication 38, p. 169-180.

Worden, R.H. and Morad, S., 2000, Quartz cementation in oil field sandstones: a review of the key controversies, *in* Quartz Cementation in Sandstones, Worden R.H., and Morad, S. eds., International Association of Sedimentologists Special Publication 29, p. 1-20.

Worden, R.H., Ruffell, A.H., and Cornford, C., 2000, Palaeoclimate, sequence stratigraphy and diagenesis: Journal of Geochemical Exploration, v. 69-70, p. 453-457.

Zhang, E., and Davis, A., 1993, Coalification patterns of the Pennsylvanian coal measures in the Appalachian foreland basin, western and south-central Pennsylvania: Geological Society of America Bulletin, v. 105, p. 162-174.

APPENDIX A
Petrographic Data Matrix

Upper Pennsylvanian Sandstones

Sample	Qm	Qp	Lm	Ls	Lv	Fk	Fp	Musc	Biot	Heav	Org	Ilm	Pp	Ps	Qcs	Kaol	Fab	Illr	Illc	Chl	Calc	Sid	Dol	Ank	Fe+3	Pyr
Grafton (M-60)																										
DDS-93	215	17	12	0	0	6	0	12	6	1	1	0	0	0	0	2	0	85	3	30	0	0	3	0	7	0
DDS-94	263	14	4	1	0	2	0	1	0	0	0	0	0	2	2	17	0	5	0	2	3	23	52	7	1	1
DDS-95	294	23	9	6	0	4	0	6	1	0	0	0	1	3	2	7	0	19	1	1	7	1	6	2	5	2
DDS-96	303	18	7	6	0	3	0	3	0	0	2	0	2	2	2	16	0	16	0	3	5	0	3	0	8	1
DDS-97	206	8	16	0	0	4	0	15	1	0	0	0	8	55	0	0	0	44	1	14	6	0	6	4	11	1
DDS-98	234	14	23	5	0	6	0	9	3	0	3	0	0	0	1	1	0	59	2	24	4	0	3	0	9	0
DDS-99	216	17	25	1	0	10	0	17	2	1	0	0	0	0	0	0	0	49	2	22	15	0	10	1	12	0
DDS-100	220	29	16	1	0	7	0	13	3	0	2	0	0	0	0	0	0	26	0	14	33	0	23	1	10	2
Saltsburg (M-60)																										
DDS-101	210	38	16	4	0	5	0	18	0	0	5	0	7	39	0	1	0	35	2	7	0	0	2	1	9	1
DDS-102	285	36	10	15	0	2	0	0	1	0	3	0	2	6	1	9	0	10	0	3	2	0	15	0	0	0
DDS-103	257	32	19	8	0	7	0	2	0	1	5	0	4	14	0	11	0	23	1	6	1	0	6	0	3	0
DDS-104	283	27	5	5	0	1	0	1	1	1	1	1	0	6	4	20	0	9	0	5	2	1	26	0	1	0
DDS-105	309	22	8	8	0	1	0	2	0	0	1	0	0	0	2	14	0	8	0	1	2	4	12	0	5	1
DDS-106	260	23	20	11	0	3	0	8	0	0	6	0	0	0	3	3	0	25	1	3	0	5	9	8	12	0
DDS-107	275	11	9	3	0	1	0	7	0	0	5	0	12	28	1	2	0	11	0	0	1	7	5	7	14	1
DDS-108	272	20	16	1	0	7	0	6	1	1	2	0	7	9	1	15	0	19	1	7	2	1	10	2	0	0
DDS-109	277	16	6	1	0	5	0	0	0	0	1	0	3	11	2	16	0	11	0	9	3	0	35	1	1	2
DDS-110	259	21	7	6	0	1	0	1	0	1	0	0	2	5	3	12	0	35	0	17	2	0	14	2	3	9
Saltsburg (USGS-3)																										
DDS-57	138	76	27	47	0	4	0	7	1	0	0	0	0	0	1	0	0	38	1	2	0	0	40	0	13	5
DDS-59	181	52	48	18	0	4	0	8	0	0	0	0	0	0	1	0	0	37	0	8	2	0	17	7	11	6
DDS-61	208	58	11	20	0	2	0	4	0	0	0	0	5	16	3	7	0	11	2	3	4	0	23	15	3	5
DDS-62	254	51	21	14	0	0	0	2	1	1	0	0	4	12	2	0	0	26	0	1	1	0	6	2	2	0
DDS-63	170	56	44	20	0	5	0	22	0	0	0	0	0	0	2	2	0	40	4	2	6	0	0	3	19	5
DDS-64	269	36	22	23	0	3	0	4	0	0	1	0	0	0	5	0	0	19	0	1	3	0	10	1	2	1
DDS-65	234	42	14	18	0	7	0	7	0	0	0	0	10	16	6	4	0	15	3	2	5	7	1	4	3	2
DDS-66	287	30	13	11	0	5	0	1	1	0	0	0	1	2	5	0	0	25	0	3	1	1	11	0	2	1
DDS-67	233	45	11	17	0	5	0	0	0	0	0	0	7	11	40	21	0	7	0	1	0	0	0	0	0	2

Sample	Qm	Qp	Lm	Ls	Lv	Fk	Fp	Musc	Biot	Heav	Org	Ilm	Pp	Ps	Qcs	Kaol	Fab	Illr	Illc	Chl	Calc	Sid	Dol	Ank	Fe+3	Pyr
DDS-68	274	32	21	18	0	4	0	3	0	1	1	0	2	5	5	0	0	29	0	0	0	0	0	0	4	1
DDS-69	208	50	40	19	0	5	0	4	0	0	0	0	1	3	5	3	0	13	1	2	1	0	0	1	12	32
Saltsburg (MD-4)																										
MD4-37	214	24	45	6	0	2	0	10	1	0	0	1	0	0	12	3	0	17	2	48	3	4	0	0	4	4
Saltsburg (USGS-1)																										
DDS-37	175	49	80	18	0	0	0	23	0	0	3	0	0	0	3	0	0	30	7	6	0	0	0	0	0	6
DDS-39	106	34	27	0	0	0	0	1	0	0	0	0	0	1	1	0	0	2	1	6	3	0	201	17	0	0
DDS-40	237	34	33	5	0	7	0	21	4	0	0	0	0	0	0	15	0	25	0	7	1	0	6	0	5	0
DDS-41	202	35	70	7	0	5	0	10	1	0	0	1	1	1	0	1	0	32	13	11	2	0	0	0	1	7
DDS-43	203	38	49	4	0	0	0	8	0	0	0	1	0	0	0	0	0	38	9	8	1	0	0	4	20	17
DDS-44	182	8	25	5	0	2	0	12	0	0	1	0	0	0	0	0	0	43	0	1	73	2	27	11	8	0
DDS-45	227	30	36	11	0	3	0	7	0	0	0	0	2	21	4	1	0	23	9	6	2	0	0	3	9	6
DDS-46	182	29	38	4	0	0	0	11	1	0	0	3	0	0	4	0	0	34	6	6	3	0	0	0	75	4
DDS-47	260	52	6	1	0	0	0	0	0	0	0	1	0	1	14	0	0	10	2	4	0	28	2	0	17	2
Buffalo (MD-4)																										
MD4-24	312	29	3	3	0	0	1	0	0	0	0	0	2	1	31	3	0	1	2	0	6	1	3	2	0	0
Buffalo (M-60)																										
DDS-111	260	26	22	7	0	3	0	6	1	0	0	0	4	6	3	4	0	25	0	4	1	0	16	2	8	2
DDS-112	211	38	22	6	0	4	0	13	1	0	4	0	3	9	0	2	0	52	3	14	1	6	5	4	1	1
DDS-113	239	45	23	6	0	3	0	4	0	0	0	0	1	12	3	7	0	30	0	8	0	0	5	2	11	1
DDS-114	246	78	10	9	0	0	0	0	0	0	0	0	0	1	0	1	0	16	0	1	3	0	33	0	2	0
Mahoning (USGS-3)																										
DDS-70	318	23	9	10	0	0	0	2	0	0	0	0	0	3	6	1	0	23	2	0	0	0	0	0	1	2
DDS-71	249	40	12	2	0	3	0	1	0	0	0	0	1	2	19	11	0	8	1	3	7	37	0	0	2	2
DDS-72	303	18	6	5	0	0	0	0	0	2	1	0	2	15	15	1	0	8	0	1	2	12	2	1	3	3
DDS-73	265	50	13	1	0	4	0	3	0	0	0	0	4	6	23	13	0	5	1	1	1	0	0	4	3	3
DDS-74	275	45	2	6	0	0	0	1	0	0	0	0	0	0	13	23	0	1	1	0	5	2	0	7	14	5
DDS-75	285	52	8	2	0	1	0	1	0	0	0	0	5	7	23	5	0	2	1	1	4	0	0	3	0	0
DDS-76	296	46	4	2	0	0	0	0	0	0	0	0	4	19	21	0	0	1	0	0	7	0	0	0	0	0
DDS-77	198	58	31	26	0	0	0	13	2	0	0	0	0	0	11	1	0	20	4	12	2	0	0	0	17	5

Sample	Qm	Qp	Lm	Ls	Lv	Fk	Fp	Musc	Biot	Heav	Org	Ilm	Pp	Ps	Qcs	Kaol	Fab	Illr	Illc	Chl	Calc	Sid	Dol	Ank	Fe+3	Pyr
Mahoning (MD-4)																										
MD4-9	239	52	37	2	0	3	0	7	0	0	0	0	2	6	14	11	0	11	0	2	10	1	0	1	2	0
MD4-7	270	48	2	0	0	1	0	0	0	0	0	1	9	6	34	1	0	2	0	5	11	7	0	0	1	2
Mahoning (M-60)																										
DDS-115	194	37	36	23	0	2	0	14	1	0	7	0	0	0	0	0	0	57	5	1	8	6	1	1	7	0
DDS-116	218	39	28	9	0	6	0	16	0	1	2	0	0	0	2	1	0	49	4	6	6	1	2	1	9	0
DDS-117	245	37	21	14	0	6	0	7	0	0	7	0	0	0	0	0	0	45	4	2	6	0	0	1	5	0
DDS-118	281	46	3	5	0	1	0	0	0	0	0	0	4	8	6	14	0	2	0	0	26	0	1	0	1	2
Mahoning (MD-5)																										
MD5-22	292	24	12	5	0	1	0	1	0	0	0	0	1	1	24	1	0	0	0	0	5	0	27	6	0	0
Mahoning (USGS-1)																										
DDS-48	203	60	27	20	0	2	0	13	1	0	0	3	2	4	3	12	0	24	5	7	5	0	0	0	2	7
DDS-49	192	50	37	16	0	0	0	18	1	0	0	0	2	4	6	11	0	27	2	1	9	10	0	2	4	8
DDS-50	210	28	27	36	0	1	0	20	1	0	1	0	0	0	0	0	0	66	2	0	6	0	0	0	1	1
DDS-51	193	48	34	12	0	1	0	8	0	0	0	0	2	5	2	10	0	41	4	4	9	9	0	0	9	9
DDS-52	211	31	31	12	0	1	0	16	0	0	0	0	0	1	0	0	0	69	4	1	5	8	4	1	4	1
DDS-53	184	40	40	15	0	2	0	23	0	0	0	0	5	4	1	13	0	39	3	3	2	0	0	0	16	10
DDS-55	209	42	37	17	0	2	0	13	0	0	0	1	1	8	4	4	0	29	2	3	6	0	3	9	6	4

Lower Pennsylvanian Sandstones

Nuttall (USGS-8)																										
DDS-80	288	10	22	2	0	13	0	8	1	1	0	0	0	2	0	25	0	19	0	2	0	1	0	0	6	0
DDS-81	294	13	6	1	0	16	0	7	0	0	0	0	0	6	1	32	0	10	1	3	1	5	1	2	1	0
DDS-82	327	21	2	0	0	9	0	6	1	0	0	0	0	2	3	21	0	2	0	0	1	0	0	1	4	0
DDS-83	324	19	2	0	0	11	0	2	0	0	0	0	4	7	2	18	0	5	0	1	0	4	0	0	1	0
DDS-84	279	12	9	1	0	4	0	2	0	0	0	0	2	9	1	18	0	1	0	0	10	45	6	0	1	0
DDS-85	230	18	37	2	0	12	0	23	2	0	2	0	0	0	1	0	0	25	0	4	20	8	2	0	14	0
DDS-87	269	16	28	0	0	11	0	16	2	0	0	0	0	0	0	0	0	24	0	3	15	6	0	0	10	0
DDS-89	168	9	12	1	0	11	0	9	0	0	1	0	0	0	0	0	1	8	0	2	161	1	12	3	1	0
DDS-90	259	16	32	1	0	6		21	3	1	2	0	0	0	0	3	0	36	1	8	0	1	5	0	4	1
DDS-91	257	20	27	2	0	8	0	18	1	0	0	0	0	0	0	10	0	29	0	3	1	3	10	2	9	0
DDS-92	254	27	17	0	0	11	0	13	1	0	15	0	0	1	0	16	0	24	0	1	2	5	6	0	7	0

Sample	Qm	Qp	Lm	Ls	Lv	Fk	Fp	Musc	Biot	Heav	Org	Ilm	Pp	Ps	Qcs	Kaol	Fab	Illr	Illc	Chl	Calc	Sid	Dol	Ank	Fe+3	Pyr
Bee Rock (98-SE-1)																										
VA98-1	226	20	17	14	0	28	2	11	6	0	1	0	0	6	3	0	1	50	2	5	0	1	1	0	4	2
VA98-2	229	24	17	23	0	26	1	15	1	3	0	0	0	12	1	0	0	34	2	5	0	0	0	0	3	4
VA98-3	201	25	22	25	0	24	4	7	2	0	0	0	0	6	1	0	4	20	0	1	53	0	0	0	5	0
VA98-4	239	29	17	36	0	18	2	10	0	0	0	0	0	0	2	0	1	26	1	4	5	8	1	0	1	0
VA98-5	237	29	15	40	0	29	2	2	2	1	0	0	0	2	2	0	0	28	0	4	0	0	0	0	7	0
VA98-6	237	19	20	25	0	12	2	17	1	2	0	0	1	10	3	0	0	35	1	6	1	3	0	1	3	1
VA98-7	218	27	11	18	0	37	4	8	3	1	0	0	4	29	1	0	1	32	1	0	2	0	0	0	3	0
VA98-8	241	21	7	16	0	49	2	3	0	0	0	0	3	20	3	0	0	30	0	2	0	0	0	0	2	1
Council (98-SE-1)																										
VA98-9	228	20	19	38	0	31	1	9	0	0	0	0	0	0	2	0	0	37	1	2	0	2	0	0	10	0
VA98-10	206	19	18	36	0	28	2	18	1	2	0	0	0	1	1	0	0	62	1	1	2	2	0	0	0	0
VA98-11	243	14	18	41	2	28	0	9	0	1	0	0	1	3	4	0	0	25	0	3	1	4	2	0	1	0
VA98-12	220	9	25	45	0	20	1	19	0	0	0	0	0	1	3	0	1	46	2	3	1	4	0	0	0	0
VA98-13	221	13	22	49	0	19	2	11	1	0	0	0	0	2	4	0	0	35	1	1	3	8	6	0	2	0
Guyandot (C-15)																										
C15-1	317	10	10	4	0	1	0	6	0	2	0	1	4	1	27	0	0	5	2	2	0	6	0	0	0	2
C15-2	236	5	10	5	0	2	2	29	2	1	0	0	0	0	2	0	0	73	9	11	0	9	2	0	1	1
C15-3	257	14	24	2	0	1	0	21	0	0	0	0	0	0	4	0	0	64	7	4	0	0	0	0	1	1
C15-4	268	7	24	4	0	3	1	23	1	0	0	0	1	0	3	0	0	49	5	9	0	0	1	0	0	1
C15-5	263	7	31	3	0	7	5	16	4	0	0	0	7	18	0	1	0	30	4	4	0	0	0	0	0	0
C15-6	269	2	22	1	0	22	6	12	7	1	0	0	2	3	1	2	0	36	6	5	0	0	1	0	2	0
C15-7	269	15	11	0	0	27	3	4	4	1	0	0	8	15	0	0	0	32	3	4	0	0	0	0	1	3
C15-8	267	9	16	0	0	20	4	8	4	0	0	0	6	9	2	1	0	38	3	8	0	0	0	0	5	0
C15-10	242	21	12	5	0	12	2	9	0	1	0	0	0	0	8	0	1	65	4	9	1	0	0	0	8	0
C15-11	227	23	19	3	0	10	3	9	0	2	0	0	1	11	1	0	1	74	5	2	0	3	1	0	5	0
C15-12	219	18	7	1	0	15	4	11	1	0	0	0	2	13	2	0	0	55	3	4	41	0	0	0	4	0
C15-13	191	12	19	4	0	11	1	9	0	0	2	0	0	1	0	0	0	39	1	4	58	11	31	0	6	0
C15-14	219	27	24	5	0	9	0	13	1	0	0	0	0	0	0	0	0	80	5	6	3	3	0	0	5	0
C15-15	233	18	25	5	0	14	2	12	0	0	1	0	0	9	3	0	1	56	2	3	1	9	0	0	6	0
C15-16	222	21	30	9	0	19	2	9	1	0	0	0	0	0	3	0	0	66	3	9	1	4	0	0	1	0
C15-17	211	16	22	2	0	9	0	9	0	1	0	0	0	0	5	1	0	45	2	1	7	68	0	0	1	0
U. Quartz Arenite (98-SE-1)																										
VA98-14	227	10	27	28	0	30	5	6	2	1	0	0	1	2	2	0	1	33	1	3	1	0	1	2	17	0
VA98-15	220	11	12	25	0	37	7	10	1	0	0	0	0	34	3	0	1	26	1	2	1	0	3	1	4	1
VA98-16	210	12	16	19	2	46	8	7	1	0	0	0	0	10	4	0	0	35	1	2	1	14	2	3	7	0

Sample	Qm	Qp	Lm	Ls	Lv	Fk	Fp	Musc	Biot	Heav	Org	Ilm	Pp	Ps	Qcs	Kaol	Fab	Illr	Illc	Chl	Calc	Sid	Dol	Ank	Fe+3	Pyr
VA98-17	241	12	18	20	0	57	2	3	0	0	0	0	0	1	2	0	0	27	1	0	0	1	2	1	12	0
VA98-18	240	13	20	25	0	44	5	3	1	0	0	0	1	1	5	0	0	23	0	0	0	3	0	1	14	1
U. Raleigh (WVGS-4)																										
DDS-1	269	10	3	0	0	4	1	0	0	0	0	0	32	20	58	1	0	0	0	0	2	0	0	0	0	0
DDS-2	288	14	13	1	0	2	0	5	0	1	0	0	2	1	45	0	0	7	1	5	1	11	3	0	0	0
DDS-3	302	22	3	2	0	3	0	0	0	0	0	0	16	12	30	9	0	0	0	0	0	0	0	0	1	0
DDS-4	331	6	5	0	0	0	0	1	0	0	0	0	4	3	40	4	0	2	0	3	1	0	0	0	0	0
DDS-5	313	6	5	0	0	7	0	0	0	0	0	0	19	13	31	5	0	0	0	0	0	0	0	0	0	1
DDS-6	332	6	5	1	0	1	0	2	0	1	0	0	2	2	30	5	0	6	1	1	0	0	4	1	0	0
DDS-7	290	17	2	1	0	9	0	0	0	1	0	0	13	16	41	6	0	0	0	1	1	0	0	2	0	0
DDS-8	330	3	5	0	0	0	0	0	0	0	0	0	4	6	37	3	0	4	0	1	1	4	1	0	0	1
DDS-9	300	10	5	1	0	1	0	0	0	0	0	0	21	13	21	1	0	0	0	1	0	23	1	0	0	2
DDS-10	340	11	1	0	0	0	0	0	0	0	0	0	9	12	19	0	0	1	1	5	0	1	0	0	0	0
DDS-11	294	14	1	0	0	9	0	1	0	0	0	0	26	6	39	2	0	1	0	1	1	5	0	0	0	0
DDS-12A	298	7	5	1	0	5	0	2	0	0	0	0	1	6	5	0	0	2	0	1	9	1	57	0	0	0
DDS-12B	308	2	4	2	0	1	0	0	0	0	0	0	1	0	15	0	0	0	0	2	5	3	57	0	0	0
DDS-13	274	15	17	1	0	9	0	1	0	0	0	0	15	16	38	9	0	0	0	2	0	0	0	0	0	3
DDS-14	324	1	9	1	0	0	0	3	0	0	0	0	4	5	41	2	0	4	0	4	0	0	2	0	0	0
DDS-15	260	26	31	5	0	7	0	2	0	0	0	0	6	6	30	8	0	3	3	13	0	0	0	0	0	0
DDS-16	259	12	26	0	0	6	0	5	0	1	0	0	6	2	45	1	0	16	5	10	2	0	1	2	0	1
DDS-17	262	17	14	10	0	4	0	4	0	1	1	0	12	13	47	0	0	10	3	0	0	1	0	1	0	0
DDS-18	368	0	4	0	0	0	0	0	0	0	0	0	4	3	19	0	0	1	0	0	1	0	0	0	0	0
DDS-19	317	14	2	0	0	4	0	0	0	0	0	0	11	5	38	1	0	1	1	2	3	0	0	0	0	1
DDS-20	233	31	8	4	0	1	0	2	0	0	0	0	2	7	21	9	0	3	0	0	5	74	0	0	0	0
L. Raleigh (WVGS-4)																										
DDS-21	278	4	22	6	0	2	0	5	0	0	0	0	3	2	9	13	0	26	2	1	0	24	1	0	0	2
DDS-22	266	25	13	2	0	11	0	0	0	0	0	0	11	8	28	15	0	4	1	0	10	5	0	0	0	1
DDS-23	305	2	5	0	0	2	0	2	0	0	0	0	7	21	19	5	0	7	3	3	0	17	0	0	0	2
DDS-26	128	25	18	7	0	6	0	3	0	0	0	1	0	0	0	0	0	3	0	1	15	0	193	0	0	0
DDS-27	209	39	55	15	0	2	0	10	0	0	0	2	2	4	2	0	0	5	2	4	8	37	0	0	0	4
DDS-28	281	4	20	9	0	0	0	21	1	0	0	0	8	7	6	3	0	21	4	6	3	5	0	0	0	1
DDS-29	265	15	10	7	0	2	0	0	1	0	0	0	3	15	25	0	0	3	0	1	14	33	3	0	0	3
DDS-30	332	7	5	5	0	1	0	1	0	0	0	0	0	1	31	0	0	3	1	0	4	9	0	0	0	0
DDS-31	244	37	30	14	0	9	0	1	0	0	0	0	3	6	36	3	0	6	4	4	3	0	0	0	0	0
Unnamed (98-SE-1)																										
VA98-19	259	16	19	30	0	23	2	6	0	1	0	0	0	0	1	0	0	25	1	2	0	6	2	0	7	0

Sample	Qm	Qp	Lm	Ls	Lv	Fk	Fp	Musc	Biot	Heav	Org	Ilm	Pp	Ps	Qcs	Kaol	Fab	Illr	Illc	Chl	Calc	Sid	Dol	Ank	Fe+3	Pyr
VA98-20	260	12	21	17	0	19	7	4	0	0	0	0	0	1	8	0	0	35	2	1	3	1	2	0	7	0
VA98-21	232	18	15	16	0	16	1	5	1	0	1	0	6	37	4	0	0	16	0	1	1	0	21	1	7	1
VA98-22	246	13	21	34	0	13	0	11	0	0	0	0	0	1	5	0	0	24	0	0	11	1	6	0	14	0
VA98-23	206	8	31	53	0	20	3	11	1	0	0	0	0	0	2	0	0	50	2	1	1	1	0	0	10	0
VA98-24	221	14	18	20	0	17	4	6	0	0	0	0	1	19	4	0	0	34	1	1	1	35	1	2	0	1
VA98-25	256	10	18	33	0	21	2	4	0	0	0	0	0	0	2	2	0	32	1	3	0	1	2	0	13	0
VA98-27	226	13	25	36	0	18	3	12	2	0	0	0	0	0	5	3	0	23	1	4	0	1	17	0	11	0
VA98-28	242	13	24	31	0	27	0	9	1	0	0	0	0	0	3	2	0	27	0	2	0	2	1	0	16	0
Quinnimont (WVGS-4)																										
DDS-32	215	35	28	6	0	15	0	5	0	0	0	0	4	1	28	0	0	30	11	4	3	11	1	2	1	0
DDS-33	252	38	17	2	0	10	0	3	0	0	0	0	10	2	37	0	0	14	7	3	1	0	0	0	1	3
DDS-34	285	40	2	0	0	6	0	0	0	0	0	0	6	6	44	0	0	2	6	2	0	0	0	1	0	0
DDS-35	263	76	3	2	0	2	0	0	0	0	0	0	7	6	26	0	0	0	2	0	6	3	0	4	0	0
Unnamed (98-SE-1)																										
VA98-29	249	14	16	27	0	8	0	4	0	0	0	0	1	37	5	0	0	35	1	0	0	0	1	0	2	0
VA98-30	252	12	24	24	0	28	0	12	0	0	0	0	0	5	1	0	0	31	1	0	0	1	5	1	3	0
VA98-31	247	10	21	23	0	23	1	7	0	0	0	0	2	9	1	0	0	46	2	0	0	0	1	0	7	0
VA98-32	238	8	25	17	0	27	3	2	2	0	0	0	2	32	3	0	0	30	2	1	0	1	0	0	4	3
VA98-33	258	12	12	21	0	30	0	5	1	0	0	0	1	6	4	0	0	35	2	0	1	0	5	0	7	0
VA98-34	253	10	12	27	0	21	2	10	2	0	17	0	0	0	2	0	0	25	0	2	0	1	0	0	16	0
VA98-35	250	10	11	23	0	32	0	9	0	1	0	0	1	10	7	0	0	35	2	1	0	0	2	0	6	0
VA98-36	266	13	13	13	0	27	3	4	1	0	0	0	1	10	3	0	0	35	1	0	1	0	6	0	3	0
White Rock (98-SE-1)																										
VA98-37	248	6	13	21	0	12	1	7	0	1	0	0	0	0	0	0	0	77	3	3	0	0	5	0	3	0
VA98-38	258	15	12	25	0	19	2	7	0	0	0	0	0	0	1	0	0	48	0	0	0	0	6	0	7	0
VA98-39	248	12	15	12	0	13	2	2	0	0	0	0	2	47	1	0	0	34	2	0	0	0	8	0	2	0
VA98-40	259	14	15	30	0	16	0	2	1	0	0	0	1	25	7	0	0	19	1	0	3	0	3	0	4	0
VA98-41	264	16	9	27	0	12	1	9	1	0	0	0	0	2	0	0	0	29	2	3	14	1	5	0	5	0

Upper Mississippian Sandstones

Glady Fork (outcrop)																										
P-1	283	10	8	15	0	12	0	0	0	1	0	0	0	0	7	0	0	8	1	1	44	0	8	1	1	0
GFO-2	268	3	9	32	0	10	0	1	0	0	0	0	0	0	0	0	0	9	0	52	14	0	0	0	2	0
GFO-4	245	4	8	32	0	12	0	6	1	0	0	0	0	0	0	0	0	37	3	49	1	0	0	0	2	0

Sample	Qm	Qp	Lm	Ls	Lv	Fk	Fp	Musc	Biot	Heav	Org	Ilm	Pp	Ps	Qcs	Kaol	Fab	Illr	Illc	Chl	Calc	Sid	Dol	Ank	Fe+3	Pyr
GFO-5	255	10	2	85	0	4	0	2	1	1	0	0	0	0	0	0	0	8	0	24	6	0	0	0	2	0
PO-1	329	6	2	24	0	3	0	0	1	0	0	0	0	12	2	3	0	2	0	0	0	0	0	0	16	0
Princeton (outcrop)																										
PO-1	329	6	2	24	0	3	0	0	1	0	0	0	0	12	2	3	0	2	0	0	0	0	0	0	16	0
PO-2	295	12	5	26	0	6	0	5	0	0	0	0	0	5	0	2	0	12	0	0	0	0	0	0	32	0
PO-3	322	5	3	32	0	2	0	2	0	0	0	0	0	4	1	5	0	5	0	0	0	0	0	0	19	0
PO-4	315	15	7	29	0	10	0	0	0	0	0	0	0	2	1	4	0	6	0	0	0	0	0	0	11	0
PO-5	326	9	1	25	0	6	0	0	0	1	0	0	0	5	3	1	0	5	0	0	0	0	0	0	18	0
Stony Gap (C-99-23)																										
C99-1	317	5	5	12	0	6	0	2	0	1	0	0	1	14	18	0	0	10	0	3	4	0	0	0	2	0
C99-2	328	4	1	6	0	10	0	3	0	2	0	0	5	16	14	1	0	2	0	0	5	0	0	0	1	2
C99-3	365	0	2	2	0	5	0	2	0	0	0	0	2	3	15	0	0	1	0	1	1	0	0	0	0	1
C99-4	335	2	1	13	0	6	0	2	0	0	0	0	0	9	5	1	0	4	0	1	18	0	2	0	0	1
C99-5	351	1	1	10	0	5	0	1	0	0	0	0	0	13	10	0	0	5	0	0	1	0	2	0	0	0
C99-6	302	7	5	29	0	17	0	5	0	2	0	0	0	2	6	1	0	13	0	8	0	0	0	0	1	2
C99-7	339	5	2	6	0	4	0	3	0	1	0	0	0	31	2	3	0	3	0	1	0	0	0	0	0	0
C99-8	338	1	1	6	0	4	0	4	0	0	0	0	1	23	3	0	0	13	0	0	4	0	0	0	0	2
C99-9	323	2	3	10	0	7	0	2	0	0	0	0	0	38	6	1	0	7	0	0	1	0	0	0	0	0
C99-10	345	0	3	1	0	8	0	2	0	0	0	0	0	29	4	0	0	3	0	0	4	0	1	0	0	0

Qm-monocrystalline quartz; Qp-polycrystalline quartz; Lm-metamorphic rock fragments; Ls-sedimentary rock fragments; Lv-volcanic rock fragments; Fk-K-feldspar (detrital); Fp-plagioclase feldspar (detrital); Musc-muscovite; Biot-biotite; Heav-heavy mineral; Org-organic; Ilm-ilmenite (detrital); Pp-primary porosity; Ps-secondary porosity; Qcs-authigenic quartz; Kaol-kaolinite; Fab-authigenic albite; Illr-replacement illite; Illc-illite cement; Chl-authigenic chlorite; Calc-calcite; Sid-siderite; Dol-dolomite; Ank-ankerite; Fe+3-Iron-oxide/oxyhydroxide; Pyr-pyrite

APPENDIX B

SAS/IML code
(Statistical Analysis Software/Interactive Matrix Language)

Michal Kowalewski and Jason Reed

```
%let vars=;
%let id=ss; * - only one variable here (will show on SAS plot);
%let label=sample;
options linesize=186;
data output;
infile cards;
input ss $ sample $ Qm Qp Lms Ls Lv Fk Fp Musc Biot Heav Org Ilm
Pp Ps Qcs Kaol  Fab Illrsm Illc Chl Calc Sid Dol Ank Fexh Pyr;
if Dol>40 then delete;
if Calc>40 then delete;
if Sid>20 then delete;
cards;
        -----------D A T A  M A T R I X----------
;
data iml1;
   set output;
   keep andvars;
PROC IML;
USE iml1;
READ all into Y;
X=t(Y);
taxsum=X[,+];
xid=loc(taxsum>0);
Y=X[xid,];
tem1=Y[+,];
tem2=shape(tem1,nrow(Y),ncol(Y));
relY=Y/tem2*100;
Z=t(relY);
sumofrows=Z[,+];
if mean(sumofrows)^=100 then print 'OH SHIT';
final=Z||sumofrows;
col1={andvars total};
CREATE out1 from final[colname=col1];
append from final;
close out1;
QUIT;
RUN;

DATA fin2;
        set out1;
```

```
DATA labid;
   set output;
   keep andid;
DATA corr;
   merge fin2 labid;
proc corresp all data=corr outc=out; * - correspondence
analysis;
var andvars;
id andid;
data report;
        set out;
        if dim1='.' then delete;
   keep dim1 dim2 andid;
data labels;
   set output;
   keep andlabel;
data final2;
   merge report labels;
proc print data=final2;
proc plot data=final2;
        plot dim1*dim2=andid;
run;
quit;
```

APPENDIX C

BOREHOLE AND OUTCROP LOCATIONS

Well	Source	Location[1]	Interval	# samples
		Upper Pennsylvanian		
USGS-3	USGS	39.44031, -79.08503	Saltsburg	13
			L. Mahoning	10
MD4	Mettiki Coal	39.31178, -79.34529	Saltsburg	1
			Buffalo	1
			L. Mahoning	2
M60	Mettiki Coal	39.27932, -79.37491	Grafton	8
			Saltsburg	4
			Buffalo	10
			L. Mahoning	4
MD5	Mettiki Coal	39.26887, -79.38707	L. Mahoning	1
USGS-1	USGS	39.19848, -79.37897	Saltsburg	12
			Buffalo	9
		Lower Pennsylvanian		
USGS-8	USGS/WVGES	38.61921, -80.75482	Nuttall	13
WVGS-4	USGS/WVGES	37.96783, -81.29867	U. Raleigh	19
			L. Raleigh	11
			Quinnimont	4
C-15	Ackenheil Engineering	37.48365, -81.58904	Guyandot	17
98-SE-1	Consol Energy	37.10441, -82.05185	Bee Rock/Nuttall[2]	8
			Council/???	5
			U. Qtz Arenite Mbr/Guyandot[2]	5
			Sewanee/Upper Raleigh[2]	10
			???/White Rock/Quinnimont[2]	8
			White Rock/Pineville[2]	5
		Upper Mississippian		
C-99-23	Army Corp of Engineers	37.64044, -80.88644	Stony Gap	11

Outcrop (Mississippian Sandstones) ----------

1	-----	37.365, -81.116	Glady Fork	4
2	-----	37.485, -81.073	Princeton	5

[1] latitude, longitude (decimal degrees)
[2]approximate West Virginia time equivalents (Virginia/West Virginia nomenclature)

APPENDIX D

VITRINITE REFLECTANCE VALUES

Core	location	stratigraphic interval	depth (ft)	%Ro
		Upper Pennsylvanian		
USGS-3	39.44031, -79.08503	black shale (unnamed)	620	0.91 1.05 1.00 1.15 1.05 0.96 1.12 1.03 mean = **1.03**
USGS-3	39.44031, -79.08503	Brush Creek Shale	818	1.45 1.40 1.40 1.35 1.35 mean = **1.39**
USGS-1	39.19848, -79.37897	black shale (unnamed)	149	0.84 0.86 mean = **0.85**
		Lower Pennsylvanian		
C-15	37.48365, -81.58904	Sewell Coal	69	1.03 0.98 0.98 1.16 1.16 1.11 1.01 1.13 1.07 mean = **1.07**
WVGS-4	37.96783, -81.29867	black shale (unnamed)	1173	0.91 1.18 1.08 0.98 0.93 1.03 1.13 1.03 1.12 1.03 mean = **1.04**
WVGS-4	37.96783, -81.29867	black shale (unnamed)	1202	0.99

				1.05 0.98 0.98 mean = **1.00**
WVGS-4	37.96783, -81.29867	black shale (unnamed)	1213	0.84 0.90 0.85 0.98 mean = **0.89**

APPENDIX E

TIMING OF MAXIMUM BURIAL AND INTERPOLATED PALEOGEOTHERMAL GRADIENTS

method	*Max burial*[1] *(Ma)*	*interpolated paleogeotherm (°C/km)*	*max. T*[2] *(°C)*	*burial depth*[3] *(km)*
		Upper Pennsylvanian		
FI, Ro	263±3	32.6	149	4.6
AFT	---	25.8	100	3.14
(U-Th)/He	---	24.5	60	1.68
		Lower Pennsylvanian		
FI, Ro	274±4	32.0	146	4.4
AFT	---	25.6	100	3.14
(U-Th)/He	---	23.3	60	1.74

[1]estimated timing of maximum burial was determined using sedimentation rates and estimates provided by Blackmer et al. (1994). Independent determination of the timing of maximum burial indicator was necessary to avoid additional assumptions concerning the paleogeothermal gradient. Maximum burial was reached 40 Myr.

[2]maximum temperatures for AFT and (U-Th)/He are annealing and closure temperatures, respectively

[3]from thermal constraints and average day formation temperatures

APPENDIX F

DECOMPACTED THICKNESS FOR NONMARINE DEPOSITS IN CENTRAL APPALACHIAN BASIN

	% of section	*thickness (m)*	*[1]decompacted thickness (m)*
		Upper Pennsylvanian	
Glenshaw Fm.			
USGS-3	100	**121.1**	**160.0**
Sandstone	39	47.1	60.2
Mudstone	59	70.6	93.9
Coal	2	3.4	5.9
		Lower Pennsylvanian	
New River Fm.			
WVGS-4	100	**266.9**	**349.0**
Sandstone	54	144.0	184.3
Mudstone	45	120.0	159.6
Coal	1	2.9	5.1
		Upper Mississippian	
[2]Mauch Chunk Grp.			
Mercer 36, 31	100	**556.0**	**735.6**
Sandstone	34	188.2	242.8
Mudstone	66	367.8	492.8

[1]Decompaction parameters according to Nadon and Issler (1997) and Nadon (1998)
[2]Mauch Chunk thickness measured from composite well log (Mercer 31, Mercer 36; Miller and Eriksson, 2000)

APPENDIX G

ESTIMATED PRESENT DAY SAMPLE TEMPERATURES FOR THERMOCHRONOLOGY

Sandstone(sample)	core	depth (m; median)	Temperature (°C; median)
	----------*Upper Pennsylvanian*----------		
Saltsburg (S):	USGS-3	170 – 190 (180)	18.4 – 18.8 (18.6)
Mahoning (M):	USGS-3	262 – 274 (268)	20.3 – 20.5 (20.4)
	----------*Lower Pennsylvanian*----------		
Guyandot (G):	C-15	25 – 38 (32)	15.5 – 15.8 (15.7)
Lower Raleigh (LR):	WVGS-4	340 – 354 (347)	21.8 – 22.1 (21.9)

(Present geothermal gradient: ~ 20 °C/km; estimated average surface temperature = 15°C)

APPENDIX H

CENOZOIC FORELAND BASIN GEOTHERMAL GRADIENTS

Basin	Geothermal Gradient	source
North Slope, Alaska	27-39 °C/km	O'Sullivan (1999)
Llanos Basin, Columbia	20-50 °C/km	Bachu et al. (1995)
Potwar Plateau, Pakiston	18.2 –27.4 °C/km (Neogene) 30.1-60.2 °C/km (pre-Neogene)	Law et al. (1998)

VITA

Jason Scott Reed

Personal:

Date of Birth: October 9, 1975
Parkersburg, West Virginia

Education:

Ph.D. (2003), Virginia Polytechnic Institute and State University, Blacksburg, VA
B.S. (magna cum laude; 1998), Marshall University, Huntington, WV

Awards and Honors:

- Nominee: Outstanding Graduate Student, College of Arts and Sciences, Virginia Tech (2003)
- Outstanding Service Recognition Award (Dept. of Geol. Sci., Virginia Tech; 2002)
- Byron Nelson Cooper Memorial Fellowship (Dept. of Geol. Sci., Virginia Tech; 2002)
- Geological Society of America Student Grant (2000 and 2002)
- Graduate Research Development Project Grant (Virginia Tech, 2002)
- Robinson-Holden Scholarship (Dept. of Geol. Sci., Virginia Tech; 2001)
- Department of Geology Endowed Scholarship (Marshall University; 1995 and 1996)
- Phi Eta Sigma National Honor Society

Experience:

- Graduate Teaching Assistant, Dept. of Geological Sciences, Virginia Tech (1998-2003):
- bp p.l.c., summer geoscience intern, Houston, TX (May – August 2001)
- NASA's Planetary Geology and Geophysics Undergraduate Research Program undergraduate researcher, Brown University, Providence RI (June-August 1997)